ABSTRACT

Title of Dissertation: IDENTIFICATION AND FUNCTIONAL CHARACTERIZATION OF THE GBF1-CONTROLLED NETWORK OF HOST PROTEINS SUPPORTING ENTEROVIRUS REPLICATION

Seyedehmahsa Moghimi,

Doctor of Philosophy, 2022

Dissertation directed by: Dr. George Belov, Associate professor

Department of Veterinary Medicine,

University of Maryland, College Park

The genus *Enterovirus* of the *Picornaviridae* family contains many established and emerging pathogens. However, licensed vaccines are currently available only against poliovirus and enterovirus A71. No therapeutics have been officially approved to treat any enterovirus infections, although some are being developed. To find suitable targets for antivirals and control the infections, we need to understand the virus's life cycle better and identify the cellular factors involved in virus infection. Enterovirus genome replication occurs on the unique membranes known as replication organelles (ROs). A Golgi resident protein, GBF1, is recruited to the ROs by a viral protein 3A. GBF1 activates small GTPases Arf, which are critical regulators of the cellular secretory pathway. Here, we investigated the mechanistic details of GBF1-dependent Arf activation during enterovirus replication

and characterized the proteome of the ROs in the vicinity of GBF1. We showed that Arf1 appeared to be the first to associate with the ROs, followed by other Arfs. Once activated and recruited to the ROs, all Arfs except Arf3 were no longer sensitive to inhibition of GBF1, suggesting that they do not actively cycle between GTP- and GDP-bound states in infected cells. siRNA depletion studies demonstrated an increased sensitivity of polio replication to inhibition of GBF1 in Arf1-, and to a lesser extent, Arf6-depleted cells, indicating the importance of GBF1-mediated activation of these Arfs for the viral replication. Taking advantage of the GBF1 recruitment to the ROs and GBF1's essential role in enterovirus replication, we used a GBF1 construct fused to APEX2 peroxidase to explore the proteome of the ROs by proximity biotinylation. Among the proteins biotinylated in infected cells were the known cellular factors recruited to the ROs, including PI4KIIIβ, OSBP, and ACBD3, indicating that these proteins are localized close to GBF1. Among the viral proteins, the intermediate products of the polyprotein processing were overrepresented, suggesting that GBF1 is localized close to the sites of active polyprotein processing. About 85% of the proteins identified by MS have not been previously associated with enterovirus infection. Gene ontology analysis revealed a significant enrichment of RNA binding and mRNA metabolic processes, suggesting a close localization of GBF1 to the RNA replication complexes. siRNA knockdown functional analysis of the selected proteins showed the recruitment of both proviral and antiviral factors to the ROs. Collectively, our work revealed important details about the involvement of Arfs in the replication process, introduced a highly efficient system to investigate the proteome of the enterovirus ROs, and provided novel data about the protein composition of the GBF1-enriched environment in the replication sites.

IDENTIFICATION AND FUNCTIONAL CHARACTERIZATION OF THE GBF1-CONTROLLED NETWORK OF HOST PROTEINS SUPPORTING ENTEROVIRUS REPLICATION

by

Seyedehmahsa Moghimi

Dissertation submitted to the Faculty of the Graduate School of the
University of Maryland, College Park, in partial fulfillment
of the requirements for the degree of
Doctor of Philosophy
2022

Advisory Committee:
Associate Professor George Belov, Chair
Professor Jeffrey DeStefano
Professor Daniel Nelson
Professor Utpal Pal
Associate Professor Yanjin Zhang

Dedication

This dissertation is dedicated to my parents, Maryam and Mousa. I will never be able to thank you enough for all your sacrifices.

Acknowledgements

First, I would like to thank my advisor, Dr. George Belov, for trusting me and giving me the opportunity to work in his lab on such tremendous projects. Dr. Belov, I have learned a lot from you, not only about viruses but how to practice critical thinking, independent judgment of data, and enjoy science. In practice, you have shown me how one can achieve success in a short amount of time by only "concentrating on their research" and keeping themselves from unnecessary distractions. You certainly are by far one of the most influential people in my life who opened new doors to success in my future career. I will always owe you for making me the best version of scientist Mahsa. I also especially thank Dr. Ekaterina Viktorova. Kate, you always were and will be my role model. I truly admire your patience in dealing with the graduate students. No matter how many times we ask you the same questions, you always guide and assist us with your extraordinary knowledge and experience with a great deal of patience and kindness. During the ups and downs of the experimental lab works, you were always by my side, excited by my excitement and upset by my disappointment. It was such a great pleasure for me to collaborate with you on several projects during the past years. I also must thank my committee members, Dr. Jeffrey DeStefano, Dr. Daniel Nelson, Dr. Utpal Pal, and Dr. Yujin Zhang. I really appreciate your taking time out of your hectic schedule to review my dissertation and provide valuable comments and ideas to improve this project.

I would like to thank my lovely friends/lab mates, Anna and Samuel. You guys are the best lab mates one can ask for. You were always there for me, helped me overcome my fears and self-doubts, and cheered me up when I was burning out from

too much work and stress. Wish you guys all the best in your life. I also thank the UMD, Department of Veterinary Medicine's Dean, faculties, staffs, postdocs, and my fellow graduate students for making our workplace such a lovely, welcoming, and relaxing environment. I was excited to go to work literally every day with a great deal of enthusiasm and passion. Please keep up the excellent job for the future scholars.

I would like to thank my parents, Maryam and Mousa, but I cannot find any suitable words to express my deep gratitude towards them. You were my first mentor in life. You taught me to be kind and respectful to everybody regardless of our differences, appreciate those who make our life easier, work with honesty, modesty, and responsibility, and always smile and spread positive energy when interacting with others. I would like to thank my lovely siblings, Saeedeh and Amir. This is such an honor to be your sis, and I cannot imagine how empty my life would be if you guys were not in it. Love you so much! I also thank my besties, Dr. Fazeleh Etebar and Dr. Sahar Hemmati, for enriching my life with their support and kindness. Although we live thousands of miles away from each other now, you always have your special place in my heart and your positive influence on my life. I must thank Kayla Itsines and Emily Skye for their outstanding HIIT programs that helped me maintain my physical and mental health at the best level during my graduate studies. This project was supported by the National Institute of Health, and I am thankful for their support.

Finally, I would like to thank Hossein, my husband, best friend, and life partner. Hossein, merci, for always being there for me during the difficult and stressful time of graduate school, patiently listening to my boring daily stories from work, and helping me make the best decisions when I was so confused. Wish you all the best!

Table of Contents

List of Tables

List of Figures

List of Abbreviations

ACBD3: Acyl CoA-binding domain-containing 3

ACSLs: Acyl-CoA synthetase enzymes

AFM: Acute flaccid myelitis

ALDOA: Fructose bisphosphate aldolase A

APEX: Ascorbate peroxidase

ARF: ADP-ribosylation factor

Arf-GAP: Arf-GTPase activating protein

Arf-GEF: Arf guanine nucleotide exchange factor

ATGL: Adipocyte triglyceride lipases

BFA: Brefeldin A

cVDPV: Circulating virus-derived poliovirus

CVB3: Coxsackie B3 virus

CRE: *cis*-acting RNA element

DMEM: Dulbecco modified Eagle's medium

dsRNA: Double-stranded RNA

eIF: Eukaryotic initiation factor

EMCV: Encephalomyocarditis virus

EV: enterovirus

EWSR1: Ewing sarcoma breakpoint region 1

ERGIC: Endoplasmic Reticulum-Golgi intermediate compartment

FBS: Fetal bovine serum

FRP: Fusion red protein

G3BP1: Ras GTPase activating protein-binding protein 1

GBF1: Golgi-specific brefeldin A-resistance guanine nucleotide exchange factor 1

GFP: Green fluorescent protein

GO: Gene ontology

GuHCl: Guanidine hydrochloride

HFMD: Hand-food-and-mouth disease

HNRNPA0: Heterogeneous nuclear ribonucleoprotein A0

HNRNPH: Heterogeneous nuclear ribonucleoprotein H

HNRNPQ (SYNCRIP): Heterogeneous nuclear ribonucleoprotein Q

HNRNPR: Heterogeneous nuclear ribonucleoprotein R

HNRNPU: Heterogeneous nuclear ribonucleoprotein U

HPI: Hours post-infection

ILF3: Interleukin enhancer-binding factor 3

IPV: Inactivated polio vaccine

IRES: Internal ribosome entry site

kDa: Kilo Dalton

KHDRBS: KH domain-containing RNA-binding protein

LDHA/B: Lactate dehydrogenase A/B

LDs: Lipid droplets

MOI: Multiplicity of infection

MS: Mass spectrometry

NT: Nucleotide

OPV: Oral polio vaccine

ORF: Open reading frame

OSBP: Oxysterol-binding protein

PFU: Plaque forming unit

PI4KIIIβ: Phosphatidylinositol 4-kinase III β

PI4P: Phosphatidylinositol 4-phosphate

PKM: Pyruvate kinase

PM: Plasma membrane

PV: Poliovirus

RBMX: RNA-binding motif protein, X chromosome

ROs: Replication organelles

SDS-PAGE: Sodium dodecyl-sulfate polyacrylamide gel electrophoresis

SGs: Stress granules

siRNA: Short interfering RNA

UTR: Untranslated region

VAPP: Vaccine associated paralytic poliomyelitis

VDPV: Vaccine-derived poliovirus

VP: Viral Protein

Chapter 1: Introduction to Enteroviruses

1.1 Enteroviruses classification

The genus *Enterovirus* of the *Picornaviridae* family contains 15 species, enteroviruses A to L and rhinoviruses A to C, which cause many established and emerging diseases in humans and animals. Enteroviruses were formerly discriminated based on criteria such as host specificity, receptor usage, disease manifestations in experimental animals and humans, and epitope specificity of the VP1 capsid protein in neutralization assays (52). Nowadays, however, enteroviruses are classified based on the VP1 capsid protein sequences (11, 156, 192). Among the enterovirus species, enteroviruses A to D and rhinoviruses can cause a wide range of illnesses in humans. Poliovirus, the representative member of the genus, belongs to the *Enterovirus* C species along with 22 serotypes of Coxsackie A viruses and several numbered enteroviruses. 25 serotypes of Coxsackie A viruses and numbered enteroviruses such as enterovirus A71 are in the *Enterovirus* A species. The *Enterovirus* B species contains 63 serotypes, some of which are important human pathogens such as Coxsackie B viruses and echoviruses. The *Enterovirus* D species comprises five serotypes of numbered enteroviruses, such as enterovirus D68 and D70 (154). Human rhinoviruses were initially divided into major and minor groups based on the usage of cell surface receptors and their sensitivity to antiviral compounds (6). Now, they are grouped based on the phylogenetic sequence analysis into human rhinoviruses A, B, and C. Human rhinovirus A contains 80 serotypes, mostly from the major receptor group, and human rhinovirus B has 32 major receptor serotypes. The more recently-defined species, human rhinovirus C, contains 57 serotypes, all from the minor receptor group.

1.2 Current enteroviruses challenges

1.2.1 Poliovirus

Poliovirus is the causative agent of poliomyelitis, and humans are the only natural hosts for the virus (212). Poliovirus is transmitted via a fecal-oral route, replicates in the gastrointestinal mucosa, and enters the blood circulation via the lymph nodes, causing viremia (64). The virus induces three different types of responses in the host, two of which are non-paralytic forms. One is called the abortive form in that no symptoms of nervous system disorder are developed in the infected individuals (154). The other form is aseptic meningitis, and the virus can be detected in the cerebrospinal fluid (CSF) (238). The paralytic form of poliomyelitis causes temporary or permanent disabilities or death due to the paralysis of the respiratory muscles. In this form of response, the virus disseminates in the central nervous system (CNS) upon either penetrating the blood-brain barrier (BBB) or retrograde axonal transport and infects motor neurons in multiple parts of the CNS (157).

It has been over three decades since the Global Polio Eradication Initiative (GPEI), led by national governments and six partners, including the World Health Organization (WHO), the U.S. Centers for Disease Control and Prevention (CDC), the United Nations Children's Fund (UNICEF), Rotary International, Bill & Melinda Gates Foundation and Gavi, the vaccine alliance, started an ambitious attempt to achieve a polio-free world. During that time, substantial progress has been made so that the number of poliomyelitis cases plummeted by more than 99% in the world, and the wild polioviruses of type 2 and 3 were eradicated with the last naturally occurring viruses detected in India in 1999 and in Nigeria in 2012, respectively (https://www.cdc.gov/cpr/polioviruscontainment/diseaseandvirus.htm) (176). However,

type 1 wild-type virus is still circulating in two endemic countries, Afghanistan and Pakistan and the vaccine-derived polioviruses (VDPVs) circulate in both endemic countries and non-endemic regions, i.e., the ones that are declared free from the wild-type poliovirus (https://www.cdc.gov/mmwr/volumes/68/wr/mm6845a4.htm). Attenuated viruses in the Sabin vaccine (OPV) can revert to the wild-type phenotype during replication in the intestine, generating VDPVs which can establish circulation in under-immunized communities, turning to circulating VDPV (cVDPV), and causing outbreaks of paralytic poliomyelitis. (173). All three serotypes of the virus caused the cVDPVs-related outbreaks over the past five years; however, more than 90% of them were associated with the type 2 cVDPV (cVDPV2). In 2020, 1,037 cases of cVDPV2 were reported from 24 countries, while the number of cases was three times less in 2019, and 15 countries were involved (https://polioeradication.org/wp-content/uploads/2021/03/GPEI-cVDPV2-nOPV2-Factsheet-20210312-EN.pdf). Multiple factors are associated with the cVDPV2 outbreaks, such as low immunization coverage, inefficient outbreak response, and elimination of type 2 from the vaccination programs. The Polio Eradication Strategy 2022-2026 was implemented by the GPEI in July 2020, offering a systematic plan to overcome these challenges and deliver on a promise of a polio-free world. The strategy includes two goals: (1) to permanently stall all wild-type poliovirus transmission in endemic countries and (2) to put a stop to cVDPVs transmission and prevent outbreaks in non-endemic regions. To achieve these goals, a set of activities has been implemented, such as developing next-generation mOPV2 vaccines that are more genetically stable, increasing the vaccination coverage in children, and establishing intensive disease surveillance in the regions with a history of cVDPV2 outbreaks (https://polioeradication.org/gpei-strategy-2022-2026/).

1.2.2 Non-polio enteroviruses

Non-polio enteroviruses can infect humans, non-human primates, and domestic animals. They are associated with a wide range of illnesses with various clinical manifestations, target organs, main target age group, severity, and prognosis.

Many enteroviruses can induce neurological disorders. Enterovirus A71 is one of the most neurotropic non-polio enteroviruses and the main cause of Hand-Foot-and-Mouth Disease (HFMD) outbreaks around the globe, especially in Southeast Asia (161). Infants and children are the main targets of the virus. The disease starts with rash and blisters in the limbs and mouth and can lead to the development of neurological symptoms such as aseptic meningitis, encephalitis, and poliomyelitis-like paralysis (161). Coxsackieviruses A6, A10, and A16 are other etiologic agents for HFMD, but they cause milder symptoms and less mortality than enterovirus A71 (187). The other neurotropic non-polio enterovirus is enterovirus D68, although it is primarily associated with respiratory-related diseases. Enterovirus D68 is the primary causative agent of Acute Flaccid Myelitis (AFM), which mainly affects the grey matter of the spinal cord, causing general weakness in the body, especially in the limbs. The epidemiology of enterovirus D68 has changed rapidly and unpredictably during the past decade worldwide. Up to 2014, enterovirus D68 cases were reported sporadically in the U.S., Europe, and Southeast Asia and were associated with mild respiratory complaints. However, several enterovirus D68 outbreaks occurred since 2014 with disease manifestation of severe respiratory infections and, in some cases, mixed with AFM. These outbreaks led to the awareness and attention towards this enterovirus and its association with AFM, so the CDC has initiated monitoring and monthly reporting of AFM cases in the U.S. since 2014 (36). Echoviruses may also show neurological

manifestations, with echovirus-A71 causing AFM and echovirus 6 and 9 causing aseptic meningitis, especially in children (123). Similarly, several serotypes of Coxsackieviruses B, such as Coxsackieviruses B2 and B5, can cause encephalitis and aseptic meningitis (4, 39).

Coxsackieviruses A and B and echoviruses can target cardiac muscles causing different presentations such as myocarditis, myopericarditis, dilated cardiomyopathy, and cardiac arrhythmia. Enterovirus-induced cardiomyopathy predominantly occurs in children and young adults, resulting in an unexpected death or a life-long heart failure in the surviving patients (63, 114).

Type 1 diabetes, an autoimmune genetic disorder, results from the damage of insulin-producing β-cells in the pancreas by autoreactive immune cells. Multiple genetic and environmental factors have been defined as the causative agents of the disease (59). Viral infection is one of the major environmental factors associated with type 1 diabetes. In particular, enteroviruses, including Coxsackieviruses B4 and B5, are the main viral candidates for the disease in humans as the viral RNA and antibodies synthesized against the viral antigens were detected in the patients with onset of the disease (158). The tropism of the virus to the pancreatic cells is associated with the expression of the viral receptor Coxsackie and Adenovirus Receptor (CAR) on the surface of these cells (180). Viral infection can trigger a robust immune response by stimulating natural killer cells (NK cells) and $CD8^+$ cytotoxic cells, which can attack the β pancreatic cells in the patients (59).

Acute hemorrhagic conjunctivitis, mainly caused by Coxsackieviruses A24 and enterovirus 70, is a highly contagious disease with severe symptoms such as hyperemia,

eye discharge, and sub-conjunctival hemorrhage. The disease occurs in all age groups with no specific preference and no treatment described (119, 154).

Human rhinoviruses are the major cause of the common cold and arguably are the main reason for the antibiotic prescription (7). They are highly contagious and mainly cause upper respiratory infections, although in certain cases, they can invade the lower parts of the respiratory tract (95). Human rhinoviruses typically cause self-limiting diseases in immunologically competent individuals; however, they are associated with life-threatening disorders such as croup, bronchiolitis, and pneumonia in infants, immunocompromised persons, and patients with pre-existing chronic obstructive pulmonary disease (35). Human rhinoviruses are also the major cause of asthma exacerbation in children and adults (66). Thus far, about 170 serotypes of human rhinoviruses have been detected, categorized into groups A, B, and C (127). Some antivirals, such as repurposed registered drugs, including capsid-binding agents (e.g., pleconaril, vapendavir, pirodavir), mRNA synthesis antagonists (e.g., ribavirin), 3C protease inhibitor (e.g., rupintivir), and immunomodulatory compounds (e.g., interferon 2α, interferon β) could successfully combat the diseases associated with these viruses (35, 95, 208).

Enteroviruses can cause infections in domestic animals, which are mostly mild to asymptomatic (97). Bovine enteroviruses (BEVs) belong to the species E and F of the genus and are endemic in cattle in many areas of the world (87). Although they are typically associated with asymptomatic infections, there have been reports of various clinical signs such as diarrhea, respiratory disorders, and abortion in infected animals (31, 97, 237, 243). BEVs transmission from animals to humans has been documented; however, they are not

associated with any clinical disorders in humans (74). Coxsackievirus B5 is a causative agent of the highly contagious swine vesicular disease (SVD) in domesticated pigs, with clinical manifestations of vesicles and erosions on the hooves and mouth. However, SVD is primarily mild and self-limiting in pigs, and no clinical signs have been reported in humans with close contact with infected animals (53). Species G of the genus *enterovirus* contains 20 serotypes of porcine enteroviruses, associated with sporadic reports of skin lesions, flaccid paralysis, and diarrhea in pigs (5, 111, 233).

1.2.3 Enteroviruses vaccines

Despite a wide range of enterovirus species and their associated illnesses, licensed vaccines are currently available only against two of them, poliovirus and enterovirus A71. Such limitation in vaccine development is due to a considerable genetic variability among enteroviruses (68). Two vaccines against poliovirus are the inactivated Salk vaccine (IPV) and live-attenuated Sabin vaccine (OPV), which were licensed in the U.S. in 1955 and 1963, respectively (47). The inactivated Salk vaccine, which has been the sole poliovirus vaccine applied in the U.S. since 2000, is administered via intramuscular or subcutaneous routes and triggers only humoral immunity in the vaccine recipients. The live attenuated Sabin vaccine is administered orally and stimulates both humoral and mucosal immunity in the vaccinees, as well as some immunization of unvaccinated individuals with close contact with the vaccine recipients (47). Compared to IPV, OPV production is less expensive, the administration is more convenient, and it induces sterilizing immunity important for the interruption of poliovirus transmission. Nevertheless, OPV is associated with the vaccine-associated poliovirus poliomyelitis (VAPP) incidence as the attenuated strains in the vaccine can revert to the wild-type phenotype. To address this issue, the polio

immunization strategy has been either completely switched from OPV to IPV administration or included a sequential IPV-OPV vaccination plan in which at least two doses of IPV are required (143). In addition to these two vaccines, new anti-poliovirus vaccines are actively being developed to contribute to the polio elimination programs, such as nOPV2-Consortium1 (nOPV2-c1), nOPV2-c2, nOPV-Codon-Deoptimized (nOPV-CD), which have higher genetic stability and lower risk of reversion to the wild-type (46, 112).

Enterovirus A71, which belongs to the enterovirus A species, is the other enterovirus that is currently controlled with vaccines. There are three monovalent inactivated whole virus vaccines approved by the Chinese Food and Drug Administration (CFDA) in 2015 to deal with the increasing number of HFMD cases in Southeast Asia (40). They were developed by three different companies, including Sinovac Biotech, Beijing Vigoo, and the Chinese Academy of Medical Science (CAMS). The efficacy and safety of these vaccines were evaluated by large phase III clinical trials, which revealed no adverse effects and 94.8%, 90.5%, and 97.4% efficacy for Sinovac, Vigoo, and CAMS vaccines, respectively (129). During the past few years, the development status of these vaccines has been carefully monitored and reviewed by the WHO, which provided recommendations to assure the efficacy, safety, and quality of the vaccines (https://www.who.int/teams/health-product-policy-and-standards/standards-and-specifications/vaccine-standardization/enterovirus-71). Recently, other types of anti-enterovirus A71 vaccines are being developed, some of which are multivalent vaccines against enterovirus A71 and other HFMD-related enteroviruses such as Coxsackieviruses A16, A6, and A10, estimated to be more efficient in controlling HFMD outbreaks (132).

1.2.4 Anti-enteroviral drugs

While the high antigenic diversity of multiple enteroviruses presents a significant challenge for vaccine development, antivirals may provide an effective way to control virus infections. Nevertheless, to date, no FDA-approved anti-enteroviral drugs are available, although some compounds targeting the viral factors such as capsid (e.g., pleconaril, V-073, disoxaril, pirodavir, and BTA-798), polymerase (e.g., ribavirin), and proteases (e.g., rupintrivir, AG7404) are in development (24, 213). Such drugs targeting viral proteins are effective only against very closely-related viruses in the *Picornaviridae* family.

The other option for antiviral development is targeting host cell factors involved in the virus's life cycle, which seem to be effective for a broad range of viruses that rely on the same cellular factors during infection (201, 214). However, host toxicity is a matter of concern for such drugs. For instance, PIK93 inhibits virus replication by blocking host phosphatidylinositol 4-kinase III β (PI4KIIIβ). However, the clinical trial for the drug was halted at phase II due to toxicity as well as the emergence of resistant viruses (24). Enviroxime-like compounds, divided into the major and minor categories, target the host cell proteins PI4KIIIβ and oxysterol-binding protein (OSBP), respectively. The major enviroxime-like drugs, including MDL-860, pachypodol, oxyglaucine, GW5074, BF-738735, and T-00127-HEV1 demonstrated significant inhibition of virus infection; however, they caused adverse side effects in the clinical trials (131, 197). The minor enviroxime-like drugs such as itraconazole, AN-12-H5, 25-HC, and T-00127-HEV2 are in the pre-clinical phase (182, 201).

To address the challenges in designing efficient and safe anti-enteroviral drugs, it is important to have a better understanding of the virus's life cycle, including the knowledge of the cellular factors involved in viral replication.

1.3 Enterovirus genome organization, particle structure, and life cycle

1.3.1 Viral genome organization

Poliovirus is the representative member of the genus enterovirus. It is a small, non-enveloped virus containing a ~7.5 kb positive-strand genome RNA. The genome consists of a 5' untranslated region (UTR), a single open reading frame (ORF), a 3' UTR, and a poly(A) tail at the 3' terminus (Figure 1.1) (149). The 5' end is covalently attached to a small viral peptide VPg (also known as 3B), which acts as the primer for viral genome replication. The first 100 nucleotides (nt) of the 5' non-coding region contain a cloverleaf structure necessary for viral genome replication. The cloverleaf contains stem loops a, b, c, and d. The dynamic binding of host and viral proteins to these stem loops mediates the transition from translation to the replication of the viral RNA (58, 68). The next 642 nt UTR of the 5' end contains an internal ribosome entry site (IRES) which consists of several stem-loop structures and is necessary for the cap-independent translation of the viral RNA (68). The single ORF codes for a polyprotein that is cleaved by viral proteases into structural and replication proteins encoded in the P1 and P2P3 regions, respectively. Typically, in enteroviruses, the 2C-coding region of the genome contains the *cis*-acting RNA element (CRE), a 61-base stem-loop structure that functions as a template for VPg uridylation. However, the CRE position varies in several human rhinoviruses; for instance, in human rhinovirus 14, CRE is located in the P1-coding part of the genome, while in

human rhinoviruses 1A, 2, and 16, CRE is in the 2A-coding region (142). The 3' UTR is about 72 nt and consists of two stem loops involved in a pseudoknot structure formation (96). The 3' UTR is terminated by a poly(A) tail with about 60 adenylate residues (234).

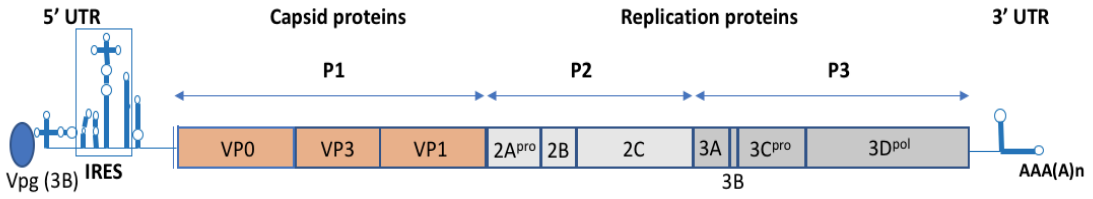

Figure 1.1 Poliovirus genome structure.

1.3.2 Viral particle structure

Enteroviruses' genome is enclosed in a naked icosahedral capsid of about 30 nm in diameter (Figure 1.2). Viral particle comprises 60 identical structural units (protomers), each consisting of one copy of viral proteins VP0, VP1, and VP3. During maturation, VP0 is autocatalytically cleaved into the VP2 and VP4, so the protomer of the mature virions consists of 60 copies of each VP1, VP2, VP3, and VP4. The C-terminal domains of VP1, VP2, and VP3 are located inside, and their N terminal parts are on the virion's surface. VP4 is entirely located internally. Five sets of the capsid proteins VP0, VP3, and VP1 assemble into a pentamer. The structure of these proteins comprises an eight-stranded antiparallel β barrel sheet. The capsid is made of 12 pentamers; each pentamer contains fivefold, threefold, and twofold axes. VP2 and VP3 surround the two and threefold axes, while the fivefold axis is surrounded by the capsid protein VP1, in which a deep depression

called “canyon” is located. The canyon is the binding site for the cell surface receptors, and its size and location differ among enteroviruses. For example, human rhinoviruses C and enterovirus D68 possess non-continuous canyons, resulting in an unusual capsid compared to other enteroviruses (11). There is an opening into a hydrophobic pocket underneath the canyon in the hydrophobic center of the capsid protein VP1, known as the “pocket factor”, which contains a combination of fatty acid-like molecules (82). However, not all enteroviruses contain the pocket factor; for instance, human rhinovirus C lacks such structure in its capsid (42, 135).

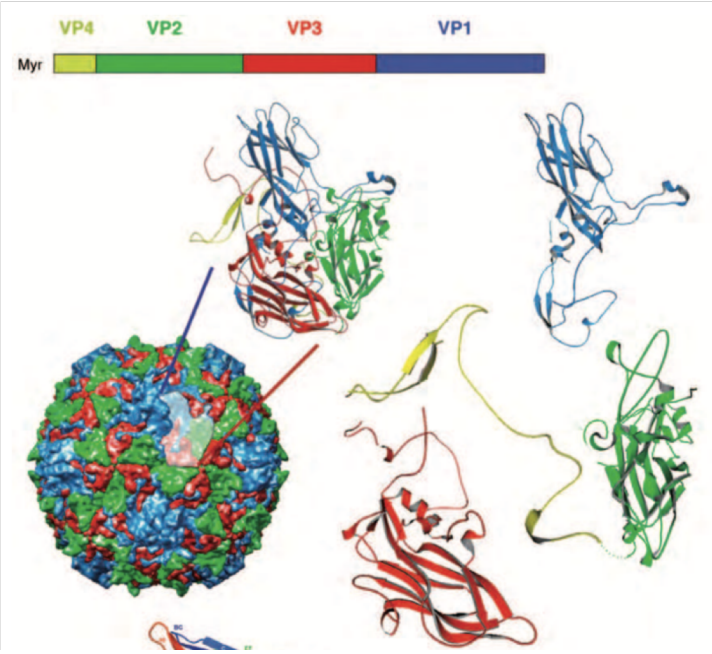

Figure 1.2 Poliovirus capsid proteins organization and structure, protomer assembly, and surface representation of the virion (109). Poliovirus structural proteins (VP1, VP2, VP3, and VP4) are located at the N-terminal domain of the viral polyprotein, modified by myristoylation (Myr). They generate a protomer with VP1-3 on the surface and VP4 hidden at the bottom. Five protomers assemble into a pentamer, 12 of which construct the icosahedral capsid structure.

1.3.3 Enterovirus life cycle

1.3.3.1 Virus attachment and entry

Enteroviruses employ various cell receptors, including the immunoglobulin (Ig)-like receptors, mucin-like domain receptors, low and very low-density lipoprotein receptors (LDLRs and VLDLRs), complement control family receptors, sialic acid, and integrins (25).

The Ig-like family receptors comprise an extracellular domain, a transmembrane domain, and a cytoplasmic domain and include poliovirus receptor (PVR), intracellular adhesion molecule-1 (ICAM-1), Coxsackie and adenovirus receptor (CAR), which are respectively used by poliovirus, major group human rhinoviruses, and Coxsackieviruses (212).

LDLRs and VLDLRs are utilized by minor group human rhinoviruses, and similar to the Ig-like receptors, they contain an extracellular, a transmembrane, and a cytoplasmic domain. Five copies of the receptor surround the fivefold axes of the viral capsid. This event enhances the avidity of the virus-receptor binding (212).

The decay-accelerating factor (DAF, also known as CD55) belongs to the complement control family of receptors, used by Coxsackie B viruses, Coxsackievirus A21, and enterovirus D70 (105, 138, 188). DAF comprises four short consensus repeats connected to the membrane by a glycosylphosphatidylinositol (GPI) anchor. The binding of DAF with the virus does not make conformational rearrangement in the capsid structure; instead, it attracts the virus to the cell surface where the second receptor triggers viral entry.

Integrins are other cell receptors used by enteroviruses, such as Coxsackievirus A9, echoviruses 1 and 9 (26, 78, 152). Integrins contain α and β subunits; each has a globular

extracellular domain, a transmembrane domain, and a cytoplasmic domain. Similar to DAF, integrins function as a co-receptor for attachment, and other receptors are required for the virus entry.

Enterovirus A71 uses two receptors, P-selectin glycoprotein ligand-1 (PSGL-1) and scavenger receptor B2 (SCARB2), for attachment and uncoating, respectively. The neurotropism of enterovirus A71 causing neurological manifestations in humans is explained by the expression of SCARB2 on neurons (98). Interestingly, receptors for enteroviruses that cause characteristics neurological clinical symptoms, such as poliovirus (CD155), Coxsackieviruses B5 and A2 (CAR), and historical enterovirus D68 (sialic acid), are expressed on the motor neurons, suggesting a direct correlation between the presence of a particular viral receptor in tissue and induction of specific clinical presentations in patients (86). However, *in vivo* studies revealed that contemporary circulating enterovirus D68 (i.e., strains collected from the outbreaks since 2014) reaches the neurons independent of sialic acid, and no receptors for these strains have been characterized yet (81).

Receptor-mediated endocytosis is the route of entry used by enteroviruses. Receptor-binding of poliovirus and many other enteroviruses triggers conformational alterations in the viral capsid such that the virions lose VP4, and most of the hydrophobic N-terminus of VP1 translocate to the particle's surface. The resulting particle is called "A" (altered) particle, which differs from the native viral particle in several characteristics, including the sedimentation value, hydrophobicity, antigenicity, stability, and the ability for receptor binding. The A particle contains the RNA genome and retains infectivity similar to the native virus. Owing to the hydrophobic feature of the A particle and the conformational modifications, the virion can interact with the membrane bilayer, leading

to the virus-membrane attachment, followed by RNA genome release into the cytoplasm (82).

1.3.2.2 Viral genome translation and polyprotein processing

After release into the cytoplasm, the positive single-strand RNA genome works as an mRNA and initiates a cap-independent translation process (Figure 1.3). Viral protein VPg is cleaved from the 5' end of the genome by a host protein 5′ tyrosyl-DNA phosphodiesterase 2 (TDP2) (220). The viral genome RNA is translated into a single polyprotein with a total molecular weight of 247 kDa in poliovirus. The polyprotein is then co- and post-translationally cleaved by the viral proteases $2A^{pro}$, $3C^{pro}$, and $3CD^{pro}$ into multiple intermediate and mature capsid and replication viral proteins (19). To compromise the limited information encoded in the small genome size, the intermediate and end cleavage products of the viral proteins have different functions during infection (232). Poliovirus structural protein precursor P1, located in the N-terminal part of the polyprotein, is separated *in cis* from the rest of the polyprotein by the activity of the viral protease $2A^{pro}$ shortly after translation. Further P1 processing occurs *in trans* by the viral protease $3CD^{pro}$ to generate VP0, VP3, and VP1 capsid proteins. During virion maturation, VP0 is autocatalytically processed into VP2 and VP4 proteins. Two scenarios have been defined for the processing of the replication proteins located in the P2P3 region. First, P2 proteins undergo rapid processing by the viral protease $3C^{pro}$ to generate the 2A, 2CB, and P3 proteins. The second way is the generation of P2 and P3 precursors, which are further processed to make multiple cleaved products. The 2BC protein is further cleaved by the viral protease $3C^{pro}$ into the 2B and 2C proteins. A rapid cleavage processing of the P3 precursor yields the viral proteins 3AB and $3CD^{pro}$, which are subsequently processed to

make the end products 3A, 3B, $3C^{pro}$, and viral RNA-dependent RNA polymerase $3D^{pol}$ (122).

Enteroviruses induce the host gene expression shutoff so that most of the cellular translation machinery is available for the viral gene expression (61). This also results in downregulation of the cellular antiviral factors expression, which contributes to the virus's evasion of the immune response. The translation initiation of cellular mRNAs is associated with the initiator tRNA, the 40S and 60S ribosomal subunits, which are assembled into an 80S ribosome by eukaryotic initiation factors (eIFs) (172). The eIF-4F cap-binding complex (containing the ATP-dependent RNA helicase eIF-4A, the eIF-4E, and the scaffolding protein eIF-4G) and the factors eIF4A and eIF4B functions in binding of 43S complexes (consisting of a 40S subunit, eIF2-GTP-Met-tRNAi complex) to the capped mRNA. To efficiently scan the ribosome for the start codon, eIF1A facilitates the assembly of 48S complex at the initiation codon. eIF5B is required for the assembly of the 48S complexes and 60S subunits (172). At the same time, the poly(A)-binding protein (PABP) attaches to the poly(A) tail of the eIF-4G-bound mRNA, bringing the 3' and 5' ends of the mRNA next to each other, which contributes to the stability of the initiation complex and enhances the efficiency of the translation (196). Enteroviruses shut down host mRNA translation machinery through the activities of the viral proteases $2A^{pro}$, which cleaves eIF-4G, and $3C^{pro}$, which cleaves eIF-5B subunit of the translation initiation complex and PABP (45, 71, 106, 181, 195).

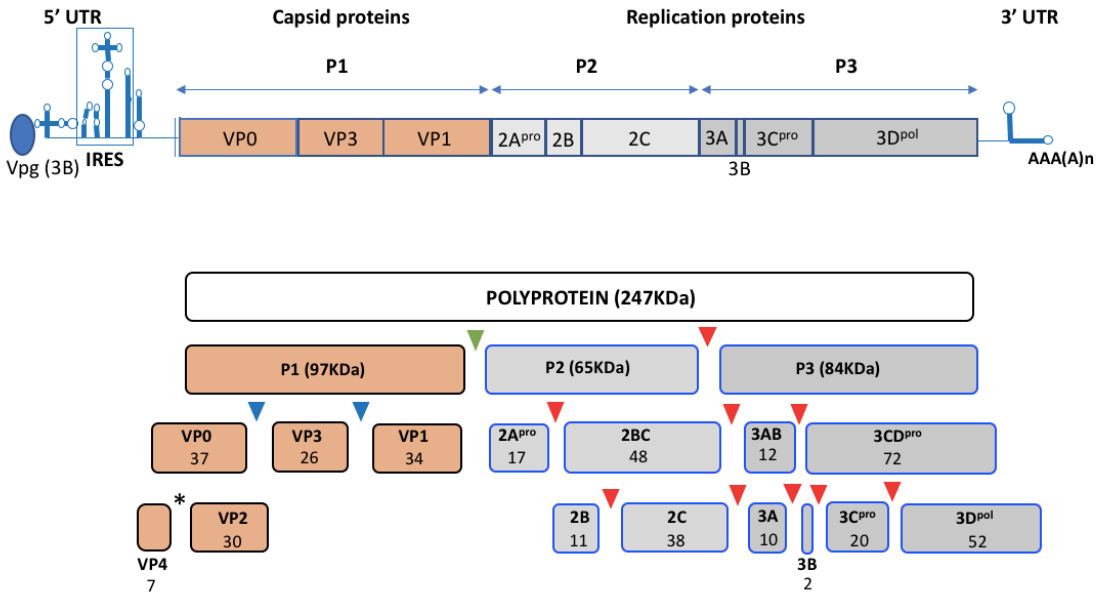

Figure 1.3 Poliovirus polyprotein processing. The molecular weights of the precursor and mature viral proteins are presented next to their names in kDa. The red triangles are the cleavage sites for the viral protease $3C^{pro}$; the green triangle shows the site cleaved by the protease $2A^{pro}$, and the blue triangles are the active sites for the protease $3CD^{pro}$. The black star indicates the autocatalytic site between the structural proteins VP2 and VP4.

Cleavage of the cellular translation initiation factors eIF-4G and PABP triggers the formation of stress granules (SGs) early in the infection cycle. SGs formation is a prompt cellular response to the environmental stress stimuli such as oxidative stress, heat shock, ultraviolet radiation, and viral infection. SGs are highly dynamic cytoplasmic aggregations containing translation initiation factors, 40S ribosomal subunits, mRNAs, and many RNA-binding proteins, such as Ras GTPase-activating protein-binding proteins (G3BP1/2), T-cell intracellular antigen 1 (TIA-1), and TIA-related protein (TIAR). These proteins play critical roles in SGs formation ad are used as the markers to recognize the SGs in the cell. Entrapping translation initiation factors, SGs temporarily stall the translation until the stress stimulus is terminated (239). However, as the infection progresses, enteroviruses

countermeasure SGs development so that the translation of the viral RNAs is minimally affected. At 4 hpi, SGs are reduced in quantity and size until they disappear by the end of the viral infectious cycle. Viral protease $3C^{pro}$ critically functions in SGs disappearance by cleaving one of the main SGs-resident proteins, G3BP1, resulting in the disassembly of the SGs (55, 239).

1.3.2.3 Viral genome replication

Viral genome replication is associated with unique membranous structures called the replication organelles (ROs), whose composition is important for the functioning of the viral replication complexes (Figure 1.4) (21). The positive single-strand RNA genome is used as a template for negative-strand RNA synthesis. Viral protein VPg serves as a primer for the synthesis of both negative and positive strands, but first, it needs to be activated. The activation requires the CRE, where the viral RNA polymerase $3D^{pol}$ uridylates VPg, generating VPg-pU-pU. Both 3' and 5' non-coding regions of the genome play crucial roles during genome replication. At the 5' end, the cloverleaf binds a host cell protein poly(rC) binding protein (PCBP), which leads to the binding of the RNA polymerase to the other side of the cloverleaf. Subsequently, the RNA polymerase $3D^{pol}$ uses VPg-pUpU as a primer to generate the complementary negative-strand RNA. During this step, a long double-stranded RNA (dsRNA) is made (replication form), which consists of one positive- and one negative-strand RNA and can be recognized by the host cell sensors such as MDA-5 (55). The next step is the synthesis of the positive-strand RNA genome from the negative-strand RNA template. During this step, a replicative intermedia) is formed, containing a full-length negative-strand RNA and multiple nascent positive-strand RNA molecules

undergoing active transcription (55). The newly generated positive-strand RNA genome molecules can enter the translation/replication pool or be encapsidated (170, 200).

1.3.2.4 Virion formation and release

P1 is the single precursor polyprotein for the viral capsid proteins VP1, VP2, VP3, and VP4. P1 is initially cleaved by the viral protease $3CD^{pro}$ into VP0, VP1, and VP3, which assemble in a protomer. Five protomers form a pentamer, twelve of which make a procapsid (an empty capsid) that comprises 60 copies of VP0, VP1, and VP3. The nascent viral genome RNAs are then packaged into these premade capsid protein shells, which are now called non-infectious provirions. During virion maturation (i.e., acquiring the RNA genome), the viral protein VP0 is autocatalytically cleaved into VP2 and VP4 capsid proteins. VP0 cleavage is dependent on RNA encapsidation and associated with a conserved histidine residue (2195H) in the close vicinity of the cleavage site (12, 80). 2195H activates local water molecules adjacent to the cleavage site, leading to a nucleophilic attack of the VP0 scissile bond. The scissile bond polarization escalates this event via the coordination of the carbonyl oxygens with RNA bases (80). Thus, the infectious particles contain a viral genome surrounded by 60 identical copies of the surface capsid proteins VP1, VP2, and VP3 and the internal capsid protein VP4 (177, 236). Empty capsids (without the RNA genome) are less stable than the mature virions (with the RNA genome) in different conditions, suggesting that VP0 cleavage into VP2 and VP4 is an indispensable event for generating stable viral particles (12).

Depending on the virus and the infected cell type, enterovirus particles egress from the cell by lytic or non-lytic pathways. Lytic release of the virions happens upon the cell death triggered by either a canonical cytopathic effect (CPE) or an apoptotic response. CPE

is manifested as extreme modifications in the morphology and location of intracellular structures, such as aggregation of membranous vesicles, nucleus shrinkage and displacement, elevated plasma membrane permeability and rounding up the cells, the specificity of biochemical events and cellular pathways involved in the development of enterovirus-induced CPE is still debated (20, 164). Apoptosis is a cell death program activated upon different stimuli, including viral infections, which is characterized by the activation of specific proteases, caspases. During enterovirus infection, the apoptotic response is activated early in the infection, while later in infection, the viral protease-mediated degradation of cellular factors required for the implementation of the apoptotic program prevents its further development. The balance of pro- and anti-apoptotic stimuli may be different upon enterovirus replication in different cell types (1, 2). The recently proposed non-lytic egress of viral particles is associated with the double-membrane vesicles. These double–membrane vesicles formed during enterovirus infection resemble autophagosomes, but their generation does not require at least some canonical autophagy factors (44, 49). The autophagosome-lysosome fusion is interrupted by enteroviruses, and autophagosomes are redirected to the autophagosome-mediated exit without lysis (AWOL), in which the vesicles containing virions fuse to the plasma membrane and egress from the cell (117). Poliovirus, Coxsackievirus B3, enterovirus A71, echovirus 7, and several human rhinoviruses induce autophagy and use this non-lytic pathway to release virions (164).

The other non-lytic viral exit pathway is through the exosomes, which are vesicles released from multi-vesicular bodies fused to the plasma membrane. Enterovirus A71 employs this type of viral exit under some circumstances. For example, the exosome-

entrapped virus was identified in the blood of the patients with viral encephalitis, whereas free viruses were detected in the feces samples of these patients (73). Such a pattern of viral egress is similar to that used by hepatitis A virus (HAV), a picornavirus that belongs to the genus *hepatovirus*. Entrapping in exosomes in the bloodstream protects the virus from being recognized by the antibodies (73, 164).

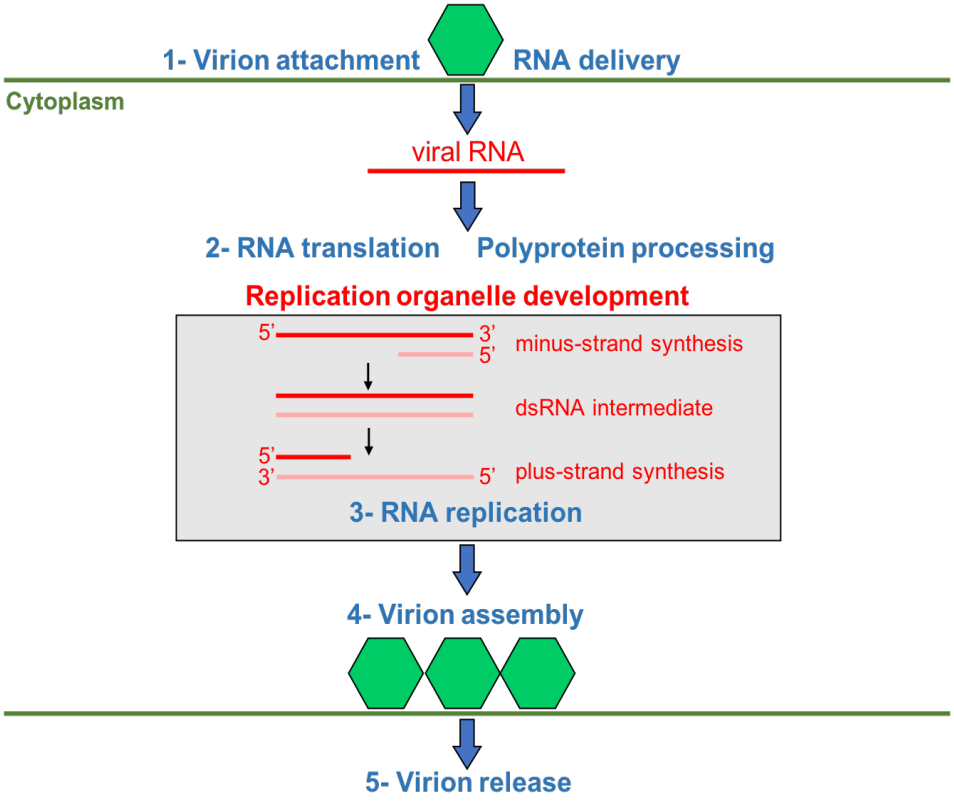

Figure 1.4 Schematic description of the enterovirus life cycle. The virus interacts with specific receptors on the cell surface and is internalized into the cell (1). Upon entering into the host cell, the viral RNA genome is released into the cytoplasm. The positive-strand RNA is translated into a polyprotein, which is co and post-translationally cleaved by viral proteases (2). In the replication organelles, the genome RNA replicates to generate negative-strand RNAs, which in turn, synthesize more positive-strand RNAs (3). The newly-made positive-strand RNAs either enter another round of translation/replication process or are encapsidated into the provirus to make the mature virions (4), which are then released from the cell (5).

Chapter 2: Rewiring the Host Cell Membrane Metabolism During Enterovirus Infection

2.1 Induction of cell membrane remodeling to develop the viral replication organelles

Enterovirus genome replication is associated with the specialized membranous structures, replication organelles (ROs) which may be beneficial for the virus by: (i) increasing the local concentration of viral and host factors required for genome replication, (ii) providing a structural scaffold and facilitating proper assembly of the replication complexes, and (iii) protecting viral replication sites from being detected and destroyed by the cellular antiviral defense mechanisms (21). The structure and composition of ROs are changing during different stages of infection. Ultrastructural analysis of the replication organelles revealed that they are formed as single-walled tubular membranous structures at the early stage nearby the Golgi compartment. As the infection progresses, they transform into double-membrane vesicles located in the perinuclear areas (19).

2.2 Host cell modifications to develop the replication organelles

Enteroviral nonstructural proteins induce the development of the ROs; however, the detailed cascade of interactions of the viral and cellular factors leading to the development of these membranous structures is not understood. The emerging picture shows that the development of the ROs includes two relatively separate components: (1) the recruitment of factors that impart a favorable biochemical environment for genome replication and (2) the activation of the phospholipid synthesis required for the expansion of their structures (205).

2.2.1 Cellular secretory pathway and enterovirus replication organelles

2.2.1.1 Overview

The secretory pathway functions in transporting, modifying, and controlling the quality of the proteins synthesized by ribosomes associated with the rough endoplasmic reticulum (RER). This pathway comprises the RER, ER-Golgi intermediate compartments (ERGIC), the Golgi complex, endosomes, and the plasma membrane (202). Proteins are carried between these compartments by specialized vesicles containing organelle-specific protein coats and targeting factors ensuring precise delivery of the cargo. Coated vesicle membrane II (COPII) and coated vesicle membrane I (COPI) mediate the anterograde protein transport from the ER to ERGIC and the *cis*-Golgi, and the retrograde protein transport back to the RER and within the Golgi complex (from *trans*-Golgi network to *cis*-Golgi network), respectively (Figure 2.1) (198).

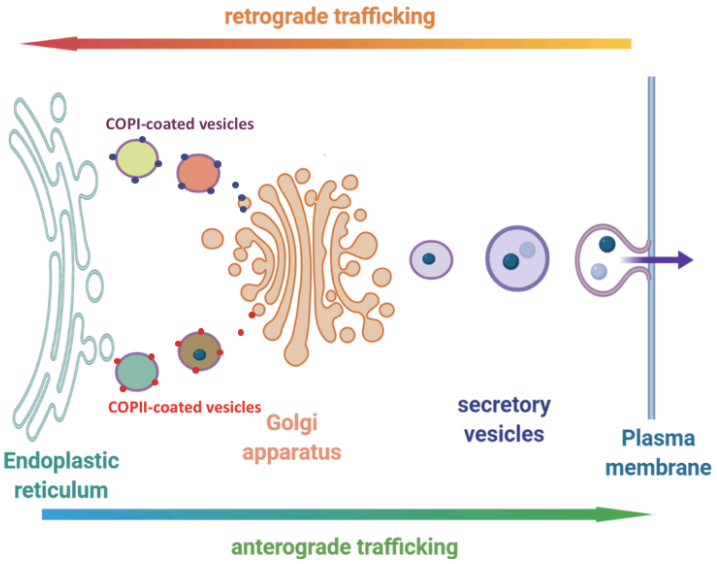

Figure 2.1 Scheme of cellular protein secretory pathway. The pathway comprises multiple compartments including RER, Golgi cisternae, endosomes, and plasma membrane. Nascent proteins synthesized in the RER are transported via COPII-coated vesicles (small red circles) to the ERGIC and *cis*-Golgi during anterograde trafficking. They are either secreted from the cell to the extracellular environment or function in the intracellular metabolic pathways. During retrograde trafficking, the misfolded proteins and ER-resident proteins are sent back to the RER via COPI-coated vesicles (small purple circles).

The enterovirus ROs are detectable as early as 2 hours post-infection (hpi) adjacent to the *cis*-Golgi and the ERGIC, the two main structures of the cellular secretory pathway (19). Furthermore, viral replication structures are strongly associated with the Golgi marker, GM130, at the early stage of infection, meaning a close relationship between the establishment of viral replication complexes and the Golgi membranes, probably because the Golgi contains some specific factors required for virus infection. Additionally, enterovirus replication is highly sensitive to a fungal metabolite named brefeldin A (BFA), which has an inhibitory effect on the secretory traffic (19). Altogether, it implies that the

virus replication depends on at least some elements of the secretory pathway, particularly those found in the Golgi apparatus.

2.2.1.2 Arf GTPases in the secretory traffic

The formation of COPI-coated vesicles requires Arf-GTPases which recruit COPI coatomer from the cytoplasm. The family of Arf-GTPases is divided into three classes based on structural homology. In primate cells, class I comprises Arf1 and Arf3, class II has Arf4 and Arf5, and class III contains the most structurally diverse Arf6. Similar to other GTPases, Arfs exist in activated membrane-bound Arf-GTP and inactive cytosolic Arf-GDP forms. Arf activation requires Arf guanine nucleotide exchange factors (Arf-GEFs), and the GTP hydrolysis is facilitated by Arf-GTPase activating proteins (Arf-GAPs) (Figure 2.2) (50). Activation of different Arf isoforms is subject to tight spatial and temporal regulation. The activated Arfs regulate multiple steps of the cellular membrane metabolism by interacting with various effector proteins (69, 94). They attract effector proteins involved in the lipid synthesis, modification, and transport, including phosphatidyl kinases, which can modify the local membrane protein and phospholipid environment, differentiating the Arf-enriched domains from the surrounding membranes (93).

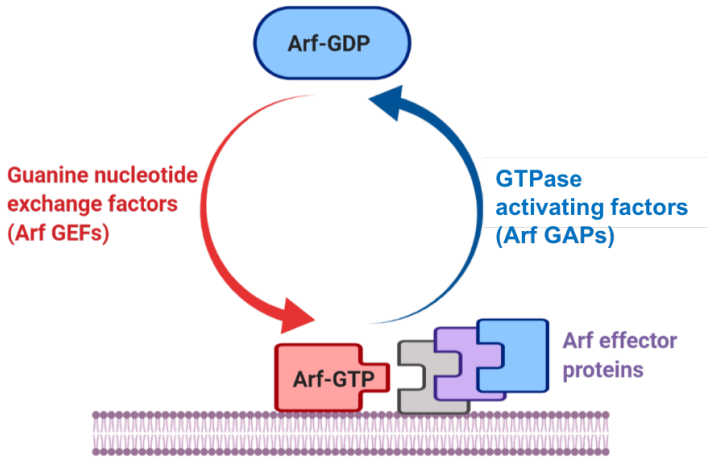

Figure 2.2 Scheme of the Arf GTPases activation cycle.

2.2.1.3 GBF1 in the secretory traffic

Various Arf-GEFs differ in cellular localization, functions, and interactions. They are categorized into six families based on domain organization and sequence homology: GBF1, BFA-inhibited GEFs (BIGs), Arf nucleotide-binding site opener (ARNO)/Cytohesins, exchange factor for Arf6 (EFA6/PSD), BFA-resistant Arf-GEF (BRAG/IQSecs), and F-box only protein 8 (FBX8) (34). Among them, GBF1 and BIG1/2 are high-molecular-weight (~200 KD), BFA-sensitive GEFs playing key functions in the secretory and endosomal trafficking (231). GBF1 typically resides in the *cis*-Golgi and mediates the Arf-GTPase activation required for the vesicle trafficking in the secretory pathway (203). It is a large protein with multiple domains, including N-terminal dimerization and cyclophilin binding domain (DCB) and homology upstream of Sec7 domain (HUS) and C-terminal homology downstream of the Sec7 domains 1, 2, and 3 (HDS1, 2, and 3), which are essential for the GBF1 membrane association. The centrally-located Sec7 domain (Sec7d) of GBF1 catalyzes GDP to GTP exchange to activate Arfs

(Figure 2.3) (22, 30). The secretory traffic inhibitor, BFA, interacts with the Sec7d of GBF1 in the junction with Arf-GDP and stabilizes the transient GBF1-Sec7-Arf-GDP complex on the membranes, thus inhibiting its catalytic activity. Introducing point mutations in the Sec7d or replacing GBF1-Sec7d with that of another Arf-GEF ARNO could rescue GBF1 from the inhibitory effect of BFA in the cell (174).

Figure 2.3 Schematic depiction of GBF1's multiple domains. GBF1 is a large protein and contains six conserved domains, including DCB1 and HUS1 in the N terminal end, the centrally-located Sec7 domain and HDS1, HDS2, and HDS3 in the C terminal end.

2.2.1.4 GBF1 during enterovirus infection

GBF1 is recruited to the enterovirus replication sites through interaction with the viral protein 3A (15). However, while GBF1 activity is essential for viral replication, the 3A-GBF1 interaction may not be a limiting factor, at least in certain cell types, since viruses with a mutation in 3A significantly reducing GBF1-3A binding can still grow efficiently in the cell culture (217). The N terminus of GBF1, including the Sec7d, is essential for viral replication, while the C-terminal part downstream of Sec7d is dispensable for replication of wild-type poliovirus. However, the defective GBF1-3A binding mutant virus requires the whole C-terminal domains of GBF1 to replicate properly (17, 217). The enterovirus replication in the presence of BFA can be rescued upon expression of GBF1 species with BFA-insensitive Sec7ds, but not with those with catalytically inactive Sec7ds,

indicating that Arf activating function of GBF1 is essential for enterovirus replication (16). However, the catalytic activity of GBF1 in Arf activation may not be the sole contribution of GBF1 to the virus replication since some level of the rescue of poliovirus replicon replication was observed upon the expression of certain catalytically inactive GBF1 mutants (217).

2.2.1.5 Arf GTPases during enterovirus infection

While the Arf-GEF function of GBF1 is essential for the enterovirus replication, the contribution of GBF1-activated Arfs to the replication process is not understood. siRNA interference experiments suggested important roles of the class I Arfs (Arf1 and Arf3) in enterovirus 71 replication. Yet, Arf3 depletion was noticeably toxic to cells, which can at least partially explain the only report of a significant decrease in an enterovirus replication after the simultaneous depletion of Arf1 and Arf3 (223). The inhibition of enterovirus infection by compounds blocking the Arf-GEF activity of GBF1, such as BFA, could be relieved only by overexpression of GBF1 itself but not by any individual wild-type Arfs or the constitutively active Arf mutants (16, 120). Moreover, the depletion or knockdown of expression of individual Arfs, or pairs thereof, was tolerated by diverse enteroviruses remarkably well, suggesting a higher level of Arf redundancy in the viral replication than in the cellular metabolism (56).

2.2.2 Cellular lipid metabolism pathway and enterovirus replication organelles

2.2.2.1 Overview

Lipids are essential building blocks of cellular life performing different functions: (i) structural lipids, including phospholipids (PLs) such as phosphatidylcholine,

phosphatidylserine, and phosphatidylethanolamine, sphingolipids (SLs), and cholesterol, which form the intracellular and plasma membranes, (ii) signaling lipids, including fatty acids (FAs), sterols, phosphatidic acid (PA), and phosphatidylinositides, , and (iii) storage lipids, such as triacylglycerol (TAG) and sterol esters, which mostly accumulate in the lipid droplets (LDs) and provide energy for the cell and building blocks for new lipid synthesis (242).

2.2.2.2 Phospholipid synthesis enhancement

During enterovirus infection, the overall cellular phospholipid synthesis is up-regulated, supporting the structural development of the membranous scaffold of the ROs (13). The phosphatidylcholine (PC) synthesis, which is the major constituent of the structural lipids in eukaryotic cells, is significantly increased during virus infection (241). The underlying mechanism includes activating the long-chain Acyl-CoA synthetase enzymes (ACSLs) and releasing the CTP: phosphocholine cytidylyltransferase from the nuclear depot. This two-step reorganization of the cellular lipid synthesizing machinery results in retargeting the long-chain fatty acid flux from the neutral lipid to phospholipid synthesis. ACSL3, in particular, has an essential role in FA metabolism during poliovirus infection as the virus replication is impaired in the cells with knocked down expression of ACSL3. Poliovirus protein 2A was shown to stimulate ACSL function (14, 151).

2.2.2.3 Cholesterol and phosphatidylinositol 4-phosphate enrichment of the replication organelles

Enterovirus infection significantly modifies the cholesterol landscape in the cell. Under normal conditions, cholesterol is internalized from the plasma membrane and

extracellular environment to the cell in the form of low-density lipoprotein (LDL) through CME. Endosomes containing LDL later fuse to the lysosomes, leading to LDL degradation and accumulation of free cholesterol. Cells maintain cholesterol homeostasis by balancing between its uptake, synthesis, distribution in the ER, storage of the esterified form in the lipid droplets (LDs), and recycling back to the plasma membrane.

During enterovirus infection, cholesterol regulates proteolysis of the viral precursor $3CD^{pro}$ into $3C^{pro}$ and $3D^{pol}$ in the replication complexes and facilitates viral RNA synthesis (91). Enteroviruses redistribute cholesterol pools from the plasma membrane, ER, endosomes, LDs, and extracellular medium to the replication complexes through harnessing different routes, including CME and recycling endosomes (91, 184). Various enteroviruses exploit different cholesterol sources in the cell. 2BC protein of poliovirus and Coxsackievirus B3 enhances cholesterol uptake and internalization from the plasma membrane and extracellular medium through CME early infection. The internalized cholesterol pools distribute into the ER and recycling endosomes. Another viral membrane-targeting protein, 3A, recruits recycling endosomes containing Rab11 into the replication membranes, resulting in additional cholesterol accumulation in these sites. Human rhinovirus A16, re-routes cholesterol stored in the LDs to the replication membranes (13).

The transfer of cholesterol from the cellular depots to the membranes of ROs relies on the PI4P-cholesterol exchange cycle mediated by the cellular proteins OSBP and PI kinases beta. OSBP is a multidomain protein with a C-terminal OSBP-related ligand-binding domain (ORD), an N-terminal pleckstrin homology (PH) domain, and a centrally-located two phenylalanine residues in an acidic tract (FFAT) domain. In uninfected cells, OSBP interacts with the Golgi-resided PI4P and the ER vesicle-associated membrane

proteins (VAPs) through its PH domain and FFAT region, respectively, forming a contact site between the ER and PI4P-enriched *trans*-Golgi membranes (159). The ORD domain of OSBP transfers cholesterol from the ER to the Golgi membranes, followed by reverse transfer of PI4P, which is enriched on the Golgi membranes to the ER. The hydrolysis of PI4P at the ER by phosphatase Sac1 maintains the PI4P gradient providing the energy for the PI4P-cholesterol exchange process (145, 146).

PI4P synthesis is mediated by phosphatidylinositol kinases 4 (PI4Ks) (48). Four PI4Ks were identified in mammalian cells, divided into type II (PI4KIIα and PI4KIIβ) and type III (PI4KIIIα and PI4KIIIβ) groups with distinct localizations and functions in the cell. Among all PI4Ks, PI4KIIIβ is shown to be recruited to the ROs during enterovirus infection. In uninfected cells, the recruitment of PI4KIIIβ to the Golgi is mediated by interaction with GBF1-activated Arfs and/or another protein ACBD3 (also known as 60-kDa Golgi complex-associated protein, GCP60) is a multifunctional protein containing an N-terminal acyl-coenzyme A binding (ACB) domain, a coiled-coil (CAR) domain, a glutamine-rich domain (Q-rich), and a C-terminal Golgi dynamics (GOLD) domain. ACBD3 is located in the Golgi membranes through the interaction of its GOLD domain with the C-terminal cytoplasmic domain of a Golgi-resident protein, giantin, which functions in Golgi structure maintenance and protein trafficking between the ER and Golgi (43, 72, 194). The major mechanism employed by enteroviruses for hijacking PI4KIIIβ is the direct interaction of the viral protein 3A with ACBD3, which results in the redistribution of PI4KIIIβ to the ROs (48). 3A protein of several enteroviruses, including poliovirus, Coxsackieviruses, enterovirus A71 and D68, and human rhinoviruses A2, A16, and B14 bind ACBD3 through its GOLD domain (136). Knockdown and knockout studies

revealed an essential function of ACBD3 in supporting enterovirus infection (204). In addition, co-immunoprecipitation studies showed a PI4KIIIβ-viral protein 2BC binding, suggesting that a portion of PI4KIIIβ is potentially recruited to the poliovirus replication organelles through direct interaction with the viral protein 2BC (13). It is also possible that GBF1/Arf1-GTPase pathway facilitates PI4KIIIβ recruitment to the enterovirus replication organelles since GBF1 is also recruited to the ROs through interaction with viral protein 3A, although this mechanism has not been experimentally demonstrated in infected cells. In addition, some *in vitro* studies revealed a direct interaction between activated Arf1 and viral protein 2BC on the replication membranes, similarly resulting in PI4KIIIβ accumulation in these regions (13).

The 3A-ACBD3-mediated recruitment of PI4KIIIβ on the ROs generates a high local concentration of PI4P and drives the OSBP-mediated enrichment of the replication membranes in cholesterol (91, 137). In addition to being associated with the cholesterol transport to the ROs, PI4P is able to bind a variety of host cell proteins containing a PH domain and recruit them to the replication complexes, likely contributing to the establishment of a membrane microenvironment required for the functioning of the viral replication complexes. Viral polymerase $3D^{pol}$ was shown to interact with PI4P in vitro, which may promote its recruitment to the replication sites (84).

2.2.2.4 Lipid droplets (LDs) engagement during enterovirus infection

LDs are highly dynamic cellular organelles functioning as lipid storage which can be rapidly mobilized or replenished depending on the cell's metabolic needs and environmental stimuli (160). They consist of a core of neutral lipids such as TAG and cholesterol esters surrounded by a phospholipid monolayer decorated by proteins

associated with lipid metabolisms. LDs are distributed throughout the cytoplasm in uninfected cells and often maintain direct contact with the ER membranes (27, 160). In enterovirus-infected cells, LDs are mostly detected in the close vicinity of the perinuclear ROs. During the time course of infection, the size and the quantity of LDs decrease, consistent with the activation of hydrolysis of neutral lipids and the retargeting of long-chain FAs for the increased PLs synthesis level during enterovirus infection (121, 219). Shuttling FAs from LDs to the replication complexes is facilitated in two ways. One is through the interaction of viral protein 2C located in the replication sites with its counterparts (other 2C protein pools) on the surface of LDs that triggers the formation of membrane contact site between these two organelles, inducing FAs flux from LDs to the replication compartments. The other way is through a direct interaction of the viral proteins 3A and 3AB, which reside in the ROs, with LD-associated lipases, including adipocyte triglyceride lipases (ATGL) and hormone-sensitive lipase (HSL), resulting in the recruitment of the cell's lipolysis machinery into the membrane contact sites, where FAs are released from the LDs by TAG lysis (121). LDs serve as the source of cholesterol for the ROs of several human rhinoviruses (23). Still, the details of LDs' engagement upon enterovirus infection are understood very cursory.

2.3 Projects Goals

Recruitment of GBF1 to the replication complexes through interaction with the viral membrane-targeted protein 3A has been reported for PV, CVB3, and EV71. Accordingly, the GBF1-directed enrichment of ROs in Arf1 has been documented. However, whether other Arfs are recruited to the ROs, and what Arf isoform(s) is actually

required to support the viral replication, as well as their mechanistic roles in the replication process, are not understood. In the first part of this project, I investigated the activation dynamics of all human Arf isoforms upon enterovirus infection and identified Arf isoforms important to support poliovirus replication.

Virtually all stages of the enterovirus replication cycle in a cell are associated with the replication organelles. While their morphological development has been extensively documented since the early days of electron microscopy, the landscape of the host and viral proteins on the membranes of the ROs and their functional associations are understood only superficially. In the second part of this project, we used a proximity biotinylation approach coupled with mass spectrometry to identify proteins localized on the replication organelles in the vicinity of GBF1.

Chapter 3: Materials and Methods

3.1 Plasmids

Retroviral vector pLNCX2 containing cytomegalovirus (CMV) promoter ahead of the multiple cloning site (MCS) and geneticin antibiotic selection properties was purchased from Takara, Bio, USA (Cat No. 631503). Plasmids pArf1-GFP, pArf3-GFP, pArf4-GFP, pArf5-GFP, and pArf6-GFP were gifts from Catherine Jackson (Université Paris Diderot-Paris). Retroviral vectors expressing individual Arf-GFP were generated by inserting each Arf-GFP fragment into the *XhoI* and *NotI* restriction sites of the pLNCX2 vector. For constructing the pLNCX2-Arf1-FRP, expressing Arf1 fused to a monomeric red fluorescent protein, FusionRed (190), an Arf1-FRP fragment maintaining the same linkers as the Arf1-GFP construct was synthesized by GeneArt (Thermo Fisher). The Arf1-FRP fragment was inserted into the pLNCX2 vector in the *XhoI* and *NotI* restriction sites for the cloning. For the construction of the pLNCX2-FLAG-APEX2-GARG-1060, which is a truncated GBF1 after HDS1 domain with Sec7d from ARNO fused with FLAG-APEX2 optimized by GeneArt service for human expression, a two-step cloning was performed. First, the plasmids GeneArt FAPEXGAG_1Xho-ApaII and GeneArt FAPEXGAG_2ApaII-NotI were respectively cut by the pair of restriction enzymes *Xho-ApaII* and *ApaII-NotI*, followed by inserting to the pCI vector to generate pCI-FAPEXGAG_Xho-NotI. For cloning into the retroviral vector, the FAPEXGAG_Xho-NotI fragment was excised with the restriction enzymes *Xho* and *NotI* and inserted into the previously linearized pLNCX2 with the same enzymes. Plasmid pXpA-RenR, coding for

a poliovirus or Coxsackievirus 3 replicons with the capsid P1 region replaced by the *Renilla* luciferase gene, was described elsewhere (15).

3.2 Cells

HeLa and RD cells were cultured in high-glucose Dulbecco's modified Eagle's medium (DMEM) supplemented with 10 mM sodium pyruvate, 2 mM L-glutamine, and 10% fetal bovine serum (FBS). Retrovirus packaging cell line GP2-293 (Takara) was maintained in DMEM supplemented with 10% FBS and nonessential amino acids.

3.3 Generation of stable cell lines using a retroviral gene transduction system

Retroviral virions were generated by transfecting the packaging cell line GP2-293 according to the manufacturer's directions. Briefly, GP2-293 cells seeded into a 6-well plate were co-transfected with pLNCX2 vectors expressing either Arf fusions or FLAG-APEX2-GARG-1060, and the plasmid coding the vesicular stomatitis virus (VSV) envelope glycoprotein. Eighteen hours after transfection, the medium was replaced with a fresh complete growth medium, and cells were kept in the incubator overnight. The infectious virions were collected in the culture supernatant 48 h after the start of transfection. HeLa cells seeded into a 6-well plate were transduced with the freshly harvested supernatant supplemented with 10 μg/ml Polybrene (Sigma-Aldrich, Cat No. TR1003). The plate was centrifuged at 1,200 X *g* for 1 h at 32°C and then incubated at 37°C for 18 h. The next day, the medium was replaced with a fresh complete growth medium, and cells were kept in the incubator overnight. Forty-eight hours after the start of transduction, cells were transferred into a T-25 flask, and the drug-resistant colonies were selected with 300 μg/ml G418 (VWR Life Science, Cat No. 97064-358) for 10 days. The

resistant colonies were pooled, and the stable cell lines were maintained in the complete growth medium supplemented with 300 μg/ml G418.

Cells co-expressing green and red Arf fusions were generated similarly, but the original HeLa culture was transduced by a mixture of retroviral vectors coding for the corresponding ARF fusions and after the G418 selection, the double-positive cells were sorted using BD FACSAria II cell sorter. This method generated cultures with 10% to 20% of cells co-expressing both green and red Arf fusions.

After a two-week course of antibiotic selection of the stable cells expressing APEX2-GBF1, approximately 60% of the cells showed the expression of the transgene indicated by FLAG staining. So, a clonal selection of the transduced cells was performed to generate pLNCX2- FLAG-APEX2-GARG-1060 expressing cells with a uniformly high level of transgene expression. Shortly, the stable cells were cultured in three 96-well plates; each contained about 30 cells so that a single cell, whether expressing the transgene or not, was plated into a separate well. Since the growth medium contains the selection antibiotic G418, only cells expressing the transgene could grow and make colonies. After expanding one of the selected clones for about three weeks, we obtained a culture with more than 90% of cells showing strong APEX2-GBF1 expression. This stable cell line was used for the rest of our study.

3.4 Virus strains and propagation

Poliovirus type I Mahoney, poliovirus type I with FLAG-Y insert in the 3A protein (206), Coxsackievirus B3 Nancy, and encephalomyocarditis virus E9 variant with a shortened poly(C) tract (76) were propagated in HeLa cells, and their titers were determined by plaque assays or TCID50. For infection, HeLa cells were seeded in either

12-well plates (with or without a coverslip depending on the future analysis) or 8-well -μ slides (Ibidi, Cat No. 80841) with a glass bottom or T225 flasks. For adsorption, the cells were incubated with the required amount of the virus re-suspended in DMEM for 30 min at room temperature and then at 37°C in DMEM with 10% FBS for the indicated times post-infection.

3.5 Chemicals and reagents

DharmaFECT1 transfection reagent was purchased from Horizon (Cat No. T-2001-02). Brefeldin A was purchased from Sigma-Aldrich. EnduRen cell-permeable substrate for *Renilla* luciferase was from Promega. DNA and RNA transfection reagents *Trans*-IT 2020 and *Trans*-IT mRNA/mRNA Boost were from Mirus. Opti-MEM Reduced-Serum Medium was from Gibco (Cat No. 31-985-062). Polybrene was from Sigma-Aldrich (Cat No. TR-1003). The cell viability luciferase-based assay kit was from Promega (Cat No. G7570). The XTT (2,3-Bis-(2-Methoxy-4-Nitro-5-Sulfophenyl)-2*H*-Tetrazolium-5-Carboxanilide) cell growth kit was from Invitrogen (Cat No. X6493).

3.6 Antibodies

Anti-poliovirus mouse monoclonal anti-2B, -2C, and -3A, rabbit polyclonal anti-3D antibodies, and human monoclonal antibody A12, recognizing a conformational epitope present only in mature poliovirus capsids were described elsewhere (17, 38, 167). Rabbit polyclonal anti-FLAG antibody was from Invitrogen (Ref No. PA1-984B). Mouse monoclonal anti-GM130 and anti-ERGIC53 antibodies were from BD Bioscience and Santa Cruz, respectively. Rabbit polyclonal anti-GFP antibodies were from Abcam. Wheat germ agglutinin, Streptavidin Alexa Fluor 594 conjugate, and secondary antibody

conjugated with Alexa fluorescent dyes (568, 488, and 594) were from Molecular Probes (Thermo Fisher). Streptavidin-horseradish peroxidase conjugate (streptavidin HRP) was purchased from Sigma-Millipore (Cat No. RPN1231). Antibodies against lactate dehydrogenase A (LDHA) (Cat No. C4B5) and pyruvate kinase (PKM) (Cat No. C103A3) were from Cell Signaling. Antibodies against aldolase A (ALDOA) (Lot No. C105938), heterogeneous nuclear ribonucleoprotein U (HNRNPU) (Lot No. A119002), RNA-binding protein EWS (EWSR1) (Lot No. R88077), and Interleukin enhancer-binding factor3-90 (Lot No. HPA001897) were from Sigma. Antibodies against LDHB (Cat No. NBP2-53421SS), EWSR1 (Cat No. NBP1-92686SS), and HNRNPA0 (Cat No. NBP1-57275) were from Novus Biological. Antibody against G3BP1 was from Cell Signaling (Cat No. 61559T). Hoechst was purchased from Thermos Fisher (Cat No. 33342). The anti-OSBP antibody was from ProteinTech (Cat No. 11096-1-AP). Antibodies against PI4KIIIβ (Cat No. 06-578) and ACBD3 (Cat No. SAB1405255) were from Millipore Sigma.

3.7 Plaque assay

RD cells were seeded into a 6-well plate and incubated at 37°C. The next day, a ten-fold serial dilution was prepared from the viral stock to be tittered in the serum-free DMEM. Viral absorption was performed by adding 400 µl of each dilution to the RD monolayer, and the plate was incubated on a shaker at room temperature for 30 min. In the meantime, the agarose cover was prepared by dissolving 500 mg agarose powder in 75 ml distilled water, followed by adding 20 ml 5X DMEM, 6 ml FBS and 2 ml penicillin-streptomycin. After aspirating the absorption medium, 4 ml of the prepared overlay solution was added to each well, and the plate was kept at room temperature till the overlay solidified. The plate was incubated at 37°C for 48 h, subsequently stained with crystal

violet, and the viral titer was calculated based on the number of plaques that appeared in specific dilutions.

3.8 Tissue culture infectious dose (TCID50) assay

HeLa or RD cells were seeded into a 96-well plate and kept at a 37°C incubator overnight. The next day, a 10-fold serial dilution was made from the viral stock in a serum-free DMEM, starting from -1 to -10. The last two columns of the plate were left uninfected as the control. 20 µl of each dilution was transferred into each well using a multichannel pipette, and the plate was incubated on the shaker at room temperature for 30 min absorption. Next, 80 µl of DMEM supplemented with 2% FBS and 1% antibiotic was added to each well to reach the final volume of 100 µl per well. The plate was incubated at 37°C for 72- 120 h, followed by staining with crystal violet. The viral titers (TCID50/ml) were calculated using Kärber's formula (104).

3.9 DNA transfection

HeLa cells were seeded into a 6 or 12-well plate, depending on the experiment's purpose, and transfected according to the manufacturer's direction. Shortly, for a 6-well plate, the transfection mix for each well was made by adding 250 µL Opti-MEM Reduced-Serum Medium, 2.5 µg DNA plasmid, and 7.5 µL *Trans*-IT-2020 Reagent and keeping at room temperature for 20 min. The monolayer was then transfected with the mixture, and the cells were incubated at 37°C overnight. The next day, transfected cells were either infected with the virus, fixed with paraformaldehyde 4%, or collected in the lysis buffer for blotting.

3.10 RNA transfection

HeLa cells were seeded into a 6 or 12-well plate, depending on the experiment's purpose, and transfected according to the manufacturer's direction. In brief, for a 6-well plate, the transfection mix was prepared for each well by adding 250 µL Opti-MEM Reduced-Serum Medium, 2.5 µg RNA stock, and 5 µL of each *Trans*-IT mRNA and mRNA Boost Reagent and keeping at room temperature for 5 min. The complex was then added to the monolayer medium, and the cells were kept either in the incubator at 37°C overnight or in a plate reader in the presence of the EnduRen cell-permeable substrate for poliovirus replicon replication assay.

3.11 siRNA nucleotide sequences and transfection

Scrambled siRNA mix siControl#1 was from Ambion. siRNAs against human ARFs and other cellular proteins, including ALDOA, LDHA, LDHB, PKM, EWSR1, HNRNPU, HNRNPH2, HNRNPH3, HNRNPA0, HNRNPR, HNRNPQ (SYNCRIP), interleukin enhancer-binding factor 3-90 (ILF/NF3-90), ILF/NF3-110, KH domain-containing RNA-binding protein (KHDRBS), and RNA-binding motif protein RBMX were ordered from Horizon according to sequences presented in Table 3.1. siRNA transfection was performed in a 96-well plate (for *Renilla* replicon replication assay), a 12-well plate with coverslips, an 8-well -µslides with a glass-bottom (for immunostaining), or a 12-well plate without a coverslip (for western blotting) according to the DharmaFECT's protocol. Briefly, for 35 wells of a 96-well plate, the siRNA mix was prepared by adding 175 µL Opti-MEM Reduced-Serum Medium, 157.5 sterile molecular grade water, 17.5 µL of 20 µM siRNA or scrambled siControl#1. The DharmaFECT transfection mix was made for the whole plate by adding 31.5 µL DharmaFECT into 1544 µL Opti-MEM Reduced-

Serum Medium and incubating at room temperature for 5 min. Then, 350 µL of the transfection mix was added to the siRNA solution and incubated at room temperature for 20 min. For each sample, about 3.5 * 10^5 HeLa cell in 3.5 ml complete growth medium was mixed with the transfection mixture and subsequently were seeded into the plate and incubated for 72 h at 37°C.

Table 3.1 siRNA sequences against human Arfs and other cellular proteins with references.

Number	Target protein	siRNA sequence	Reference
1	Arf1-A	ACCGUGGAG UACAAGAACA	(221)
2	Arf1-B	UGACAGAGAGCGUGUGAAC	(221)
3	Arf3-A	UGUGGAGACAGUGGAGUAU	(221)
4	Arf3-B	ACAGGAUCUGCCUAAUGCU	(221)
5	Arf4-A	UCUGGUAGAUGAAUUGAGA	(221)
6	Arf4-B	AGAUAGCAACGAUCGUGAA	(221)
7	Arf5-A	UCU GCUGAUGAACUCCAGA	(221)
8	Arf5-B	ACCAUAGGCUUCAAUGUAGA	(221)
9	Arf6-A	CGGCAUUACUACACUGGGA	(148)
10	Arf6-B	UCACAUGGUUAACCUCUAA	(148)
11	Aldo-A	CCGAGAACACCGAGGAGAA	(240)
12	LDHA	AAGACAUCAUCCUUUAUUCCG	(99)
13	LDHB	GUACAGUCCUGAUUGCAUC	(141)
14	PKM	CCACGAGCCACCAUGAUCC	(240)
15	EWSR1	CUACUAGAUGCAGAGACCC	(3)
16	HNRNPU	AAAGACCACGAGAAGAUCAUG	(128)
17	HNRNPH2	CAUGAGAGUACAUAUUGAA	(62)
18	HNRNPH3	GACAGUACGACUUCGUGGA	(54)
19	HNRNPA0	CAGACCAAGCGCUCCCGUU	(54)
20	HNRNPR	GGAGUAUGGAGUAUGCUGU	(54)
21	HNRNPQ (SYNCRIP)	GCUACUUGCACAUAGUGAU	(54)
22	ILF/NF3-90	CUUCCUAGAGCGUCUAAAAGU	(150)
23	ILF/NF3-110	GCGGAUCCGACUACAACUACG	(150)
24	KHDRBS	GGACCACAAGGGAAUACAA	(33)
25	RBMX	CGGAUAUGGUGGAAGUCGA	(139)

3.12 Enterovirus replicon replication assay

The polio replicon replication assay was performed as described elsewhere (218). Briefly, HeLa cells grown in a 96-well plate or cells previously (72 h) transfected with siRNA against Arfs or other cellular proteins were transfected with a purified RNA coding for a polio *Renilla* replicon using Mirus mRNA transfection reagent (Mirus Bio). The cells were incubated in the growth medium supplemented with 5 μM EnduRen cell-permeable *Renilla* luciferase substrate in the heated chamber of a multi-well plate reader (ID3; Molecular Devices) at 37°C, and the *Renilla* signal was measured in live cells every hour for 18 h after replicon RNA transfection. The signal from at least 16 wells was averaged for each sample for each time point. The total replication signal was calculated as the area under the curve for the replication kinetics signal. To study the effects of the inhibitors (BFA or GuHCl) on the replication, the enterovirus replicon assay was performed in the cells previously prepared based on the experiment's purpose. The polio replicon replication was assessed in the HeLa cells transfected with FLAG-APEX2-GARG-1060, a plasmid coding for EGFP-GARG-1060, or an empty vector (pUC) or in the HeLa cells stably expressing FLAG-APEX2-GARG-1060 along with a control HeLa in the absence or presence of 2 μg/ml BFA. The single Arf knocked down cells were incubated for 72 h after siRNA transfection, and a polio replicon replication was performed in the absence or presence of 125 or 500 ng/ml of BFA. Polio or CVB3 replicon replication was measured in the individual host protein-depleted cells at 72 h post-transfection in the absence or presence of 2mM of GuHCl (Sigma). Each data point on the replication graph is an average signal from at least 24 wells.

3.13 Immunofluorescent staining

HeLa monolayer was fixed with paraformaldehyde 4% diluted in phosphate-buffered saline (PBS) for 20 min, followed by three times washing with PBS. Fixed cells were then permeabilized with 0.2% triton for 5 min, with consequent washing with PBS three times. After 30 min blocking with blocking reagent (Amersham ECL Blocking Agent, RPN2125) dissolved in PBS, cells were incubated with primary antibody for 1 h, followed by three times washing with PBS. Cells were then incubated with appropriate anti-mouse, rabbit, or human secondary Alexa Fluor Conjugate or the streptavidin Alexa conjugate and Hoechst for 1 h, then washed with PBS three times and imaged by confocal microscope Zeiss LSM 510 microscope.

3.14 Microscopy

Confocal images were taken with either Zeiss LSM 510 or Zeiss LSM 800 microscope systems or a PerkinElmer Ultraview ERS 6FE spinning disk confocal attached to a Nikon TE 2000-U microscope. Non-confocal images were taken with a Zeiss Axiovert 200M microscope. For image analysis, several random fields with at least 100 total cells were analyzed.

3.15 Western blot

Cells lysed in mild lysis buffer (100 mM Tris-HCl pH=7.8, Triton-100X 0.5%) or RIPA lysis buffer (150 mM NaCl, 50 mM Tris-HCl pH=7.5, Triton-100X 1%, sodium dodecyl sulfate 1%, sodium deoxycholate 0.5%) supplemented with 1X proteinase inhibitor or the streptavidin-enrichment eluates were separated in the SDS-PAGE gel (either 12% or a gradient gel 4-15% (Bio-Rad, Cat No. 4568081)). Proteins were then

transferred to the nitrocellulose membrane, immersed in the 2% blocking solution in washing buffer (2 L distilled water, 100 mM NaCl, 2 mM Tris-HCl pH= 7.5, and 0.2% Tween-20) for 30 min. The membranes were then incubated with primary antibodies for 1 h, followed by three times washing with washing buffer and incubation with appropriate secondary antibodies or Streptavidin-horseradish peroxidase conjugate (Sigma-Millipore, Cat No. RPN1231) for 1 h. After three-time washing, the membrane was developed using ECL Select western blotting detection reagent (Bio Health, Cat No. PRN2235) and imaged by Azure Biosystems C500 Chemiluminescence.

3.16 APEX2-based biotin-labeling

Depending on the future analysis, HeLa cells stably expressing FLAG-APEX2-GARG-1060 were seeded in either a 12-well plate with or without coverslips, a T-25 or a T-225 cm^2 flask, and infected (or mock-infected) with 10 PFU/ml of poliovirus for certain time points in the presence of 2 μg/ml BFA. The biotinylation process was initiated half hour before each time point by replacing the medium with DMEM containing 500 μM biotin phenol (Chemodex CAS No. 41994-02-9) and incubating the cells at 37°C for 30 min. Next, the medium was replaced with PBS containing 20 mM hydrogen peroxide (H_2O_2) (Sigma Millipore, Cas No. 7722-84-1), and the reaction occurred for 3 min at 37°C. Cells were then washed three times by PBS and either fixed with paraformaldehyde 4% to visualize *in situ* or lysed in RIPA lysis buffer supplemented with a 1X proteinase inhibitor cocktail (Sigma, Cat No. P8340), followed by a 2-min sonication for SDS-PAGE or blotting analyses. Controls were made by omitting either biotin phenol, or H_2O_2, or both to confirm the specificity of the reaction.

3.17 Streptavidin beads pull-down assay

The whole-cell lysates were mixed with the equilibrated streptavidin magnetic beads (Pierce, Cat No. 88817) and incubated at room temperature on a rotator for 1 h. Next, the beads attached to the biotinylated proteins were precipitated in a magnetic rack, and the supernatant was collected as the flow-through containing the non-biotinylated proteins. After washing the pellets with RIPA lysis buffer three times, the biotin-labeled proteins were eluted from the beads by boiling the samples in 40 µL of 3X sample buffer supplemented with 2 mM biotin 20 mM and dithiothreitol (DTT) for 10 min. The streptavidin-enriched eluates were separated from the beads on the magnetic rack and kept at -80°C for further analysis.

3.18 Sample preparation for mass spectrometry

HeLa cells expressing FLAG-APEX2-GARG-1060 were seeded into 10 T-225 cm^2 flasks; half of them were infected with 10 PFU/ml of poliovirus for 6 h in the presence of 2 µg/ml BFA, and the other half were mock-infected in the same condition. The cells were then treated with 500 µM biotin phenol at 5 and a half hpi in the presence of BFA for 30 min, followed by the biotinylation reaction for 3 min at 37°C. Cells were then washed with PBS three times, collected in versene (PBS containing 2mM ethidium bromide), and centrifuged at maximum speed for 5 min at 4°C. Cell pellets were lysed in RIPA lysis buffer supplemented with 1X proteinase inhibitor cocktail and sonicated for 2 min. The streptavidin pull-down was performed to purify the biotin-labeled proteins. The biotinylation reaction was evaluated in the eluates collected from each flask separately by blotting with the streptavidin-HRP conjugate. A mixture of the five replicates for mock and PV-infected samples was loaded in the SDS-PAGE gel. The bands of interest were

visualized by immersing the gel in the Coomassie Blue solution made of 0.1% Coomassie Blue Dye (VWR Life Science, Cas No. 6104-58-1), 10% acetic acid, 50% methanol, and 40% distilled water for 40 min on a shaker at room temperature. The gel was then de-stained with a solution of 10% acetic acid, 50% methanol, and 40% distilled water three times for a total period of 3 h on a shaker until the gel's background color disappeared. After visualizing the bands of interest using the C500 UV reader, they were excised, placed into the Eppendorf tubes containing 50% acetonitrile**,** and submitted to the Harvard FAS Division of Science, Center for Mass Spectrometry Proteomics (https://proteomics.fas.harvard.edu/) for mass spectrometry analysis.

3.19 Mass spectrometry analysis and data processing

The LC-MS/MS experiment was performed on a Lumos Tribrid Orbitrap Mass Spectrometer (Thermo Fischer, San Jose, CA) equipped with Ultimate 3000 (Thermo-Fisher, CA) nano-HPLC. Peptides were separated onto a 150 µm inner diameter microcapillary trapping column packed first with approximately 2 cm of C18 Reprosil resin (5 µm, 100 Å, Dr. Maisch GmbH, Germany) followed by PharmaFluidics (Gent, Belgium) 50 cm analytical column. Separation was achieved by applying a gradient from 5– 27% ACN in 0.1% formic acid over 90 min at 200 nl/min. Electrospray ionization was enabled by applying a voltage of 2 kV using a homemade electrode junction at the end of the microcapillary column and sprayed from metal tips (PepSep, Denmark). The mass spectrometry survey scan was performed in the Orbitrap in the range of 400–1,800 m/z at a resolution of 6×10^4, followed by the selection of the twenty most intense ions (TOP20) for CID-MS2 fragmentation in the Ion trap using a precursor isolation width window of 2 m/z, AGC setting of 10,000, and a maximum ion accumulation of 100 ms. Singly charged

ion species were not subjected to CID fragmentation. The normalized collision energy was set to 35 V and an activation time of 10 ms. Ions in a 10-ppm m/z window around ions selected for MS2 were excluded from further selection for fragmentation for 60s.

Raw data were submitted for analysis in Proteome Discoverer 2.4 (Thermo Scientific) software. Assignment of MS/MS spectra was performed using the Sequest HT algorithm by searching the data against a protein sequence database, including all entries from our Uniport_Human2018_SPonly database as well as other known contaminants such as human keratins and typical lab contaminants. Searching the identified spectra against the UniProt database provided a unique "accession number," enabling us to directly find the protein of interest and complete information in the database. Quantitative analysis between samples was performed by label-free quantitation (LFQ). Using the SEQUEST search algorithm, the company provided a protein score which is the sum of the ion scores of individual peptides that were identified. The percentage of a protein sequence covered by the identified peptides gave us the percent coverage, ranging from 1-71%; the higher number is better, which shows a better coverage of the protein of interest. SEQUEST searches were performed using a 10-ppm precursor ion tolerance and requiring N-/C termini of each peptide to adhere to Trypsin protease specificity while allowing up to two missed cleavages. Methionine oxidation (+15.99492 Da) was set as a variable modification as well as deamidation (+ 0.98402 Da) of Asparagine and Glutamine amino acids. Special modification of 1xBiotin-tyramide (+361.14601 Da) on Tyrosine amino acid residues was used as variable modification. All Cysteines were set to permanent modification with Carbamidomethyl (+ 57.02146 Da) due to an alkylation procedure. All MS2 spectra

assignment false discovery rate (FDR) of 1% on both protein and peptide levels was achieved by applying the target-decoy database search by Percolator (103).

The sets of proteins identified in the infected and mock-infected samples were analyzed for Gene Ontology (GO) term enrichment using PANTHER classification system web tool (147) against all *Homo sapiens* protein-coding genes using Fisher's exact test and Bonferroni correction for multiple testing. Only the statistically significant enrichment results with $p<0.05$ are reported. The high-confidence proteins identified in the replication complexes by mass spectrometry were searched in the literature available in the PubMed database to detect the proteins that have not been previously reported to be involved in enterovirus replication.

3.20 Data analysis

Digital images were processed with microscope operating software Zen (Zeiss) or Volocity 6.2 (PerkinElmer) and Adobe Photoshop. All images belonging to one experiment were processed the same way, and the adjustments were applied evenly to the whole image area. Statistical calculations were performed using the GraphPad Prism software package; all calculations are presented as mean values and standard deviation bars. Data comparison for statistical significance was performed using the two-tailed unpaired *t*-test.

Chapter 4: Enterovirus Infection Induces Massive Recruitment of All Isoforms of Small Cellular Arf GTPases to the Replication Organelles

4.1 Introduction

Enteroviruses are small positive-stranded RNA viruses of eukaryotes, which are fully dependent on the host cells to replicate and produce viral progeny. During infection, the virus induces a massive remodeling of the cell membranous structures to build a safe, confined environment to replicate without being interrupted by the host antiviral immune factors. These membranes, called the replication organelles (ROs), contain a unique combination of viral and host factors required for proper genome replication. Viral antigens are associated with the *cis*-Golgi marker, GM130, at the early stage of infection, meaning a close relationship between the establishment of viral replication complexes and the Golgi membranes, presumably because this organelle contains some specific factors required for virus infection. In addition, the ROs are detectable nearby *cis*-Golgi and ERGIC, the two compartments of the cellular protein secretory machinery early on infection, supporting that the virus requires a Golgi-like environment for genome replication. Moreover, inhibition of the secretory traffic by BFA blocks enterovirus replication. Collectively, these data suggest that at least some elements of the secretory pathway are involved in the virus replication process.

One of the key elements of the secretory pathway is the family of ADP-ribosylation factor (Arf) GTPases, which are divided into three classes based on their structural homology. In primate cells, Arf1 and Arf3 belong to class I, Arf4 and Arf5 are in class II, and Arf6 is the only member of class III. Similar to other GTPases, Arfs cycle between an

activated membrane-bound Arf-GTP and inactive cytosolic Arf-GDP forms. Arf activation is mediated by Arf guanine nucleotide exchange factors (Arf-GEFs), and the GTP hydrolysis is facilitated by Arf-GTPase activating proteins (Arf-GAPs) (50). The active form of Arfs interacts with various effector proteins, including those engaged in membrane remodeling, lipid synthesis, and trafficking (69, 94). Activation of different Arf isoforms is subject to tight spatial and temporal regulation and is important for regulating multiple steps of the membrane metabolism in the cell.

GBF1 is one of the Arf-GEFs, which is typically located in the *cis*-Golgi. GBF1 and Arf1-GDP are recruited to the Golgi membranes, in which the GDP-GTP exchange occurs. GBF1 is then released from the membranes while the activated Arf1-GTP stays associated with the membranes, where they recruit many effector proteins with various functions. BFA interacts with GBF1-Sec7d in the junction with Arf-GDP and stabilizes the GBF1-Arf-GDP complex on the membranes, resulting in inhibiting GBF1's catalytic function. As a consequence, the flow of the secretory pathway is disturbed. During enterovirus infection, the interaction of GBF1 with the viral protein 3A relocates GBF1 to the replication organelles in which it attracts and activates Arf1. Viral protein 2BC also interacts and recruits Arf1 into the replication sites. However, whether other Arfs are associated with the replication organelles and what Arf isoform(s) is actually required to support the viral replication, as well as their mechanistic roles in the replication process, are not understood.

Published data show some disagreement over the significance of human Arf isoforms in the enterovirus replication process. Knockdown and knockout studies of individual Arf isoforms or pairwise combinations indicated no significant inhibition of

Coxsackieviruses B3 and B4 replication (56, 120), while simultaneous depletion of Arf1 and Arf3 impaired enterovirus 71 replication in the cell (223). Although GBF1-controlled Arf activation is required for enterovirus replication, the inhibitory effect of BFA on enterovirus replication is relieved by overexpression of GBF1 but not any of Arf isoforms, remaining the roles of individual Arfs in the replication process undefined.

To get a better insight into the role of different Arfs in enterovirus infection, we established cell lines stably expressing all human Arfs fused to fluorescent proteins. Such a system allowed us to observe the dynamics of Arf recruitment to replication organelles upon viral infection without the artifacts usually associated with transient transfections, such as activation of antiviral signaling due to the presence of plasmid DNA in the cytoplasm. Using these cell lines and other experimental systems, we systematically investigated the contributions of different Arf isoforms to the replication of enteroviruses.

Here, we report that poliovirus induces a complex pattern of engagement of different Arfs. Only Arf1 was rapidly recruited to the replication membranes in the early-middle stages of the infectious cycle, while a significant proportion of other Arfs was not associated with viral antigens at early times. However, by the end of the replication cycle, all Arfs, including Arf6, were massively associated with the replication membranes. The different dynamics of Arf isoform recruitment were confirmed in cells expressing pairs of Arfs fused to different fluorescent proteins. Among the different viral antigens, 2B and mature virions demonstrated the strongest association with Arf1-enriched membranes, while the signal for double-stranded RNA (dsRNA) was strongly separated from that of Arf1, suggesting that dsRNA is sequestered biochemically distinct membranous domains.

Interestingly, only Arf3 required a continuous BFA-sensitive GEF activity to remain associated with the membranes in infected cells. Knockdown of expression of individual Arf isoforms had minimal effect on viral replication, confirming the previously reported data (19, 22). However, the knockdown of expression of Arf1 and, to a certain extent, Arf6, but not other Arfs, significantly increased the sensitivity of enterovirus replication to BFA, suggesting that GBF1-driven activation of Arf1 and, to a lesser extent, Arf6, directly supports the development and/or functioning of the viral replication complexes.

4.2 Results

4.2.1 Stable cell lines expressing Arf-GFP constructs recapitulate normal Arf phenotypes.

To visualize the location of Arf isoforms in the cell and their redistribution profile during viral infection, we generated stable HeLa cell lines expressing individual human Arfs (Arf1, 3, 4, 5, and 6) C-terminally tagged to a green fluorescent protein (GFP). DNA transfection-based systems are not well-suited for studying viral infection since the presence of DNA in the cytoplasm triggers innate immune signaling, which interferes with authentic viral infection responses (85). Therefore, we transduced HeLa cells with retroviral vectors expressing individual Arf-GFP constructs and isolated the successfully transduced cells by applying selective antibiotic pressure. Approximately 80% of the stable cells displayed Arf signals with various intensities. The heterogeneous composition of cells expressing Arf-GFP constructs allows minimizing possible artifacts associated with

different provirus integration sites and the level of transgene expression in a particular population of transduced cells.

As shown in Fig. 4.1A, the fluorescent signal was observed mainly in the Golgi and *trans*-Golgi network (TNG) areas in the Arf1 and Arf3 expressing cells. In contrast, the signals for Arf4 and Arf5 were predominantly detected in a rather diffuse perinuclear pattern, the characteristics of the ER and ERGIC regions. Arf6 was concentrated mainly on the plasma membrane. To see whether the fluorescently-tagged Arf isoforms behave as authentic proteins, we assessed their colocalization with markers for the *cis*-Golgi (GM130), ERGIC (ERGIC53), and plasma membrane (wheat germ agglutinin-WGA). As expected, Arf1 and Arf3 colocalized with the GM130 marker, whereas Arf4 and Arf5 showed colocalization with the ERGIC53 marker. The strong colocalization of Arf6 with the WGA marker confirmed that Arf6 is mostly associated with plasma membrane; however, a small portion of Arf6 was detected on the intracellular structures, suggesting Arf6 association with endosomal pathways in the cell (Fig. 4.1A). These data demonstrate that stably expressed Arf-GFP constructs recapitulate the behavior expected from functional Arf isoforms.

Finally, we tested if the expression of the Arf-GFP constructs interferes with poliovirus replication. As shown in Fig. 4.1B, the accumulation of poliovirus proteins upon infection of Arf-GFP-expressing cell lines was the same as that in control HeLa cells. It should be noted that sometimes we observed additional weak GFP-positive bands on the western blots upon analysis of Arf-GFP fusions (see, for example, Fig. 4.1B, Arf5 sample). Analysis of lysates from infected and mock-infected cells did not reveal any differences (Fig. 4.1C), thereby excluding infection-specific modification of Arf-GFP fusions. Such

bands likely correspond to posttranslational modifications, such as phosphorylation or acetylation of Arf molecules (83). We also analyzed the virus yield by plaque assay and found it the same in Arf-GFP-expressing cells and the original HeLa cell line (data not shown). Thus, cell lines expressing Arf-GFP constructs recapitulate normal Arf phenotypes and provide a convenient tool for studying the role of these small cellular GTPases in enterovirus infection.

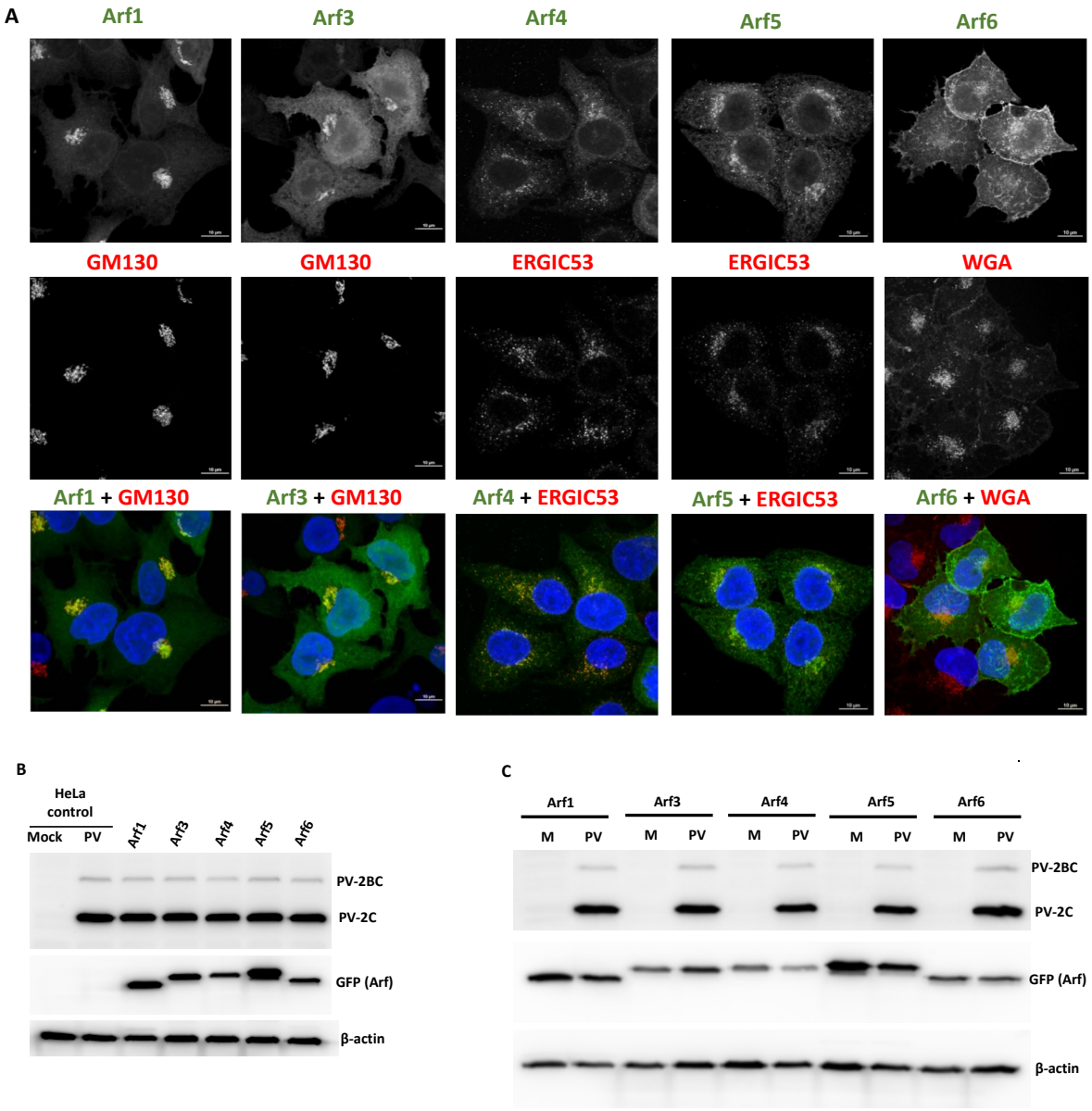

Figure 4.1. Characterization of stable cell lines expressing human Arf-GFP isoforms. (A) HeLa cells stably expressing individual Arf-GFP isoforms were analyzed with antibodies against *cis*-Golgi and ERGIC markers GM130 and ERGIC53, respectively. Plasma membrane was stained with wheat germ agglutinin (WGA). Nuclear DNA was stained by Hoechst 33342 (blue). Fluorescently tagged Arfs demonstrated the expected behavior. **(B)** Expression of fluorescently tagged Arfs does not interfere with poliovirus replication. The original HeLa cell line and its derivatives stably expressing individual Arf-GFP were mock infected or infected with poliovirus (50 PFU/cell), the cells were lysed in RIPA buffer at 6 hpi, and the total cell lysates were analyzed by western blotting with an antibody against viral antigen 2C and anti-GFP antibodies that recognize the Arf-GFP fusions. Actin is shown as a loading control. **(C)** Arf-GFP fusions are not significantly affected by poliovirus infection. Cell lines expressing corresponding Arf-GFP fusions were infected with poliovirus (PV; 50 PFU/cell) or mock infected (M), the cells were lysed in RIPA buffer at 6 hpi, and the total cell lysates were analyzed by western blotting with an antibody against viral antigen 2C and anti-GFP antibodies that recognize the Arf-GFP fusions. Actin is shown as a loading control.

4.2.2 Poliovirus infection induces the dynamic of recruitment of multiple Arfs to the replication organelles.

To monitor the pattern of Arf activation during the time course of poliovirus infection, cells expressing Arf-GFP fusions were infected with 50 PFU/cell of poliovirus type I Mahoney (so that all of the cells are infected) and fixed at 2, 4, and 6 hpi. By 6 h the replication cycle of poliovirus in HeLa cells is complete. Activation of Arfs induces their association with membranes, and, to maximally preserve the Arf localization pattern, the cells were not processed for any additional staining after fixation.

In mock-infected cells, the distribution of Arf isoforms was similar at all the time points. Arf1, 3, 4, and 5 were concentrated in the perinuclear area, reflecting their association with the Golgi and the ERGIC, and Arf6 was associated with the plasma membrane (Fig. 4.2, mock infection). Poliovirus infection induced dramatic changes in the distribution of all Arf isoforms, including Arf6. As early as 2 hpi, Arf1, 3, and 5 were redistributed in a noticeable percentage of the cells (up to 20% for Arf3) in multiple dots, likely reflecting Golgi fragmentation known to occur early in enterovirus infection (28, 178) (Fig. 4.2, 2 hpi). Arf4 was mostly associated with perinuclear structures, possibly Golgi remnants. Arf6 was still almost exclusively associated with the plasma membrane in the infected cells, similar to control cells (Fig. 4.2, 2 hpi).

In the middle of the infectious cycle, at 4 hpi, in the majority of Arf1-GFP- expressing cells (~80%) the signal was found in bright perinuclear rings, characteristic of localization of poliovirus replication organelles, while Arf3, 4, and -5 signals were found in almost equal numbers of cells either in distinct punctae (~60%, ~30%, and ~30%, respectively) or in perinuclear rings (~42%, ~60%, or ~62%, respectively). Interestingly, a redistribution of

the Arf6-GFP signal from the plasma membrane to the perinuclear region was also observed in almost all of the cells (80%); however, the level of Arf6 signal on the replication organelles was relatively low at this time point, especially compared to the bright, highly concentrated signal of Arf1 (Fig. 4.2, 4 hpi).

By the end of the replication cycle, at 6 hpi, all Arf isoforms in poliovirus-infected cells were found highly concentrated in perinuclear rings in 90 to 100% of cells (Fig. 4.2, and 6 hpi). It should be noted that starting from 4 hpi, the confocal images demonstrate a much stronger signal of membrane-associated Arf1, 3, 5, and 6 in any section plane in infected than in mock-infected cells, reflecting a significantly higher level of Arf activation upon infection (Fig. 4.2).

Thus, during the poliovirus replication cycle, Arf1, 3, 4, 5, and 6 demonstrate distinct dynamics of recruitment to the replication organelles, suggesting that the biochemical properties of the replication membranes change during the time course of infection.

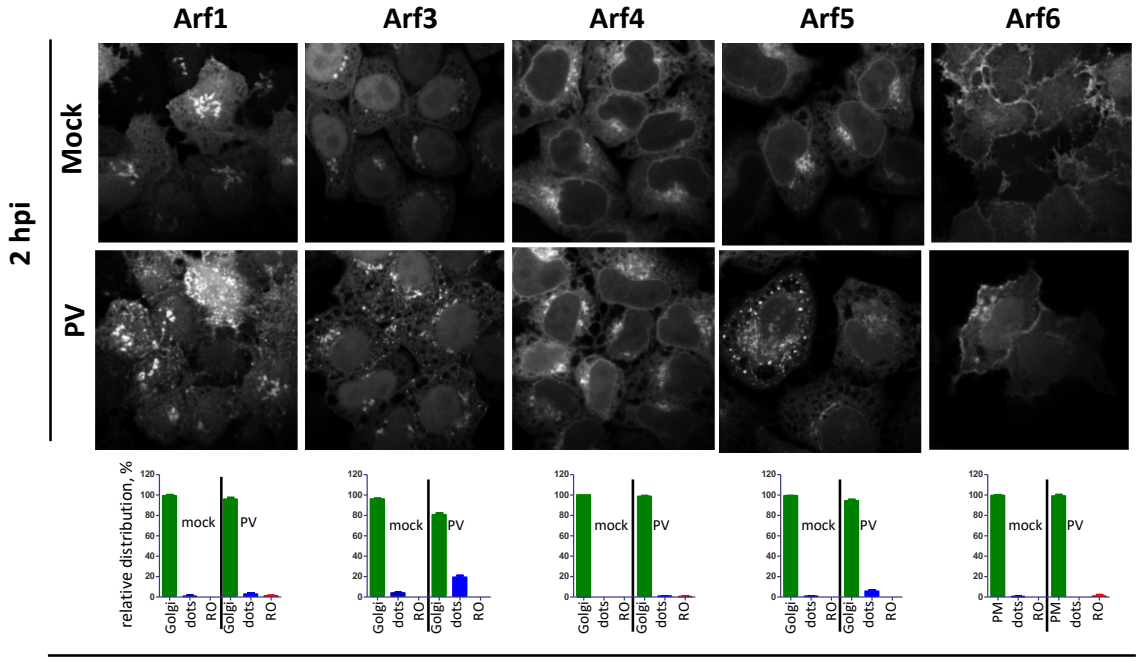
Arf1
Arf3
Arf4
Arf5
Arf6
2 hpi
Mock
PV
relative distribution, %
mock
PV
Golgi
dots
RO
PM

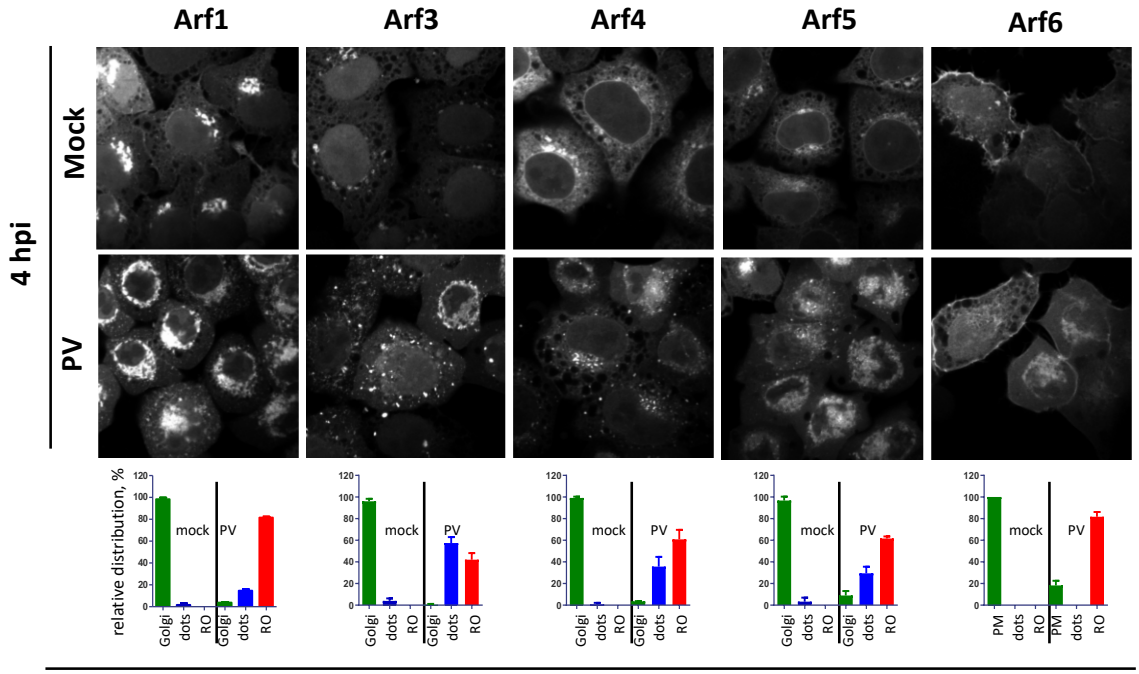
Arf1
Arf3
Arf4
Arf5
Arf6
4 hpi
Mock
PV
relative distribution, %
mock
PV
Golgi
dots
RO
PM

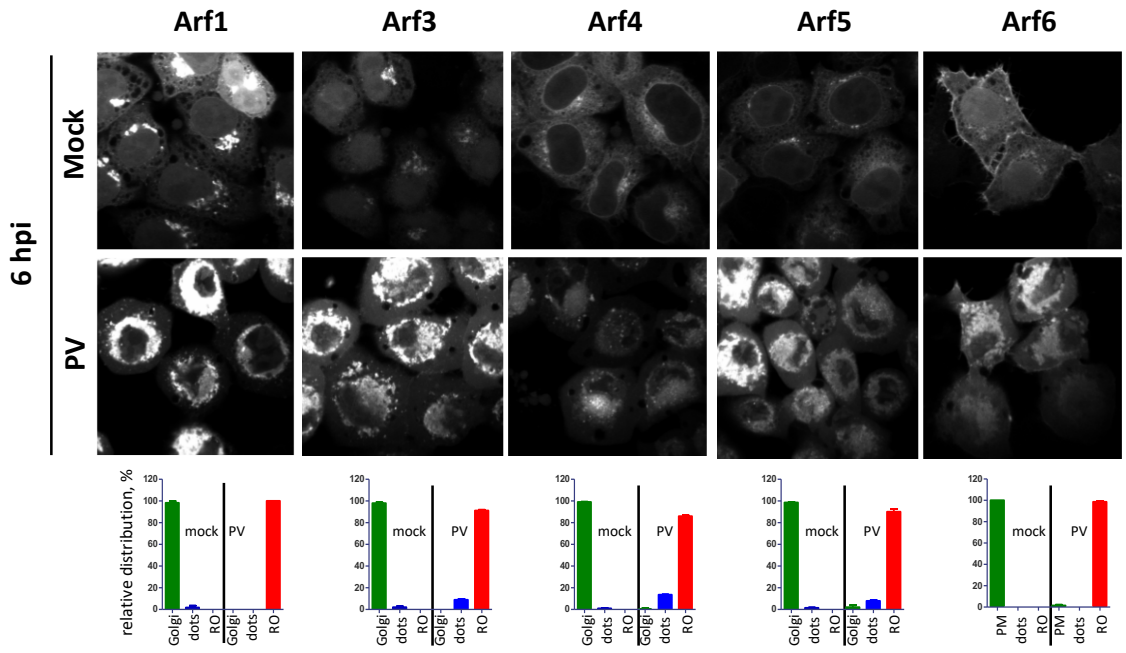

Figure 4.2. Recruitment of Arfs to the replication organelles in poliovirus-infected cells. HeLa cell lines expressing individual Arf-GFP were mock infected or infected with poliovirus type I Mahoney at 50 PFU/cell and fixed at the indicated times post-infection. To maximally preserve the pattern of Arf recruitment, no other manipulations with cells were performed. For quantifications, several random fields with no fewer than 100 total cells were counted. The cellular phenotypes were defined as Arf1 to -4, mostly at the Golgi membrane (Arf6 was at the plasma membrane), Arfs mostly distributed at the cytoplasmic dots, and Arfs mostly recruited to the perinuclear rings of the RO.

4.2.3 Diverse enteroviruses induce the same pattern of Arf activation.

To see whether the pattern of Arf recruitment to the replication organelles is virus specific, we infected cells expressing Arf-GFP with CVB3, an enterovirus distantly related to poliovirus. Poliovirus is classified within the enterovirus species C, while CVB3 belongs to the enterovirus species B in the *Enterovirus* genus of the *Picornaviridae* family (222). We also infected cells with EMCV, a murine picornavirus of the *Cardiovirus* genus, which is known not to be sensitive to BFA and, thus, is unlikely to depend on Arf activation (65).

CVB3 and EMCV replicate in HeLa cells with kinetics similar to that of poliovirus (the replication cycle is complete within 6 to 8 h).

Infection with CVB3 induced a pattern of Arf redistribution similar to that observed in poliovirus-infected cells so that by the end of the replication cycle (6 hpi), all Arfs were found on the replication organelles (Fig. 4.3A).

In contrast, in cells infected with EMCV, none of the Arfs was recruited to the replication organelles, even in cells with strong cytopathic effects, i.e., those at the end of the infectious cycle. Nevertheless, the effect of EMCV infection on Arf distribution was clearly visible. In infected cells, there were much less membrane-associated Arfs than in control cells, indicating that Arf-GEF activity is likely severely inhibited during cardiovirus infection. In some cells, Arf1 and Arf4 were found in multiple membrane-associated dots (Fig. 4.3B and data not shown), but whether these dots represent the remnants of preexisting Arf-enriched structures, like the Golgi, or have an infection-specific significance requires further investigation.

Thus, the recruitment of multiple Arfs to the replication organelles is a shared feature of enterovirus, but not cardiovirus, infection even though both enteroviruses and cardioviruses belong to the same family and induce the formation of specialized replication membranes.

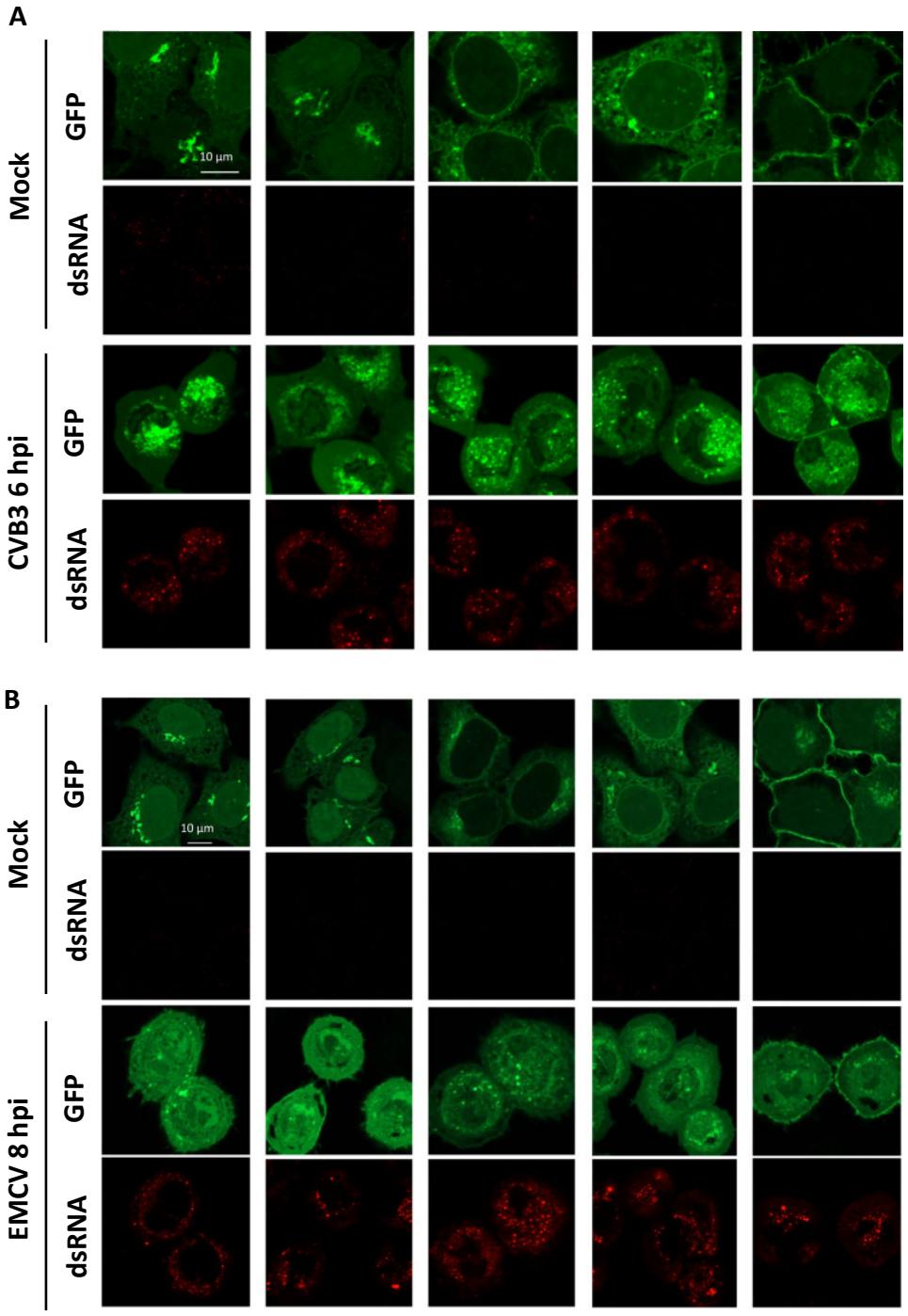

Figure 4.3 Recruitment of Arfs to the enterovirus but not cardiovirus replication organelles. HeLa cell lines expressing individual Arf-GFP were mock infected or infected with 50 PFU/cell of CVB3 (an enterovirus) **(A)** or EMCV (a cardiovirus) **(B)** and fixed at 6 and 8 hpi, respectively. The cells were counterstained for dsRNA, an intermediate product of replication of RNA viruses, to confirm the infection.

4.2.4 Arf1 is the first to associate with the functional replication organelles.

To directly compare the recruitment of different Arf isoforms to the replication organelles in the same cell, we developed cell lines co-expressing pairs of Arfs fused to either green or red fluorescent reporter proteins. As the red fluorescent reporter, we used FusionRed protein (FRP) that was specifically designed to be strictly monomeric (190), so that the residual propensity for oligomerization common to other red fluorescent reporter proteins do not interfere with Arf targeting. First, we verified that Arf1 tagged with FRP behaves the same as GFP-tagged Arf1 and monitored the colocalization of red and green signals in a HeLa cell line co-expressing Arf1-GFP and Arf1-FRP. As shown in Fig. 4.4A, in both control and infected cells, the red and the green Arf1 signals were perfectly colocalized, confirming that the Arf1-FRP construct recapitulates the same Arf1 behavior.

We then analyzed the recruitment of different Arfs relative to Arf1 by co-expressing Arf1-FRP with other Arf isoforms fused to GFP. The cells were infected (or mock-infected) with poliovirus type I Mahoney at a multiplicity of 50 PFU/cell, and the subcellular localization of both Arfs was analyzed at 3 hpi (early-middle time of the infectious cycle). At this multiplicity of infection at 3 hpi, viral antigens are readily detectable, while the cells still maintain overall normal morphology.

As shown in Fig. 4.4B, in mock-infected cells, the Arf1 signal showed extensive colocalization in the Golgi area with all the Arfs except the plasma membrane-localized Arf6. However, in infected cells, the recruitment of Arf1 to the perinuclear replication organelles preceded the recruitment of other Arf isoforms. At later time points (4 to 6 hpi), all Arfs were extensively colocalized with Arf1 on the replication organelles (data not shown).

To directly identify the Arf isoforms that associate early in infection with the functional replication organelles, we took advantage of the fact that the assembly of poliovirus virions is tightly coupled to RNA replication (155). At 3 hpi, the accumulation of the progeny virus first becomes apparent; thus, the virion signal should be localized at least close to the functional replication complexes. Cells expressing individual Arf-GFP were infected with poliovirus at a multiplicity of infection of 50, fixed at 3 hpi, and subsequently stained with a monoclonal antibody A12 that recognizes only the fully mature virions (38). As shown in fig. 4.4C, Arf1-GFP but not the other Arfs strongly colocalized with the virion signal.

Collectively, these observations indicate that Arf1 appears to be the first to associate with the ROs, followed by other Arf isoforms, which suggests that the composition of the proteins associated with the ROs may be significantly different at different stages of the infectious cycle.

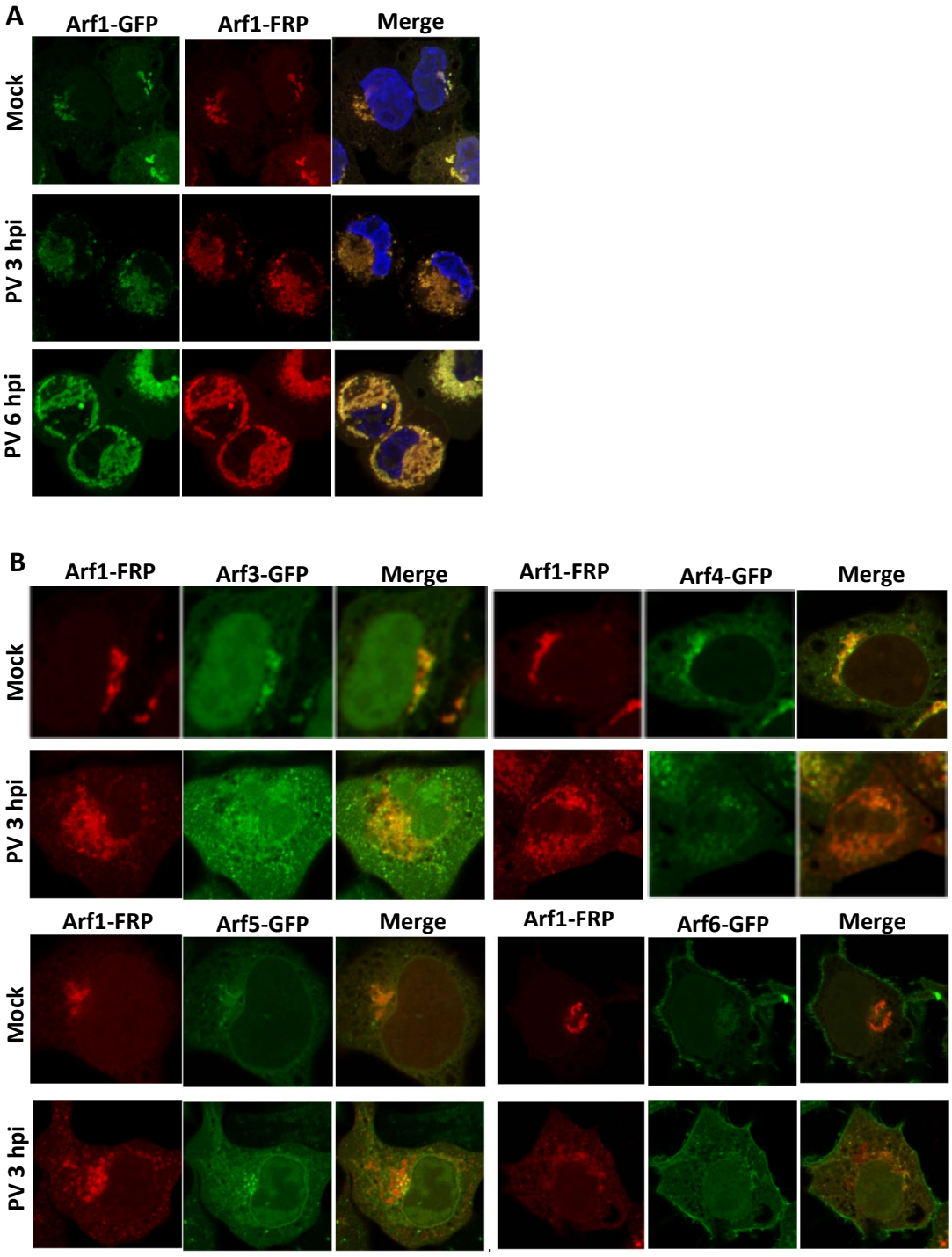
A
Arf1-GFP
Arf1-FRP
Merge
Mock
PV 3 hpi
PV 6 hpi
B
Arf1-FRP
Arf3-GFP
Merge
Arf1-FRP
Arf4-GFP
Merge
Mock
PV 3 hpi
Arf1-FRP
Arf5-GFP
Merge
Arf1-FRP
Arf6-GFP
Merge
Mock
PV 3 hpi

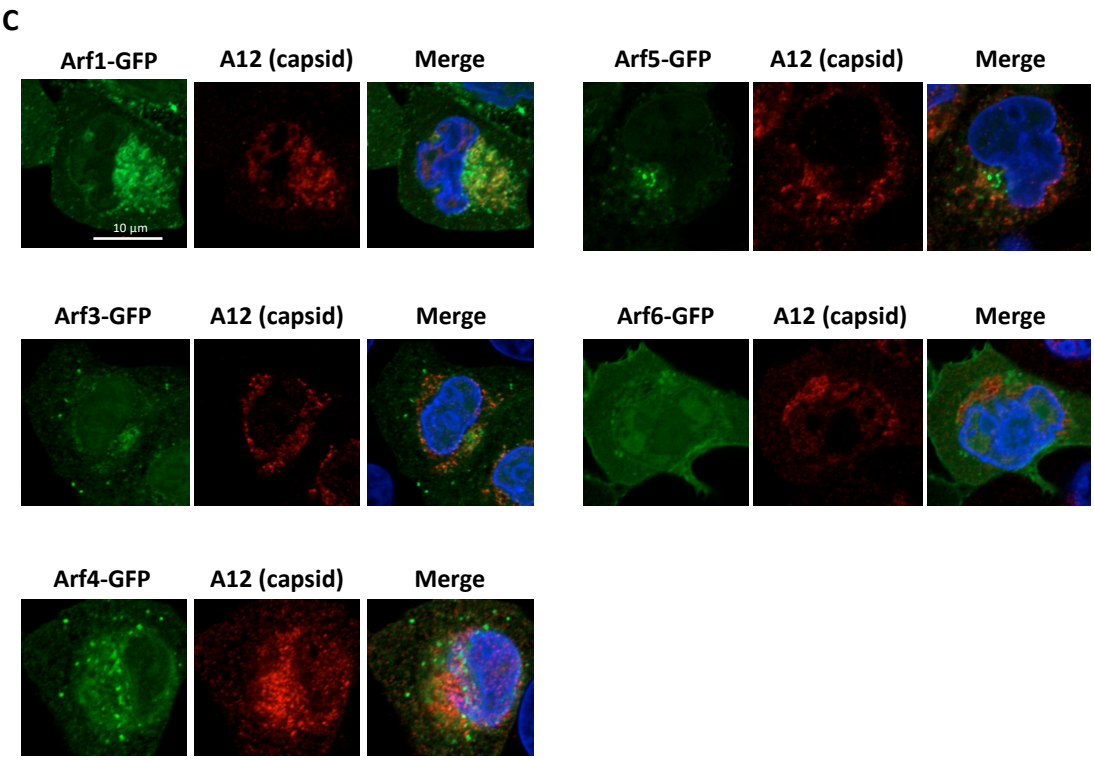

Figure 4.4. Arf1 is the first to be recruited to the functional replication organelles. **(A)** Arf1 fusions with red and green fluorescent proteins recapitulate the same Arf1 behavior. HeLa cells co-expressing Arf1-GFP (green) and Arf1-FRP (red) fusions were mock infected or infected with poliovirus type I Mahoney at 50 PFU/cell, and the cells were fixed at the indicated times post-infection. Nuclear staining was performed with a cell-permeable dye, Hoechst 33342, in live cells 30 min before fixation. To maximally preserve the pattern of Arf recruitment, no other manipulations with cells were performed. **(B)** HeLa cells co-expressing pairs of Arf1-FRP (red) with other Arf-GFP (green) fusions were infected with poliovirus type I Mahoney at 50 PFU/cell and fixed at 3 hpi. To maximally preserve the pattern of Arf recruitment, no other manipulations with cells were performed. **(C)** HeLa cells co-expressing pairs of Arf1-FRP (red) with other Arf-GFP (green) fusions were infected with poliovirus type I Mahoney at 50 PFU/cell and fixed at 4 hpi. The cells were stained with antibody A12 that recognizes only mature poliovirus capsids, and early in infection denotes the localization of the active replication organelles, since the assembly of poliovirus virions is intimately linked to active RNA replication. Nuclear DNA was stained by Hoechst 33342 (blue).

4.2.5 Viral antigens show a distinct pattern of association with the Arf1-enriched domains on the replication organelles.

Enterovirus proteins are expressed as a single polyprotein, which is co- and post-translationally processed by three viral proteases 2A, 3C, and 3CD (Fig 4.5A). Although it is assumed that synthesis of the polyprotein results in a similar spatiotemporal distribution of viral antigens, it has not been explicitly addressed. Thus, we analyzed the localization of viral antigens relative to Arf1-enriched membranes. Arf1-GFP expressing cells were infected with 50 PFU/cell of poliovirus type I Mahoney and fixed at 4 hpi in the middle of the infectious cycle. The cells were then stained with antibodies to dsRNA, an intermediate product of the viral RNA replication, or with antibodies for the mature capsid (A12) or the non-structural proteins 2B, 2C, 3A, or 3D. Because of the polyprotein synthesis and processing scheme, the antibodies recognize the mature proteins as well as all the intermediate cleavage products containing the corresponding antigens (Fig 4.5A). The level of the colocalization of the viral antigens with the Arf1-GFP signal varied in different cells and was, in general, higher in cells expressing more of the viral proteins, i.e., those further in the replication cycle progression.

At 4 hpi, Arf1 is strongly associated with the perinuclear rings of replication organelles (compare the distribution of Arf1-GFP in mock-infected cells [Fig. 4.5B] with that in the infected cells in Fig. 4.5C). We confirmed a very strong colocalization of the signal of the mature virions with Arf1-enriched membranes, similar to that observed at 3 hpi (Fig. 4.4B), indicating that at least at the early-middle stage of infection, the major part of the progeny virus is still tightly associated with the membranes of the replication

organelles and is not significantly exported from the cell via possible nonlytic pathways (Fig. 4.5C).

The non-structural proteins exhibited qualitatively distinct types of behavior. While we observed the strongest Arf1 colocalization with the 2B antigen, the signal for the membrane-targeted proteins 2C and 3A was less colocalized with Arf1. Furthermore, the signal for the 3D antigen colocalized poorly, with most of the protein found outside of the areas enriched in Arfs. Interestingly, while the signal for dsRNA was in close vicinity to that of Arf1, the two signals were clearly separated such that the Arf1 signal appeared to encircle the dsRNA-enriched regions (Fig. 4.5C, dsRNA panel, arrows). This phenomenon was observed in all cells analyzed, arguing that exclusion of dsRNA from Arf-enriched regions is an important feature of the fine organization of the replication organelles.

Viral antigens did not show any specific associations with other Arfs early in the infection cycle, and when, at the middle-late stage of infection, other Arfs were massively recruited to the replication organelles, their colocalization with viral antigens was similar to that of Arf1 (data not shown).

To confirm that in the same cell viral nonstructural membrane-targeted proteins could have a significantly different localization relative to Arf-enriched membranes of replication organelles, we infected Arf1-GFP-expressing cells with a poliovirus with a modified FLAG insert (FLAG-Y) in the protein 3A. This virus replicates with almost wild-type kinetics (206). The simultaneous staining of cells infected with this virus with anti-FLAG and anti-2C antibodies at 5 hpi demonstrated that both viral antigens have distinct localizations relative to Arf1, with a substantial amount of 2C still outside the Arf1-enriched area (Fig. 4.5D).

These data demonstrate that the full complement of viral proteins is assembled on the Arf1-enriched replication organelles at the early-middle stages of replication. However, at least some of the nonstructural proteins, including the membrane-targeted proteins 2C and 3A, could have an extended localization outside the replication complexes. This suggests the existence of replication-independent functions of these proteins.

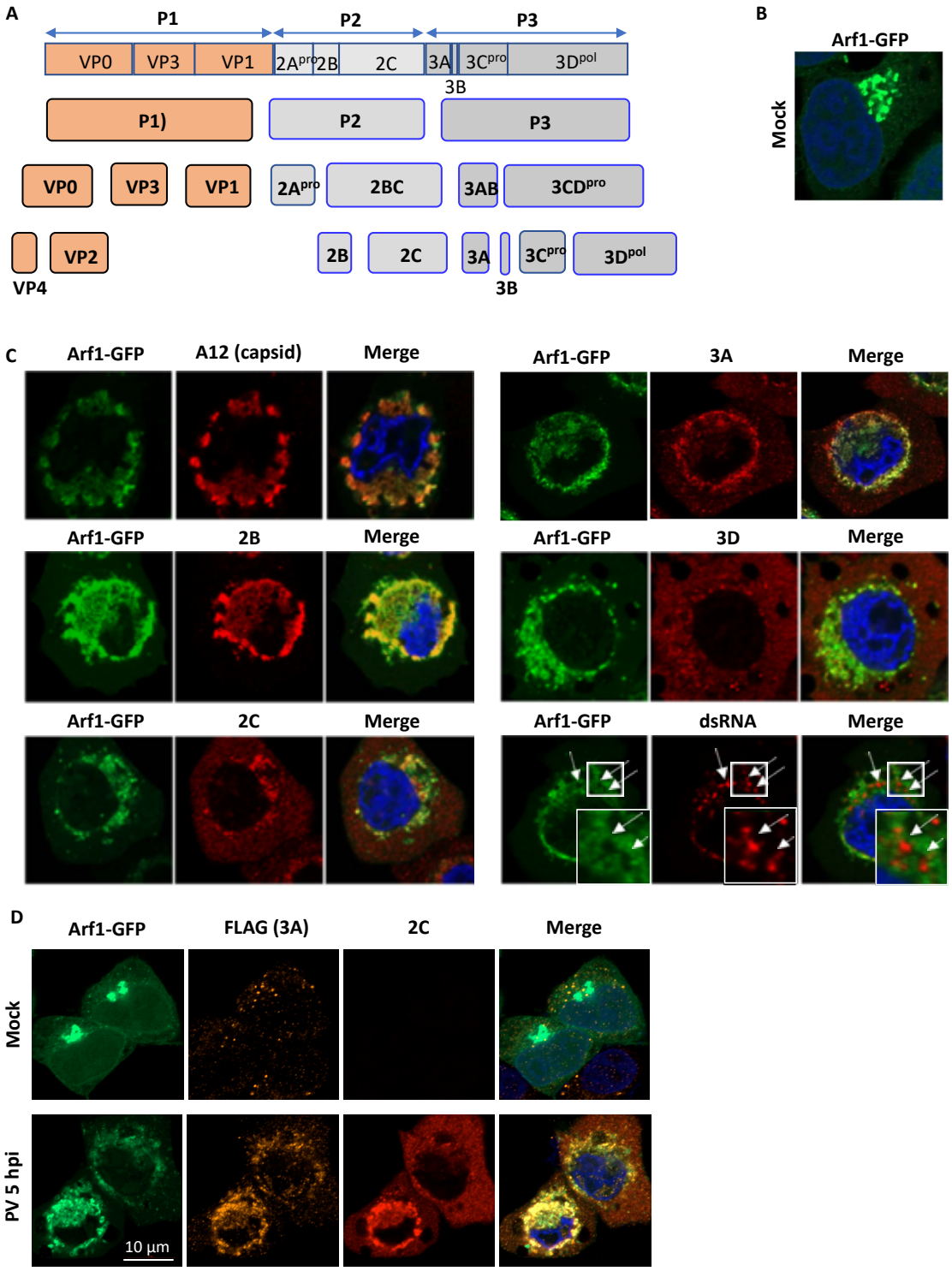
A
P1
P2
P3
VP0
VP3
VP1
2A^pro
2B
2C
3A
3B
3C^pro
3D^pol
P1)
P2
P3
VP0
VP3
VP1
2A^pro
2BC
3AB
3CD^pro
VP4
VP2
2B
2C
3A
3B
3C^pro
3D^pol
B
Arf1-GFP
Mock
C
Arf1-GFP
A12 (capsid)
Merge
Arf1-GFP
3A
Merge
Arf1-GFP
2B
Merge
Arf1-GFP
3D
Merge
Arf1-GFP
2C
Merge
Arf1-GFP
dsRNA
Merge
D
Arf1-GFP
FLAG (3A)
2C
Merge
Mock
PV 5 hpi
10 µm

Figure 4.5 Highly diverse association of different human Arf isoforms with poliovirus antigens in the replication sites. (A) Scheme of the processing of poliovirus polyprotein. **(B)** Mock-infected HeLa cells expressing Arf1-GFP. **(C)** HeLa cells expressing Arf1-GFP were infected with poliovirus type I Mahoney at 50 PFU/cell, fixed at 4 hpi, and stained with antibodies recognizing dsRNA, mature poliovirus capsid (A12), or the antigens in the viral nonstructural protein 2B, 3A, 2C, or 3D. **(D)** HeLa cells expressing Arf1-GFP were infected with 50 PFU/cell of a poliovirus type I Mahoney mutant with FLAG-Y inserted in the nonstructural protein 3A. The cells were stained with anti-FLAG and anti-2C antibodies simultaneously. Nuclear DNA was stained by Hoechst 33342 (blue).

4.3.6 Only Arf3 requires constant GEF activity to remain associated with the replication membranes.

Under normal conditions, cellular Arfs constantly cycle through activated, GTP-bound and inactivated, GDP-bound states. To determine whether Arfs recruited to the viral replication organelles still undergo cycles of GDP/GTP exchange, we infected (or mock-infected) cells expressing Arf-GFP constructs with poliovirus type I Mahoney at 50 PFU/cell and incubated them for 5 h so that the Arf-enriched replication organelles are well developed. At this point, the medium was supplemented with BFA and the cells were monitored to track the behavior of the Arfs (Fig. 4.6A). If the GTP hydrolysis arm of the Arf cycle is still functional, Arfs whose activation depends on BFA-sensitive GEFs are expected to be released from the membranes (Fig. 4.6B).

In mock-infected cells, after BFA addition, Arf1 and 3 entirely lost their association with the Golgi membranes. Arf4 and 5 were mostly released into the cytoplasm, although a small portion of these proteins was still associated with membranes, likely the remnants of the Golgi and ERGIC (Fig. 4.6C, mock). Arf6, which is activated by a BFA-insensitive GEF called ARNO, remained associated with the plasma membrane, as expected (Fig. 4.6C, mock). In contrast, in PV-infected cells, Arf1, 4, 5, and 6 showed an intact

localization in the ROs in the presence of BFA (Fig. 5.6C, PV 5 hpi). Arf3, however, was released into the cytoplasm after BFA addition. These data suggest that contrary to the rapid activation-deactivation cycle in non-infected cells, once recruited to the replication membranes, all Arfs, except Arf3, likely remain for a prolonged time in the GTP-bound state.

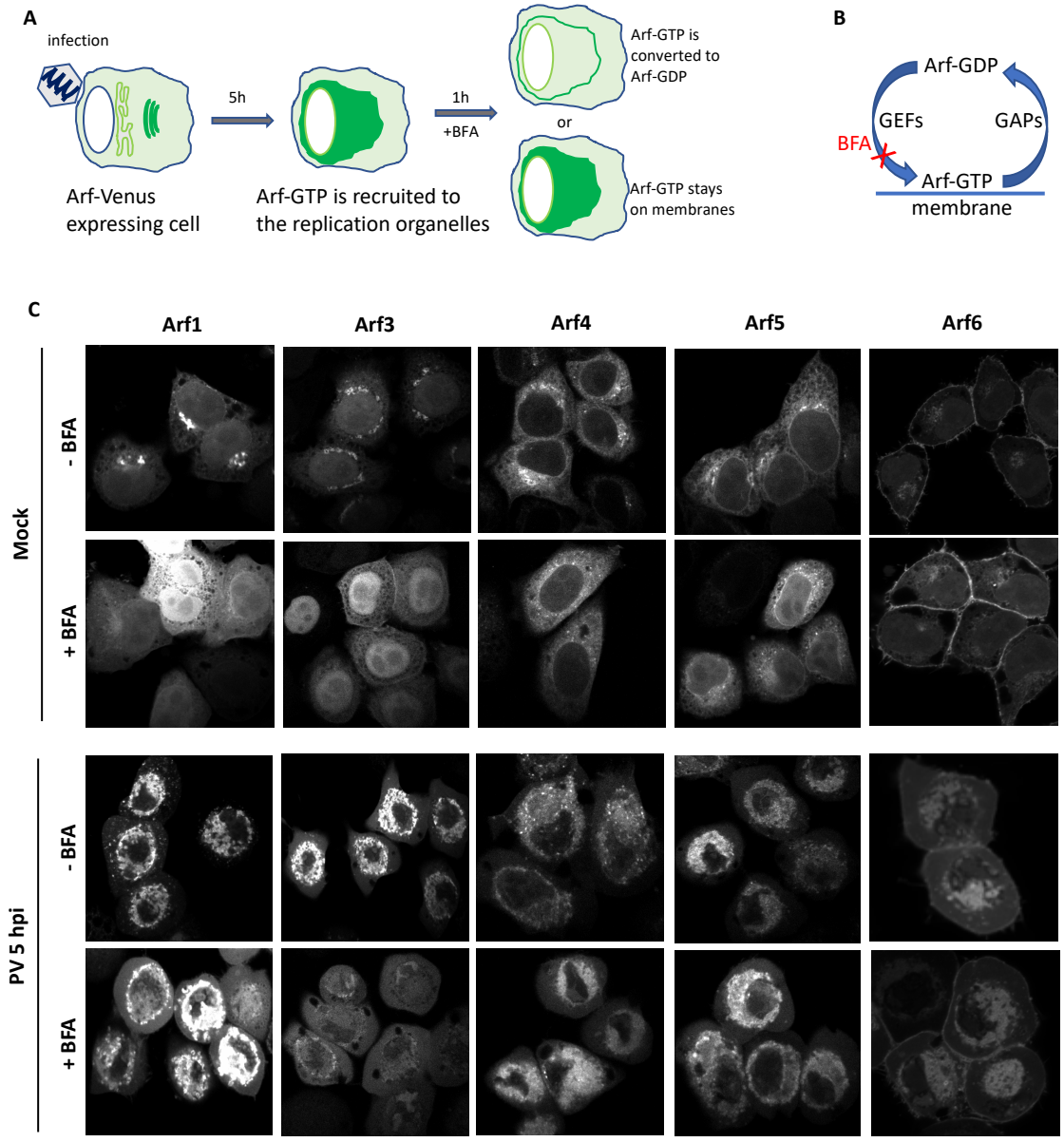

Figure 4.6 Only Arf3 requires constant GEF activity to stay associated with the replication membranes. (A) Scheme of the experiment with the addition of brefeldin A (BFA), an inhibitor of GBF1, to the infected cells upon the formation of well-developed replication organelles. **(B)** Scheme of Arf cycling through membrane-bound GTP- and cytoplasmic GDP-bound forms. The guanidine nucleotide activating factors (GEFs) may be inhibited by BFA, while the GTPase-activating proteins (GAP) are still functional. **(C)** Arf-GFP expressing cells were infected (mock-infected) with 50 PFU/cell of PV for 5h, followed by 1h treatment with 1 μg/ml BFA. No other manipulations with cells were performed to maximally preserve the pattern of Arf recruitment.

4.3.7 Arf1 depletion strongly increases the sensitivity of viral replication to GBF1 inhibition.

The results obtained here and previously reported data suggest that activated Arfs constitute an important component of the specific biochemical environment of the enterovirus replication organelles, yet their mechanistic role in the replication process remains enigmatic. Moreover, conflicting data are available regarding the functions of distinct human Arf isoforms in enterovirus replication. Small interfering (siRNA)-mediated depletion or CRISPR/CAS-mediated knockout of an individual or pairwise combinations of Arfs did not demonstrate a significant effect on the replication of Coxsackievirus B3 or B4, but the simultaneous depletion of both Arf1 and Arf3 was reported to inhibit replication of enterovirus 71 (56, 120, 223).

We hypothesized that since enterovirus replication depends on the activity of GBF1 and is inhibited by BFA (16, 120), the depletion of the Arf isoform(s) that are important for the replication process will increase the sensitivity of infection to BFA. Since reliable Arf isoform-specific antibodies are not readily available, we first evaluated the efficacy and specificity of the previously reported Arf isoform-specific siRNAs (148, 221) using our cell lines expressing individual Arf-GFP constructs. Each Arf isoform was individually targeted by two different siRNAs. The loss of the corresponding fluorescent signal and the western blot performed with anti-GFP antibodies confirmed the high specificity of the siRNAs, with the maximum depletion level achieved 72 h after siRNA transfection (Fig. 4.7A and data not shown). We observed that treatment with one siRNA from the pair was sometimes more toxic to the cells, even though they showed similar depletion efficiency, and the siRNAs with the least toxicity were always chosen for subsequent experiments. To

monitor the effect of individual Arf depletion on the sensitivity of replication to GBF1 inhibition, a quantitative polio replicon replication assay was performed on the third day after siRNA transfection in the absence or the presence of 0.125 and 0.5 μg/ml of BFA, which only partially (down to ~40% to 50% and ~10% to 20% of the control, respectively) inhibit polio replication in the cells transfected with scrambled siRNA control.

In the absence of BFA, PV replication was supported in the individual Arf knocked down cells at the same level as in control siRNA-transfected cells except for Arf3, whose depletion was the most toxic to cells (Fig. 4.7B). This suggests that either a small portion of a particular Arf remaining after siRNA treatment was sufficient to support replication or that other Arfs can compensate for a single Arf loss. However, the relative replication efficiencies of the polio replicon in Arf3-depleted cells were the same as those in control cells throughout the range of BFA concentrations (Fig. 4.7B). Similarly, in the cells depleted of Arf5, the replication was indistinguishable from that in control cells either in the presence or in the absence of BFA. The depletion of Arf4 repeatedly demonstrated a noticeable stimulatory effect on replication, regardless of the presence of the inhibitor. The most dramatic effect on BFA sensitivity was observed in Arf1-depleted cells. In the presence of even the smaller concentration of BFA, the replication was virtually completely inhibited, even though it was still effective in control cells (Fig. 4.7B). Surprisingly, replication of the polio replicon in cells with knockdown Arf6 expression was slightly but statistically significantly inhibited in the presence of BFA.

Collectively, these data support the conclusion that Arf1 account for the most essential Arf isoform critically involved in the BFA-sensitive GBF1-controlled complex of

reactions supporting enterovirus replication. In addition, our results suggest that Arf6 also specifically contributes to the development and functioning of the replication organelles.

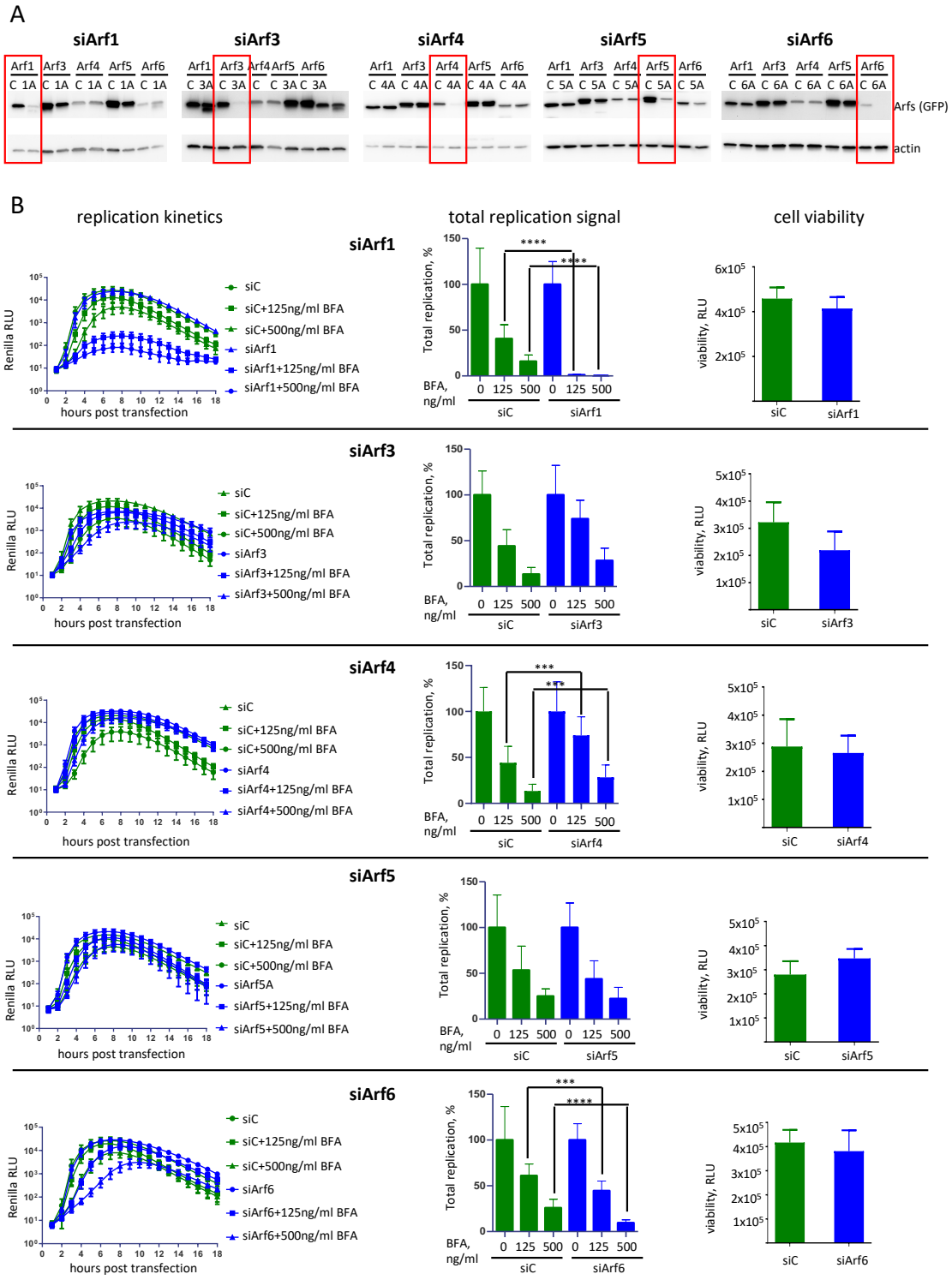
A
siArf1
siArf3
siArf4
siArf5
siArf6
Arf1 Arf3 Arf4 Arf5 Arf6
C 1A C 1A C 1A C 1A C 1A
C 3A C 3A C 3A C 3A C 3A
C 4A C 4A C 4A C 4A C 4A
C 5A C 5A C 5A C 5A C 5A
C 6A C 6A C 6A C 6A C 6A
Arfs (GFP)
actin
B
replication kinetics
total replication signal
cell viability
siArf1
siArf3
siArf4
siArf5
siArf6
Renilla RLU
hours post transfection
siC
siC+125ng/ml BFA
siC+500ng/ml BFA
siArf1
siArf1+125ng/ml BFA
siArf1+500ng/ml BFA
siArf3
siArf3+125ng/ml BFA
siArf3+500ng/ml BFA
siArf4
siArf4+125ng/ml BFA
siArf4+500ng/ml BFA
siArf5A
siArf5+125ng/ml BFA
siArf5+500ng/ml BFA
siArf6
siArf6+125ng/ml BFA
siArf6+500ng/ml BFA
Total replication, %
BFA, ng/ml
0 125 500 0 125 500
viability, RLU

Figure 4.7 Arf1 accounts for the determining factor in the sensitivity of replication to GBF1 inhibition. (A) Specificity and efficiency of siRNA targeting were assessed after siRNA gene silencing followed by immunoblotting. HeLa cell lines expressing individual Arf-GFP fusions were transfected with isoform-specific siRNAs (e.g., 1A corresponds to anti-Arf1 siRNA) or scrambled siRNA control. The cells were lysed on the third day after siRNA transfection and analyzed by western blotting with anti-GFP antibodies. **(B)** HeLa cells were treated with Arf isoform-specific siRNAs (or scrambled siRNA, siC) and on the third day after siRNA transfection were transfected with a polio replicon RNA coding for a *Renilla* luciferase gene. The cells were incubated with the indicated concentrations of BFA and the *Renilla* signal was monitored in live cells every hour for 18 h after replicon RNA transfection. The total replication signal was calculated and normalization was performed for each sample for the replication signal in the absence of the inhibitor. A parallel sample of siRNA-transfected cells was used for cell viability assay.

4.3 Discussion

Enteroviruses are non-enveloped viruses containing a ~7.5 kb positive single-strand RNA. Due to the small genome size synthetizing a limited number of proteins, enteroviruses depend entirely on host cell factors to complete their replication cycle. During infection, enteroviruses generate unique membranous structures called the replication organelles. The development of these structures is an essential step during virus infection in that they harbor the viral replication complexes. The viral proteins reorganize multiple cellular membrane metabolisms and highjack host cell proteins to the replication sites. Thus, the ROs are enriched in certain cellular membrane trafficking and lipid metabolism proteins whose activity is required to support the effective functioning of the viral replication machinery. However, the mechanistic details of how the cellular factors contribute to viral RNA replication are still poorly understood.

A Golgi resident protein, GBF1, is a guanine nucleotide exchange factor for small cellular Arf GTPases (Arf-GEF) and is recruited to the replication organelles through interaction with the viral protein 3A. It is well established that GBF1's Arf-GEF activity is

essential for viral replication (16, 120, 217, 228-230). However, it is much less clear which Arf isoforms activated by GBF1 are required to support the replication and how these GTPases are involved in the replication process. In this study, we generated cell lines stably expressing individual human Arf isoforms C-terminally tagged to a fluorescent protein, enabling us to investigate the dynamics of each Arf isoform during enterovirus infection.

We showed that Arf1 accounts for the first isoform that is recruited to the replication organelles. By the end of the replication cycle, all Arfs were observed in the replication sites in almost all cells. Surprisingly, even Arf6, which in non-infected cells is almost exclusively localized on the plasma membrane and is not normally activated by GBF1, was significantly enriched on the replication organelles by the end of the infectious cycle. Detecting all Arf isoforms in the replication organelles indicates that these newly reorganized membranes have a unique environment with a particular composition of Arfs and their effector proteins that never exist in a normal cell since there is not a single place containing all Arfs in an uninfected cell. Importantly, the similar recruitment of all Arfs to the replication organelles was observed upon infection of such distantly related enteroviruses as poliovirus and CVB3, suggesting that it represents a commonality of requirements for enterovirus replication.

In non-infected cells, Arfs undergo rapid cycling between active membrane-associated GTP-bound and inactive cytoplasmic GDP-bound forms. However, after recruitment to the replication organelles, all Arfs except Arf3 became insensitive to the inhibition of Arf-GEF activity, indicating that they remain for a prolonged time in a GTP-bound form. These data indicate that the metabolism of Arf-associated reactions is very

different between infected and non-infected cells. Whether the distinctive behavior of Arf3 has a particular significance for infection requires further investigation.

The detailed analysis of the localization of viral antigens and dsRNA relative to the Arf1-enriched domains on the ROs revealed distinct types of behavior. Among the nonstructural proteins, only 2B showed a strong colocalization with the Arf1-contained membranes, whereas the membrane-targeting proteins 3A and 2C were less associated with these regions, especially at the early stages of infection. Only a minimal amount of the RNA-dependent RNA polymerase 3D colocalized with Arfs on replication membranes, with most of the protein found in the cytoplasm without apparent association with any membranous structures. This is consistent with the earlier reports of a significant amount of 3D in the soluble cytoplasmic fractions of infected cells (153, 215). Such extensive localization of the viral nonstructural proteins outside the replication organelles suggests that they have important replication-independent functions that remain virtually unexplored. The fully assembled virions also showed a strong association with the Arf1-enriched domains at the early-middle stage of infection, indicating that at least at these steps, the major part of the progeny virus is still tightly associated with the membranes of the ROs, and is not significantly exported from the cell via possible non-lytic pathways. Interestingly, the signal for dsRNA, an intermediate of the RNA replication process, was localized adjacent to the Arf1-enriched areas but was often strictly separated in distinct Arf-free loci. Such sequestration of dsRNAs within biochemically distinct membranous domains may be functionally analogous to the confinement of the dsRNA within membrane invaginations and double-membrane vesicles observed in other (+) RNA virus systems (57, 110, 115, 183, 186, 193, 227). This may explain the importance of the proper

development of the membranous scaffold of the enterovirus replication organelles in evading the innate immune response (219).

Conflicting data are available regarding the contribution of distinct Arfs to the enterovirus replication process. The knockout or knockdown of expression of individual Arfs, or pairs thereof, was tolerated by diverse enteroviruses remarkably well, suggesting a higher level of Arf redundancy in the viral replication than in the cellular metabolism (56, 120). Besides, the inhibition of enterovirus infection by compounds blocking the Arf-GEF activity of GBF1 could be relieved only by overexpression of GBF1 itself but not by any individual Arf in either the wild-type or the constitutively active form (16, 120). In this study, we observed similar results for poliovirus replication in the individual Arf knocked-down cell such that viral RNA replication remained intact in the individual Arf knocked-down cells. This suggests that either a small portion of a particular Arf remaining after siRNA treatment was sufficient to support replication or that other Arfs can compensate for a single Arf loss.

Here, we investigated if depletion of individual Arfs changes the sensitivity of infection to inhibition of the Arf-GEF activity of GBF1. We observed that knockdown of Arf1 and, to a lesser extent, Arf6 significantly decreased replicon replication in the presence of an inhibitor of GBF1 at concentrations that only partially suppressed the replication in control cells. Curiously, depletion of Arf4 was somewhat stimulatory for viral replication both in the absence and in the presence of BFA, suggesting that Arf4 may be competing with another GBF1-activated Arf(s) that promotes replication. Together with the observations that Arf1 was the first Arf associated with the replication organelles at the

beginning of infection, our data suggest that the GBF1-Arf1 axis is the most important contributor to the development and/or functioning of the replication organelles.

Overall, our work elucidated important details of the dynamic changes in the GBF1-dependent activation of small Arf GTPases during enterovirus infection and documented that unique Arf-mediated alterations in cellular membrane metabolism occur at distinct stages of viral replication. Our work provides foundational knowledge that could be exploited in the development of therapeutics targeting only infected cells.

Chapter 5: APEX2-GBF1 Proximity Biotinylation Revealed Multiple Host Factors Modulating Enterovirus Replication

5.1 Introduction

Enteroviruses' small genome size and consequently a limited repertoire of viral proteins implies that multiple host factors should support the viral replication process. Over the years, multiple host proteins that are required for or facilitate the development of enterovirus infection have been identified (133, 163); however, the full catalog of all the cellular proteins that have been implicated in the enterovirus life cycle is yet to be compiled. The two major groups are the host nucleic acid metabolism proteins that modulate translation and/or replication of the viral RNA and membrane metabolism proteins that are hijacked to support the structural and functional development of the viral replication organelles. Currently, neither the stoichiometry of the viral proteins nor the full spectrum of the cellular factors required for the activity of the enterovirus replication complexes is known.

Previously, we showed that the cellular protein GBF1 is recruited to the replication organelles through direct interaction with the enterovirus non-structural protein 3A, and its activity is required to support the viral RNA replication (16, 120, 230). Thus, GBF1 is likely localized close to the active replication complexes on the replication organelles. In this study, we took advantage of a strict dependence of enterovirus replication on GBF1 to perform a proteomics characterization of the replication organelles. GBF1 is a large multi-domain protein normally engaged in multiple protein-protein and protein-membrane interactions (100). Our previous systematic analysis of the GBF1 determinants required to

support enterovirus replication revealed that protein's C terminal part is dispensable for virus replication, but essential for cellular metabolisms (17, 216). Such different requirements for GBF1's domains for supporting the cellular metabolisms and virus replication bring the possibility that the interactome profile of GBF1 varies in non-infected and enterovirus-infected cells. 3A recruitment of GBF1 into the replication organelles may change the protein's structure so that some GBF1's partners in non-infected cells are no longer interacting with the protein during virus infection, while some new proteins interact with the 3A-recruited GBF1 in the replication membranes. Here, to reduce the background of the proteins that are not likely to be important for viral replication, we used a C-terminally truncated GBF1 to generate a fusion with a peroxidase APEX2 (118).

The proximity biotin-labeling technique is a powerful tool for identifying the proteome composition of intracellular compartments and structures as well as protein-protein interactions in living cells. In this technique, a bait protein tagged to an enzyme (either a biotin ligase or a peroxidase) is introduced into a cell where the enzyme utilizes biotin or its phenolic derivatives, such as biotin phenol, as a substrate to label the proteins in the vicinity of the bait protein (67, 108). Since the biotin-labeling reaction occurs in a living cell, nearby proteins can be labeled during their natural dynamics and movement. The strong interaction of biotin with streptavidin allows easy and efficient purification of biotinylated proteins. The biotin-labeled proteins are then identified and characterized by blotting and mass spectrometry. Thus far, this technique has been applied to identify the localization and dynamics of various cellular proteins.

The first-established biotin-labeling method, BioID, was defined by Roux et al. in 2012. In this method, a construct containing a bait protein tagged to an engineered

Escherichia coli-derived biotin ligase (BirA*) is introduced into a cell in which the labeling process happens after adding biotin into the cell culture medium. The biotin-labeled proteins are then isolated and detected by mass spectrometry (185). This method has been used to identify and characterize the localization and dynamics of the vicinal and potential interactors of various proteins in the inner nuclear membrane, nuclear pore complex, and stress granules (107, 235).

The most recent proximity-based labeling technique applies an engineered ascorbate peroxidase (APEX) or its more-catalytically active form, APEX2, as the enzyme to initiate the reaction by generating short-lived biotin-phenoxyl radicals from biotin-phenol in the presence of H_2O_2 (Fig. 5.1) The radicals covalently tag the electron-rich amino acids such as tyrosine of the proteins in the vicinity of the bait. The biotin-labeled proteins are then purified by streptavidin pull-down assay and identified and characterized by blotting or mass spectrometry (118). To date, a proteomic map of different cellular organelles, including mitochondria (inner and outer membranes, intermembrane space, and mitochondrial matrix spaces), ER and ER-PM junction, and lipid droplets (LDs), has been identified by this method (27, 88, 89, 125).

Compared to BioID, the peroxidase labeling approach is significantly faster (2-5 min vs. 12-24 h), so the chances of missing the reactions occurring at the beginning of the process and the toxicity of the biotinylated proteins for some specific cell types are diminished. Besides, the neighboring proteins are biotinylated in a broader radius in the peroxidase labeling technique than BioID (~20 nm vs. ~10), enabling us to determine protein interactions and dynamics in larger cellular compartments. Another difference between APEX and BioID is the smaller molecular weight of APEX than BirA* (27 vs. 35

kDa) (211). In our study, the GBF1 nearby proteins in the replication sites are detected at 2, 4, and 6 h after poliovirus infection, which requires the biotin-labeling reaction to be carried out very quickly. Thus, the APEX-based biotinylation is a better option than the time-consuming BioID for our experiments.

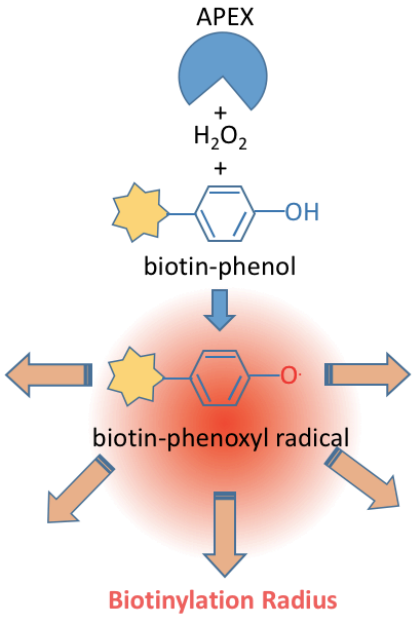

Figure 5.1 Illustration of the APEX-based biotinylation reaction. APEX is an engineered ascorbate peroxidase, which is used as an enzyme in the biotinylation process. The enzyme is tagged to a bait protein, together are introduced into a cell. In the presence of the substrate, biotin phenol, and the activator, H_2O_2, APEX converts biotin phenol to short-lived biotin-phenoxyl radicals, which covalently tag to the electron-rich amino acids such as tyrosine in the nearby proteins. The strong interaction of biotin with streptavidin allows us to efficiently purify the biotinylated proteins using a streptavidin pull-down assay or visualize the regions enriched with biotin-labeled proteins by streptavidin Alexa staining.

Here, we established a cell line stably expressing APEX2-truncated BFA-resistant GBF1 (APEX2-GARG-1060). After performing the biotinylation reaction, in non-infected cells, the truncated APEX2-GBF1 construct diffusely localized in the cytoplasm, but was effectively recruited to the replication organelles and was fully functional in supporting poliovirus replication. Accordingly, the profile of the biotinylated proteins isolated from mock- and poliovirus-infected cells was significantly different. Interestingly, among the biotinylated viral proteins, i.e., those localized close to GBF1, the intermediate products of

the polyprotein processing were overrepresented, suggesting that either the GBF1 environment may be associated with active polyprotein processing or that those incomplete products of proteolysis may perform specific functions in the GBF1-enriched domains of the replication organelles. Among the biotinylated cellular proteins in infected cells were the known cellular factors recruited to the ROs, including PI4KIIIβ, OSBP, and ACBD3, indicating that these proteins are localized close to GBF1. About 15% of the proteins identified in MS have been previously reported in the supporting enterovirus replication, validating our approach. The rest, 85% of the proteins identified by MS, have not been previously associated with enterovirus infection. Gene ontology analysis revealed a significant enrichment of RNA binding and mRNA metabolic processes, suggesting a close localization of GBF1 to the RNA replication complexes. siRNA knockdown functional analysis of the selected proteins showed the recruitment of both proviral and antiviral factors to the ROs.

5.2 Results

5.2.1 Establishment and characterization of an APEX2-GBF1 system for proximity biotinylation

We adapted the APEX2 biotinylation system to efficiently identify proteins localized nearby GBF1 in the replication organelles. First, we introduced several modifications to GBF1's structure. Previously published data showed that the C terminal part of GBF1 is required for cellular metabolism but is dispensable for polio replication (17, 217). Thus, we used a C-terminally truncated GBF1 mutant downstream of the HDS1

domain, which is expected to have a lower level of interactions with proteins non-essential for viral replication. We also previously developed a GBF1 construct containing a Sec7d from another cellular Arf-GEF, ARNO, which is not sensitive to BFA (GARG, from GBF1-ARNO-GBF1) (29). The advantage of such BFA-insensitive constructs is that BFA can inactivate the endogenous GBF1 so this exogenously introduced BFA-insensitive GBF1 derivative will exclusively support the replication functions in the experiments. Finally, a FLAG-tagged APEX2 was N-terminally fused to the GARG truncated at the end of the HDS1 domain (APEX2-GARG-1060 construct) (Fig. 5.2A).

To see if APEX2 fusion is compatible with the functioning of the GARG construct in viral replication, a polio replicon replication assay was performed in the HeLa cells transfected with a plasmid expressing either APEX2-GARG-1060 construct, EGFP-GARG-1060 (positive control), or an empty vector, pUC, (negative control) in the absence or presence of BFA. As shown in Fig 5.2B, a robust polio replicon replication was observed in HeLa cells transiently transfected with either EGFP-GARG-1060 (positive control) or APEX2-GARG-1060 in the absence or the presence of 2 μg/ml BFA. In contrast, polio RNA replication was blocked in the cells transfected with an empty vector in the presence of BFA. Thus, the APEX2-GARG-1060 construct is fully functional in polio replication. The slight replication decrease observed in the EGFP-GARG-1060- and APEX2-GARG-1060- transfected cells after BFA addition is due to the low transfection efficiency, such that only about 60% of the cells were transfected with the corresponding plasmid.

Transiently transfection of DNA is not well suited for viral infection, and proteomics studies since the level of transgene expression varies greatly and the presence of the DNA in the cytoplasm triggers innate immune signaling (85). To address these

issues, we generated a cell line stably expressing APEX2-GARG-1060. Further, to generate a culture with a uniformly high level of transgene expression, we performed a clonal selection of transduced cells. After expanding one of the selected clones, we obtained a culture where more than 90% of cells showed strong APEX2-GARG-1060 expression. We then confirmed that these cells are suitable for further proteomics studies by performing polio replicon replication and protein biotinylation assays in the presence of BFA. While RNA replication was inhibited in control HeLa cells in the presence of BFA, it was robustly supported in the HeLa cells stably expressing APEX2-GARG-1060 when the endogenous GBF1 was blocked by the inhibitor (Fig. 5.2C). This stable cell line was used for all further experiments which were performed in the presence of BFA so that the replication was supported exclusively by APEX2-GARG-1060.

Next, we assessed the biotin-labeling process in the stable cells expressing APEX2-GARG-1060 (mock and PV-infected) in the presence of BFA by microscopy. Cells were infected (or mock-infected) with poliovirus at a MOI of 10 PFU/cell. At 4 hpi (in the middle of the infection cycle), the reaction was performed for 3 min by adding H_2O_2 for a final concentration of 20 μM in the presence of 500 μM biotin-phenol. Cells were then stained with a fluorescent streptavidin conjugate to visualize the biotinylated proteins and with an antibody against the viral non-structural protein 3A. As shown in Fig 5.2D, a diffused cytoplasmic biotin-labeling pattern was observed in mock-infected cells, consistent with the lack of specific membrane-targeting determinants of APEX2-GARG-1060 at the C-terminal domain. At the same time, the biotin-labeled proteins were detected exclusively on the ROs membranes, where they colocalized with the viral protein 3A. These

observations revealed that the APEX2-GARG-1060 construct is translocated to the viral replication organelles, where it can efficiently biotinylate nearby proteins.

The specificity of the biotinylation reaction was further characterized by omitting either the substrate biotin-phenol, the activator H_2O_2, or both from the system. HeLa cells stably expressing APEX2-GARG-1060 were infected (or mock-infected) with 10 PFU/cell of poliovirus. At 4 hpi, cells were incubated with a medium containing either biotin-phenol, H_2O_2, both, or neither of the compounds. Western blot analysis with streptavidin-HRP conjugate showed two endogenous bands of similar intensity in all the samples, likely corresponding to the pyruvate carboxylase and mitochondrial 3-methylcrotonyl carboxylase, biotin-containing enzymes previously reported in studies with APEX biotinylation (77, 89, 90). At the same time, only samples incubated in the presence of both compounds showed extensive biotinylation of additional proteins, confirming the specificity of the biotinylation reaction (Fig. 5.2E).

These data indicate that the APEX2-GARG-1060 construct efficiently supports poliovirus replication; it is recruited to the replication organelles and can specifically biotinylate proteins associated with these structures.

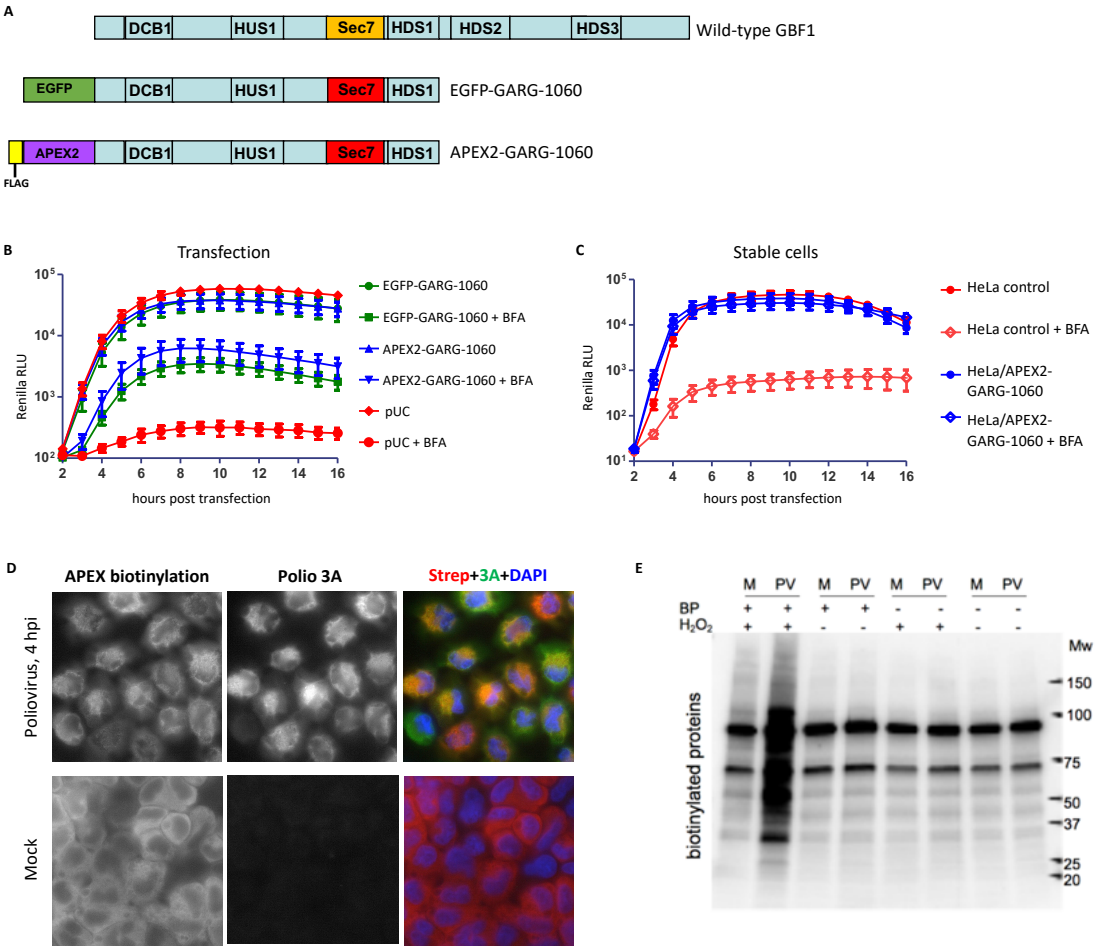

Figure 5.2 Establishment and characterization of an APEX2-GBF1 system for proximity biotinylation. (A) Illustration of full-length wild-type GBF1 (upper) and EGFP-GARG-1060 and APEX2-GARG-1060 (lower). The GARG-1060 constructs are C-terminally truncated downstream of the HDS1 domain and the Sec7d was replaced by a Sec7d from ARNO, a BFA-insensitive GEF. **(B)** A polio replicon replication assay was performed in the HeLa cells transiently transfected with either EGFP-GARG-1060 (positive control), APEX2-GARG-1060 or an empty vector, pUC, (negative control) in the absence or presence of 2 μg/ml BFA. **(C)** A polio replicon replication assay was performed in the HeLa control or HeLa cells stably expressing APEX2-GARG-1060 in the absence or presence of 2 μg/ml BFA. **(D)** The stable cells expressing APEX2-GARG-1060 were infected (or mock-infected) with 10 PFU/cell of PV and treated with BFA for 4 h, followed by the biotin-labeling reaction for 3 min and staining for the viral protein 3A (green) and streptavidin Alexa conjugate (red) and Hoechst (blue). (**E**) The specificity of the biotinylation was confirmed by omitting either H_2O_2, biotin, or both form the reaction in mock (M) and polio-infected (PV) cells. The two strong bands in all samples correspond to the endogenous biotinylated proteins, pyruvate carboxylase and mitochondrial 3-methylcrotonyl carboxylase.

5.2.2 Initial characterization of biotin-labeled proteins during a time course of infection using western blot

5.2.2.1 3A-GBF1-enriched domains on the replication organelles have a unique combination of host proteins.

First, we detected the biotinylation level during the time course of poliovirus infection. HeLa cells stably expressing APEX2-GARG-1060 were infected (or mock-infected) with 10 PFU/cell of poliovirus in the presence of 2 μg/ml BFA, followed by running the biotinylation reaction at 2, 4, and 6 hpi for 3 min. The biotinylated proteins were isolated by streptavidin columns and analyzed in a western blot type assay for a global biotinylation pattern using a streptavidin-HRP conjugate (Fig. 5.3A and B). Early on infection at 2 h, no difference was observed in the amount of biotinylated proteins between mock and virus-infected samples. As the infection progressed, the level of biotinylation has not significantly changed in the mock. In contrast, a considerably higher level of biotinylated proteins was detected in the virus-infected samples collected at 4 and 6 hpi compared with the one isolated at an earlier time point, and they were distributed throughout multiple ranges of molecular weights (Fig. 5.3A). Although the pattern of biotinylated proteins was similar in the samples collected at 4 and 6 hpi, the amount of the biotinylated proteins was higher in the sample isolated at 6 h after infection. The total protein level was similar in both samples (mock and virus-infected) at all the time points as indicated by Coomassie Blue staining (data not shown).

We then analyzed whether several cellular factors known to be recruited to the replication organelles are recovered in the biotinylated fraction, which would indicate that they localize close to GBF1 in infected cells. Similar protocols for infection, biotinylation

reaction, and protein purification were applied as described in Fig 5.3B. Similar level of all proteins tested was observed in the whole cell input collected from mock and virus-infected samples. In contrast, in the streptavidin-enriched samples, we observed a specific increase of the signals only in the infected samples collected at 4, and especially 6 hpi, for ACBD3, OSBP, and PI4KIIIβ, which are involved in the PI4P and cholesterol enrichment of the replication organelles (Fig. 5.3C) (9, 10, 84, 137). Biotinylated OSBP signal was always observed only in infected samples, while traces of PI4IIIKβ and ACBD3 were also visible in the material recovered from mock-infected samples (Fig. 5.3C).

We also analyzed the biotinylation of endogenous GBF1, and the APEX2-GARG-1060 construct itself. Since the APEX2-GARG-1060 construct lacks the C-terminal part containing the epitope recognized by the anti-GBF1 antibody, it was detected by an anti-FLAG antibody. Again, the strongest signals for both biotinylated GBF1 and APEX2-GARG-1060 were observed in the 4 and 6 h infected samples (Fig. 5.3C). The increase of the signal for the APEX2-GARG-1060 constructs in 4 and 6 hpi samples coincided with a noticeable decrease of the corresponding signal in the total input material, likely reflecting the degradation of the cytoplasmic, but not replication organelles-associated pools of the protein (Fig. 5.3C). Surprisingly, we did not detect biotinylated Arfs, even though they are enriched on the replication organelles and at least a fraction of Arf molecules is expected to be localized close to GBF1 (data not shown). Similarly, no signal for ATGL and ACSL3 were identified in the biotinylated fractions. This indicates that either they are not in the direct vicinity of 3A-GBF1-enriched domains on the replication membranes or they are not exposed to the phenoxyl radicals in the electron-rich amino acids position so simply they did not get biotinylated.

Collectively, these data reveal that the proteome of the replication organelles nearby GBF1 is not enriched in all of the known cellular proteins involved in the development/functioning of the replication organelles, suggesting that these membranes are not biochemically homogeneous and likely have specialized domains containing a particular combination of proteins with potentially different functions.

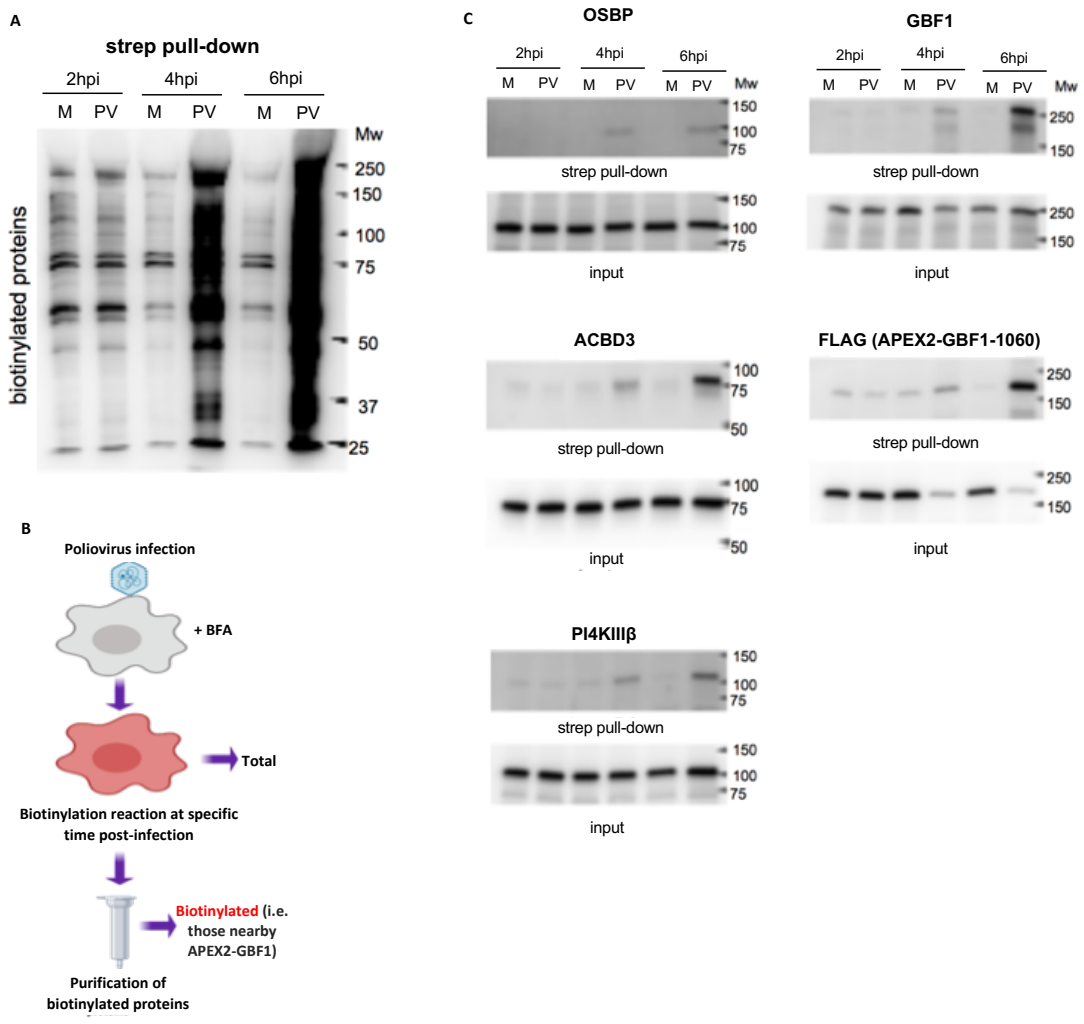

Figure 5.3 Known cellular proteins recruited to the replication organelles are biotinylated by FLAG-APEX2-GARG-1060. (A) HeLa/APEX2-GARG-1060 stable cells were infected (PV) or mock-infected (M) with 10 PFU/cell poliovirus in the presence of 2 μg/ml BFA. At certain time point after infection, the biotinylation was performed, the biotinylated proteins were collected on streptavidin beads, resolved on SDS-PAGE and analyzed in a Western blot with streptavidin-HRP conjugate. **(B)** Scheme of the biotinylation experiment for comparison of the biotinylated protein fraction (strep pull-down) with the total proteins in the cellular lysates (input). **(C)** The stable HeLa cell line expressing FLAG-APEX2-GARG-1060 was infected (PV), or mock-infected (M) with 10 PFU/cell of poliovirus in the presence of 2 μg/ml BFA, the biotinylation reactions were performed at 2, 4, and 6 hpi, and the unfractionated cellular lysates (input) and the biotinylated proteins isolated by streptavidin beads (strep pull-down) were analyzed with the indicated antibodies against known cellular factors recruited to the replication organelles in a western blot. Anti-FLAG antibody recognizes the FLAG-APEX2-GARG-1060 protein.

5.2.2.2 Viral proteins are not equally represented in the GBF1 environment.

Next, we searched the GBF1-enriched domains on the replication membranes for the viral polyprotein fragments. Since the poliovirus genome is expressed as a single polyprotein undergoing a proteolytic processing cascade, the antibodies can recognize both mature and precursor forms of that corresponding antigen. The available panel of antibodies suitable for western blot (VP3, 2B, 2C, 3A, 3D) covers all known intermediate fragments of the poliovirus polyprotein processing and almost all individual proteins except capsid proteins VP0 and VP1, proteases 2A and 3C, and the RNA replication protein primer 3B (Vpg) (Fig. 4.5A, poliovirus genome and polyprotein processing scheme). All the tested viral antigens were present in the biotinylated fraction. Interestingly, while in the input material, the largest amount of the viral antigens was found in the final polyprotein cleavage products, in the biotinylated protein fraction, the antigens of the replication proteins were overrepresented in the intermediate compared to the final polyprotein

cleavage products. For example, an uncleaved precursor P2P3 was clearly detected in the biotinylated fraction with an anti-3A antibody in 6 hpi sample, while this piece of the polyprotein was not visible in the input material (Fig. 5.4B, anti-3A panel). This indicates that the composition of the 3A-recruited-GBF1 domains of the ROs is different from that of the total replication complexes. We also observed a specific increase in the biotinylated fraction of the viral antigen-positive fragments that do not correspond to the canonical products of the viral polyprotein processing. Note the red asterisks marking a 3A-positive fragment in the 15-20 kDa range (Fig 5.4C, anti-3A panel, 6 h p.i), or a 3D-positive fragment of a molecular weight slightly higher than 3D (Fig. 5.4C, anti-3D panel, 6 hpi). This may suggest that the GBF1 environment is associated with active polyprotein maturation, although a preferential enrichment of larger polyprotein fragments due to a higher degree of biotinylation cannot be excluded.

Collectively, these results demonstrate that APEX2-GARG-1060 in infected cells can specifically biotinylate both viral and host proteins associated with the replication organelles and that the samples collected at 6 hpi are the most representative fraction for the characterization of the proteome of the replication organelles.

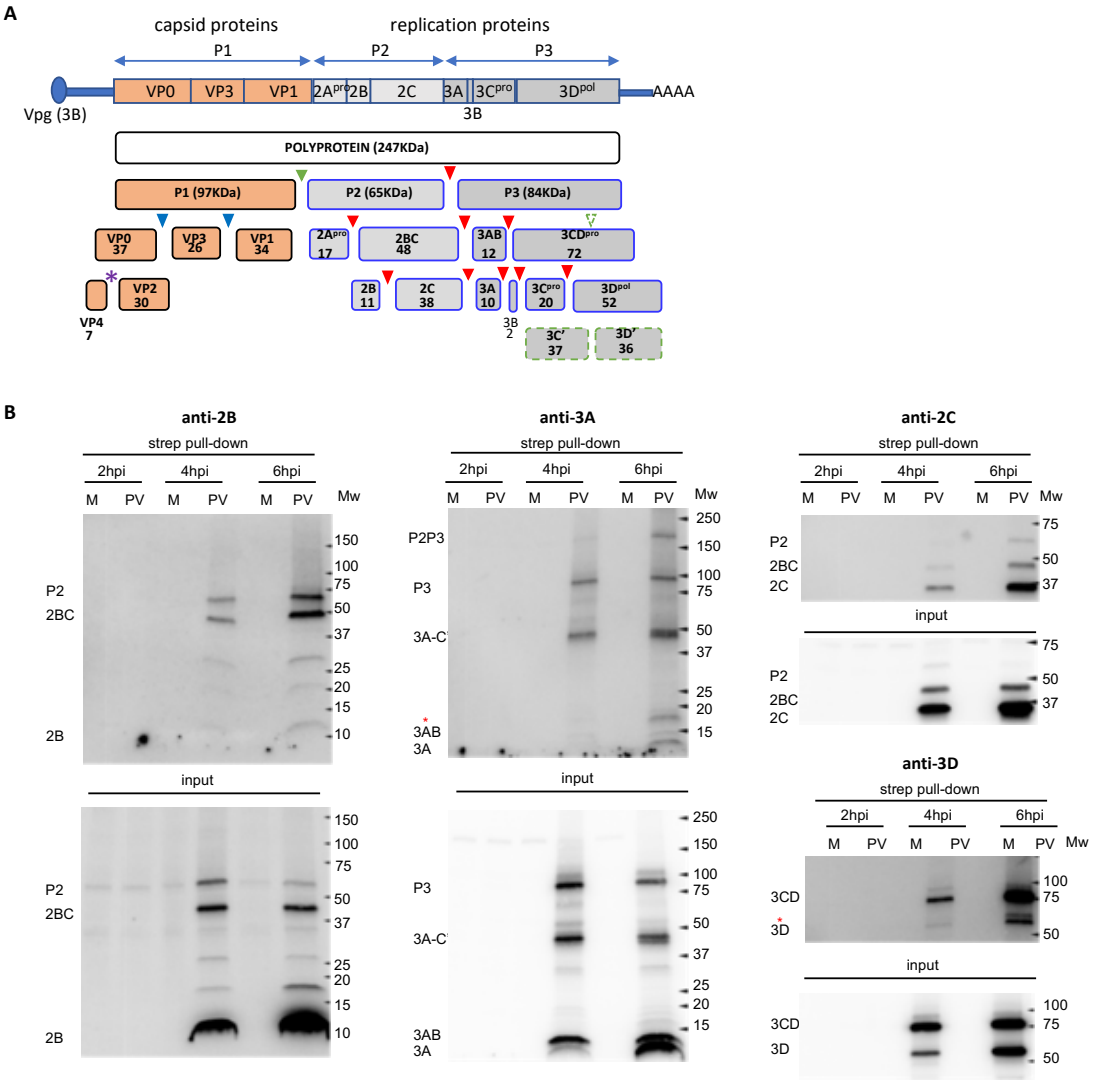

Figure 5.4 Biotinylation of the viral proteins by APEX2-GARG-1060 (A) Schematic illustration of poliovirus genome and polyprotein processing. The cleavage sites for the viral proteases 2A, 3C, and 2CD are indicated by green, red, and blue filled triangles, respectively. The dashed empty green triangle indicates a 2A cleavage site in 3D believed to be dispensable for replication, the purple star indicates an autocatalytic cleavage site in VP0. **(B)** The stable HeLa cells expressing APEX2-GARG-1060 were infected (or mock-infected) with 10 PFU/cell poliovirus in the presence of 2 µg/ml BFA. At 6 hpi, the biotinylation was performed, the biotinylated proteins were collected on streptavidin beads, resolved on SDS-PAGE and analyzed in a western blot with antibodies against indicated viral antigens (VP3, 2B, 2C, 3A, 3B, and 3D). The antibodies recognize the final and intermediate polyprotein cleavage products containing the corresponding antigen. Red stars on anti-3A and anti-3D panels indicate polyprotein fragments that do not match the known stable polyprotein cleavage products. Note the red asterisks marking a 3A-positive fragment in the 15-20 kDa range, or a 3D-positive fragment of a molecular weight slightly higher than 3D.

5.2.3 Characterization of biotin-labeled proteins identified in mass spectrometry (MS)

5.2.3.1 Sample preparation for MS

For the proteomics analysis, HeLa cells stably expressing APEX2-GARG-1060 were seeded into T-225 cm^2 flasks and infected (or mock-infected) with 10 PFU/cell of poliovirus for 6 h in the presence of 2 μg/ml BFA. The biotinylation reaction was performed at 6 h p.i, for 3 min. Five independent replicates were prepared for mock and virus-infected samples, and the aliquots of the isolated proteins were individually assessed in a western blot assay with a streptavidin-HRP conjugate. In all experiments, a similar pattern of a highly increased amount of biotinylated proteins in infected samples was observed, as expected (Fig. 5.5.A). The rest of the purified biotinylated proteins were pooled together and processed for mass-spectrometry protein identification and label-free quantitation (LFQ).

5.2.3.2 Preliminary analysis of the proteins identified in MS

After filtering the identified proteins from common contaminants, as well as carboxylases which contain naturally covalently attached biotin, and proteins with peroxidase activity which can likely be biotinylated independently of APEX2, 369 and 43 proteins were enriched in the infected and mock-infected sets, respectively. 331/369 proteins were found exclusively in the infected sample, while only 5/43 proteins from the mock-infected sample were not identified in the infected sample. A total of 192 proteins in the infected sample and 37 proteins in the mock-infected sample were detected from two or more peptides. Among the cellular proteins that we previously confirmed to be present

in the biotinylated pool by the western blot analysis (Fig. 5.3C), GBF1 (Q92538) was identified from a total of nine peptides, five of them unique (9 total:5 unique) (further on this designation is used for peptides detected for each protein), while ACBD3 (Q9H3P7) and OSBP1 (P22059) proteins were identified from one peptide each, and PI4KIIIβ (Q9UBF8) was not found.

Since GBF1 was used as the bait protein in this proximity biotinylation system, the presence of at least some known interactors of GBF1 and/or Arf GTPases would be expected. In fact, the protein analysis using the BioGRID database of curated interaction data (162, 199) identified 17 Arf1, one Arf3, four Arf4, three Arf5, and four Arf6 interactors. All Arf4 and Arf5 as well as 12 Arf1 and two Arf6 interactors were identified exclusively among the proteins from the infected sample. Also, 44 proteins were identified as GBF1 interactors, 34 of which were found only in the infected sample.

The global association of the proteins with cellular structures and pathways was analyzed by Gene Ontology (GO) enrichment for the cellular component, molecular function, and biological process categories using the PANTHER classification system (147). In general, the GO enrichment of the proteins collected from the infected sample demonstrated a much higher statistical significance than those isolated from the mock-infected cells, which is consistent with the larger number of proteins identified in the infected isolates (Fig. 5.5B). In both samples, the most statistically significantly enriched categories included proteins associated with the cellular secretory pathway and the chaperon-assisted protein folding. In the mock-infected sample, proteins associated with the proteasome-dependent protein degradation were among the highly enriched proteins. In the infected sample, a significant amount of proteins was also associated with the

cytoskeleton function. Yet, the nucleic acid, and in particular RNA metabolism, emerged as the predominantly enriched GO terms from the infected sample. Interestingly, 17 proteins were associated with dsRNA binding, 10 of which were present only in the infected sample.

We then searched the literature for 369 proteins identified in the poliovirus replication complexes to determine whether they have already been reported in the replication sites of enteroviruses. About 15% of the proteins from the poliovirus-infected sample (55/369) were previously recognized to be involved in replicating enteroviruses, validating our approach. Importantly, our set of proteins from the infected sample contained 38 out of 82 proteins previously identified as interacting with poliovirus RNA using a thiouracil-mediated covalent binding of proteins and RNA (126). The known constituents of the poliovirus replication complex, KH domain-containing, RNA-binding, signal transduction-associated protein 1 (KHDRBS1, Sam68) (140) was identified from 8 total: 2 unique; splicing factor, proline- and glutamine-rich (SFPQ) (60) from 10 total: 6 unique, and polyadenylate-binding protein 1 (PABCP1) (79) from 3 total: 2 unique peptides, exclusively in the infected sample. 6 totals:3 unique peptides shared between poly-(rC)-binding proteins 1 and 2 (PCBP1, 2) (32, 166, 210) were identified in the infected sample while one unique peptide for each PCBP1 and PCBP2 was detected in the mock-infected control. Polypyrimidine tract-binding protein 1 (PTB1) involved in the activation of the enterovirus IRES-driven translation (101, 102) was detected by one peptide in both infected and mock-infected samples.

The poliovirus-specific peptides (207 total: 64 unique) identified by MS analysis were distributed along the whole viral polyprotein, with an intriguing absence of peptides

covering 2B and 3A-3B regions. An increased clustering of the detected peptides was observed in the N-terminus of a capsid protein VP1, 3C-3D junction, and in particular in the 2C region (Fig. 5.5C). This pattern is consistent with the data shown in Fig. 5.4B and confirms that the GBF1 environment on the replication organelles is enriched in the viral structural and replication proteins.

Overall, these data validate the relevance of the identified cellular proteins for poliovirus replication and provide an important insight into the viral and cellular protein environment of the replication organelles nearby GBF1.

A

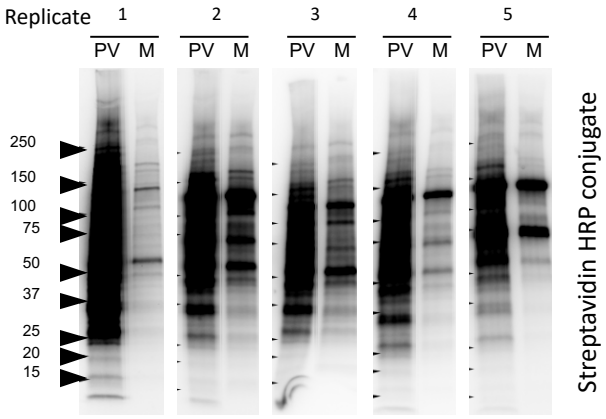

B

GO: cellular component

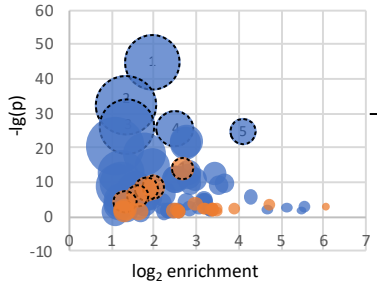

	PV	Size	Gene Ontology	
1.		147	extracellular vesicle (GO:1903561)	secretory pathway
2.		179	vesicle (GO:0031982)	
3.		155	extracellular space (GO:0005615)	
4.		68	ribonucleoprotein complex (GO:1990904)	RNA metabolism
5.		34	melanosome (GO:0042470)	secretory pathway
	Mock	Size	Gene Ontology	
1.		28	extracellular vesicle (GO:1903561)	secretory pathway
2.		28	extracellular space (GO:0005615)	
3.		29	vesicle (GO:0031982)	
4.		28	extracellular region (GO:0005576)	
5.		29	organelle lumen (GO:0043233)	

GO: molecular function

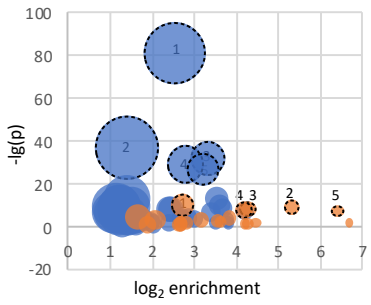

	PV	Size	Gene Ontology	
1.		175	RNA binding (GO:0003723)	RNA metabolism
2.		189	nucleic acid binding (GO:0003676)	
3.		57	cadherin binding (GO:0045296)	cytoskeleton
4.		66	cell adhesion molecule binding (GO:0050839)	
5.		51	mRNA binding (GO:0003729)	RNA metabolism
	Mock	Size	Gene Ontology	
1.		23	RNA binding (GO:0003723)	RNA metabolism
2.		10	unfolded protein binding (GO:0051082)	protein metabolism
3.		12	ubiquitin protein ligase binding (GO:0031625)	
4.		12	ubiquitin-like protein ligase binding (GO:0044389)	
5.		7	protein folding chaperone (GO:0044183)	

GO: biological process

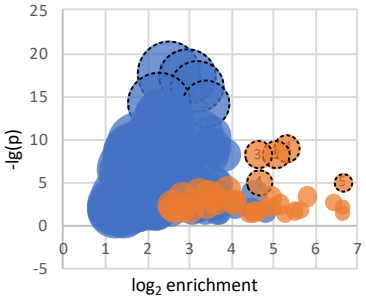

	PV	Size	Gene Ontology	
1.		51	posttranscriptional regulation of gene expression (GO:0010608)	RNA metabolism
2.		40	regulation of mRNA metabolic process (GO:1903311)	
3.		34	protein folding (GO:0006457)	protein metabolism
4.		49	mRNA metabolic process (GO:0016071)	RNA metabolism
5.		28	regulation of RNA splicing (GO:0043484)	
	Mock	Size	Gene Ontology	
1.		10	response to unfolded protein (GO:0006986)	protein metabolism
2.		10	response to topologically incorrect protein (GO:0035966)	
3.		11	protein folding (GO:0006457)	
4.		8	regulation of RNA splicing (GO:0043484)	RNA metabolism
5.		5	protein refolding (GO:0042026)	protein metabolism

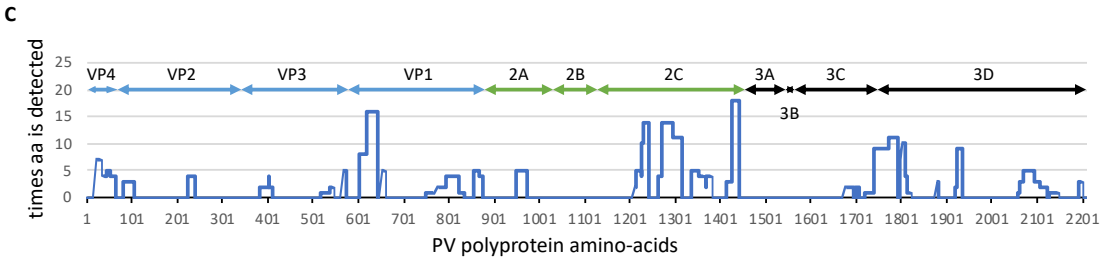

Figure 5.5 MS samples reparation and primary data analysis. (A) Five sets of mock and polio-infected samples were prepared separately as follows: The stable HeLa cells expressing APEX2-GARG-1060 were infected (PV) or mock-infected (M) with 10 PFU/cell poliovirus in the presence of 2 μg/ml BFA. At 6 hpi, the biotinylation was performed, the biotinylated proteins were collected on streptavidin beads, resolved on SDS-PAGE and analyzed in a Western blot with streptavidin-HRP conjugate. The samples from each group (mock or polio) were then pooled for further proteomics analysis. **(B)** Gene ontology (GO) enrichment analysis of the proteomics data was performed using PANTHER classification system. The bubble graphs show the number of proteins associated with a particular GO term. The orange circles represent the mock data, and the blue ones are for the virus-infected cells. The larger the circles, the more proteins associated with that particular GO term. The x-axis shows the $\log_2$ of enrichment over the expected non-specific associations of genes in the dataset with a particular GO term. The y-axis represents the statistical significance of the observed enrichment (negative $\log_{10}$ of P value). The five of the most statistically significantly enriched GO terms for proteins from infected and mock-infected samples are shown. **(C)** The distribution of the poliovirus-specific peptides identified by mass-spectrometry analysis throughout the poliovirus polyprotein. The x-axis shows the reference poliovirus polyprotein based on the number of amino-acids. The y-axis shows how many times a particular peptide is detected.

5.2.3.3 Functional validation of several high-confidence host proteins localized nearby GBF1 in the replication organelles

One of the major goals of this study was to identify novel host factors important for viral replication. Due to some limitations, the functional validation could have not proceeded for all of the newly-identified proteins in the MS data. Thus, we selected a total of 15 proteins (including a positive control for screening experiments) based on the criteria that they should be detected from multiple peptides in the infected sample (i.e. highly

enriched), with the previously uncharacterized role in enterovirus replication, and representing different functional clusters. The selected proteins are grouped as follows:

(1) Glycolytic enzymes: Fructose-bisphosphate aldolase A (AldoA), pyruvate kinase (PKM), L-lactate dehydrogenase chain A and B (LDHA and LDHB) detected from (32 total:15 unique), (15 total:11 unique), (6 total:2 unique) and (4 total: 2 unique) peptides in the infected sample, respectively. Besides being highly enriched, the group of glycolytic enzymes was selected because LDHA and LDHB are reported as Arf interactors, and also the glycolytic pathway provides substrates for *de novo* nucleotide synthesis, which may be important for rapidly replicating RNA viruses (8, 162, 171, 199, 224).

(2) Highly enriched RNA-binding proteins: Heterogeneous nuclear ribonucleoproteins A0, H2, H3, R, U (HNRNPA0, H2, H3, R, U), heterogeneous nuclear ribonucleoprotein Q (SYNCRIP), Ewing Sarcoma Breakpoint Region 1 (EWSR1), and RNA-binding motif protein, X chromosome (RBMX) were among the most enriched in the infected sample (10:3, 15:6, 8:5, 10:6, 27:11, 8:6, 12:5, and 7:6 of total: unique peptides, respectively). SYNCRIP and HNRNPU were previously reported to bind poliovirus RNA in a proteomics screen; however, the depletion of HNRNPU did not affect the virus yield, and the contribution of SYNCRIP was not analyzed (126).

(3) A potential antiviral factor: A dsRNA binding protein ILF3 was identified from 8 total:4 unique peptides in the infected sample. This protein was shown to be important for the establishment of dsRNA-induced antiviral signaling and to either promote or inhibit the replication of diverse viruses (70, 92, 130, 179, 225). The ILF3 gene is expressed as multiple isoforms of the two major variants of 90 kDa and 110 kDa proteins, all of which have two dsRNA binding domains, with an extended C-terminal GQSY-reach region in

the latter (169). A 90 kDa isoform of ILF3 was demonstrated to inhibit translation of a poliovirus-rhinovirus chimera RNA in a cell-type dependent manner by binding to the rhino- but not poliovirus IRES (144).

First, the importance of the selected proteins for the poliovirus infection was assessed using siRNA-mediated knockdown of expression followed by a polio replicon replication or western blot to detect the viral protein 2C accumulation level. This fast and convenient method allows rapid screening of multiple infection samples. The replicon replication assay is independent of virus entry, so it reflects the RNA translation-replication steps of the viral life cycle, while the 2C accumulation during infection also represents the effects of virion-receptor interaction, penetration, and uncoating. Among all the proteins tested in screening, only the depletion of LDHA showed a great deal of cytotoxicity, so its specific effects on polio replication could not be evaluated in this system. As a control for the screening methods, we included siRNA against KHDRBS1 (Sam68) (identified from 8 total: 2 unique peptides in our proteomics dataset), previously shown to bind poliovirus polymerase $3D^{pol}$ and promote viral replication (140). Depletion of Sam68 inhibited polio replication in both replication and infection assays, validating our approach (Fig 5.6A and B- KHDRBS1 panel).

The signal for the viral protein 2C was weaker in the cells treated with siRNA against EWSR1 and AldoA than in the control in western blot, while the 2C level was at least twice as much as the control in the knocked-down HNRNPR, HNRNPH2, HNRNPH3, ILF3-90, and SYNCRIP cells. No significant variation in the 2C level was observed between the control and the cells depleted in HNRNPA0, HNRNPU, LDHB, PKM, RBMX, ILF3-110, and a combination of ILF3-90 and ILF3-110. The blotting results

are representative of two independent experiments for each protein of interest (Fig. 5.6A). In the screening tests, the siRNA knockdown of the protein of interest relies on the sequences that have been previously characterized to be efficient in depleting the corresponding protein in cell (Table 3.1).

Poliovirus replicon replication was decreased in the EWSR1 and AldoA-depleted cells compared to the control, suggesting the importance of these host proteins in supporting poliovirus replication. At the same time, the replicon replication was increased in the ILF3-90 and RBMX knocked-down cells (Fig. 5.6B). The depletion of other proteins demonstrated no considerable changes in polio replicon replication compared with the control (Fig 5.6.B). The replication data were achieved from two or three independent experiments for each protein of interest.

Thus, our screening results reveal novel host factors with stimulatory or inhibitory effects on poliovirus replication.

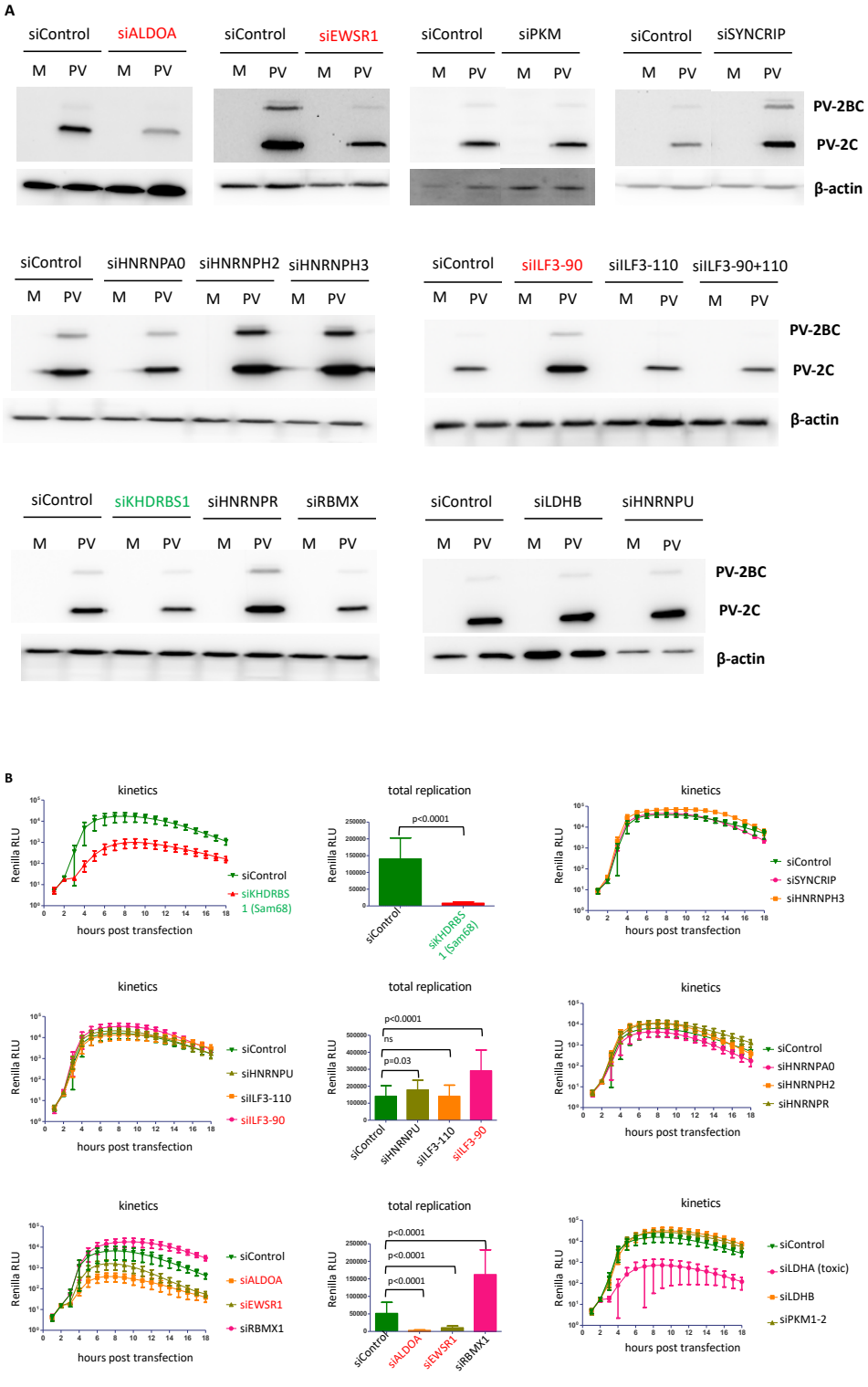
A
siControl
siALDOA
siEWSR1
siPKM
siSYNCRIP
M
PV
PV-2BC
PV-2C
β-actin
siHNRNPA0
siHNRNPH2
siHNRNPH3
siILF3-90
siILF3-110
siILF3-90+110
siKHDRBS1
siHNRNPR
siRBMX
siLDHB
siHNRNPU
B
kinetics
total replication
Renilla RLU
hours post transfection
p<0.0001
ns
p=0.03
p=0.0001
p=0.068
siControl
siKHDRBS 1 (Sam68)
siHNRNPU
siILF3-110
siILF3-90
siSYNCRIP
siHNRNPH3
siHNRNPA0
siHNRNPH2
siHNRNPR
siRBMX1
siLDHA (toxic)
siLDHB
siPKM1-2

Figure 5.6 siRNA-gene silencing screening of the selected proteins, followed by a polio replicon replication assay and western blot. HeLa cells were transfected with siRNAs specific against a protein of interest, or non-targeting control siRNA. **(A)** At 72 h post-transfection, cells were infected with 10 PFU/cell of poliovirus (PV) or mock-infected (M) for 4 h. Cell lysates were collected in the mild lysis buffer and subjected to western blot with an antibody against viral protein 2C and beta-actin as the loading control. **(B)** 72 h after siRNA transfection, a polio replicon replication assay was performed. The total replication was calculated as the area under the corresponding kinetics curves.

For further detailed analysis, we narrowed down the selected proteins into three of them (AldoA, EWSR1, and ILF3-90) whose depletion showed consistent significant effects on polio replication in multiple independent experiments. As shown before, polio replication was decreased in the AldoA and EWSR1-knocked sown cells, while ILF3-90 depletion stimulated polio replication (Fig. 5.7A). At the same time, cell viability and transfection efficiency were monitored in the siRNA-depleted cells using an ATP viability test and western blot, respectively. While similar ATP level was observed in the EWSR1- and ILF3-90-knocked down cells to the control, AldoA depletion resulted in a significantly lower ATP value although no obvious sign of cytotoxicity was observed for these cells. We compared the ATP measurement viability test with another assay based on the activity of mitochondrial dehydrogenase enzymes in reducing tetrazolium salt XTT to a highly colored formazan. Unlike the ATP assay, the XTT test demonstrated no difference in the mitochondrial enzyme activity in the siRNA-depleted cells, suggesting that the negative effect of AldoA depletion on the virus replication may be due to its requirement for ATP production in HeLa cells (Fig. 5.7B).

We then measured the effects of the individual depletion of the selected proteins on the yield of infectious virions using TCID50. At the same time, cell viability and

transfection efficiency were monitored in the siRNA-depleted cells using an ATP viability test and western blot, respectively (Fig. 5.7C). At 72 h post-siRNA transfection, cells were infected with 1 PFU/cell of poliovirus for 6 h, and the viral stocks were harvested after three times freeze-thaw cycles. HeLa cells were infected (or mock-infected) with 10-fold serial dilutions of each viral stock and incubated for 72 h. At least seven separate experiments were performed to determine the viral yield of each sample. The average titer of control cells was about 1*10^8 PFU/ml, while the titer dropped 2 and 3 folds after AldoA and EWSR1 depletion, respectively (5.6*10^7 and 3.6*10^7 PFU/ml). At the same time, the titer of the virus harvested from ILF3-90-knocked down showed about a 2-fold increase to the amount of 2*10^8 PFU/ml (Fig. 5.7C).

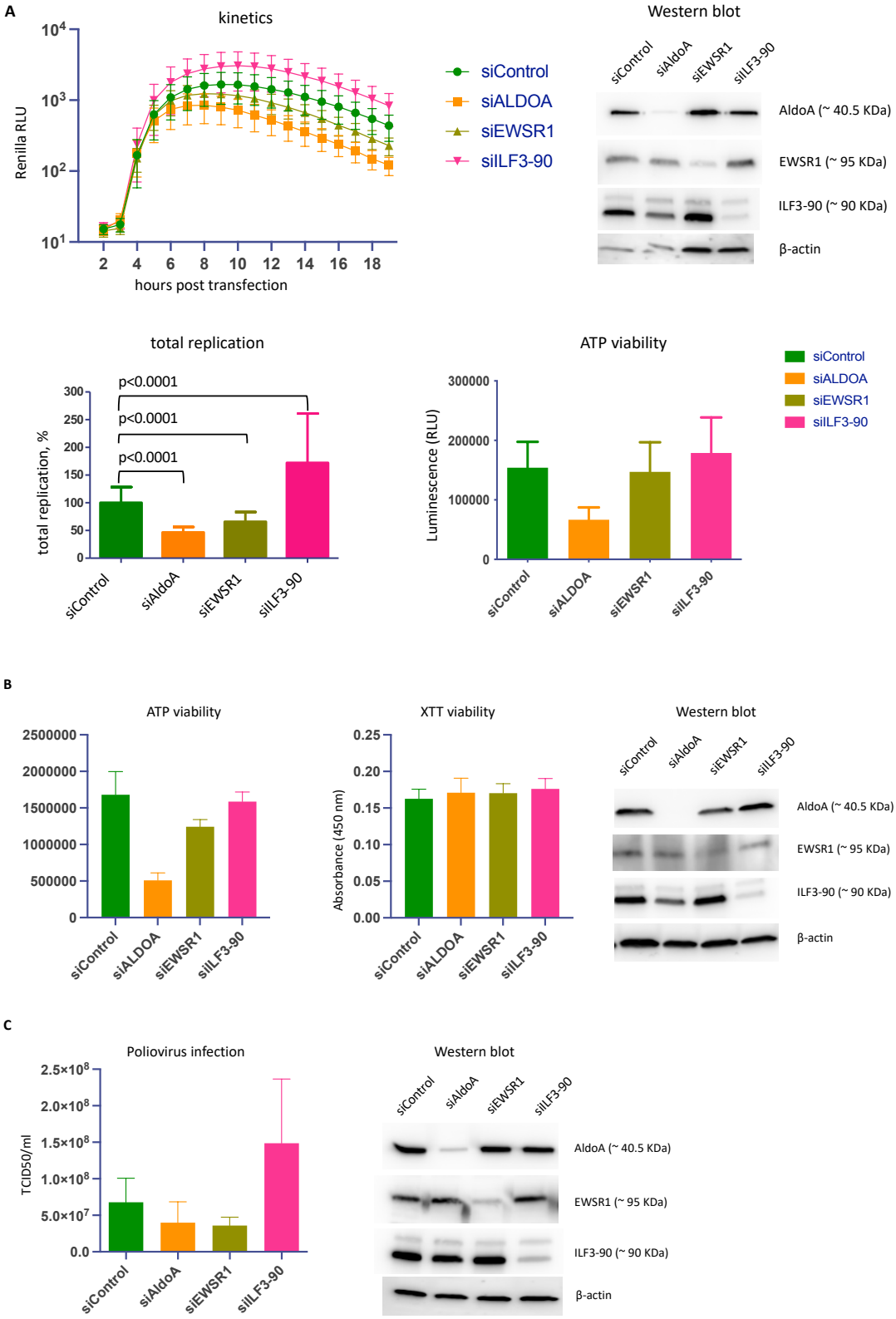
A
kinetics
Renilla RLU
hours post transfection
siControl
siALDOA
siEWSR1
siILF3-90
Western blot
siControl
siAldoA
siEWSR1
siILF3-90
AldoA (~ 40.5 KDa)
EWSR1 (~ 95 KDa)
ILF3-90 (~ 90 KDa)
β-actin
total replication
total replication, %
p<0.0001
p<0.0001
p<0.0001
ATP viability
Luminescence (RLU)
B
ATP viability
XTT viability
Absorbance (450 nm)
Western blot
C
Poliovirus infection
TCID50/ml
Western blot

Figure 5.7 Distinct behavior of the selected proteins on the poliovirus RNA replication. **(A)** HeLa cells were transfected with siRNAs specific against AldoA, EWSR1 and ILF3-90, or non-targeting control siRNA, and polio replicon replication assay was performed 72 h post siRNA transfection**.** The total replication was calculated as the area under the corresponding kinetics curves. No significant cell toxicity was observed after siRNA gene silencing for an individual protein of interest. The transfection efficiency for each protein knock down experiment was evaluated by western blot. **(B)** HeLa cells were transfected with siRNAs specific against AldoA, EWSR1 and ILF3-90, or non-targeting control siRNA. 72 h after siRNA transfection, cell viability was measured with an ATP test and an XTT growth assay. The transfection efficiency for each protein knock down experiment was evaluated by western blot. **(C)** TCID50 assay was performed to measure viral yield after knocking down of an individual protein. The transfection efficiency for each protein knock down experiment was evaluated by western blot.

Next, we examined how different the selected proteins control the replication of diverse enteroviruses. We observed similar results for CVB3 RNA replication in the AldoA and EWSR1-depleted cells such that the replication was decreased by about two folds (Fig. 5.8A). However, unlike polio, CVB3 replicated in the ILF3-90 depleted cells at the same level as control. Parallel samples were prepared for cell viability and western blot. The yield of the infectious CVB3 virions propagated in the AldoA and EWSR1 knocked-down cells was consistent with the replication data (Fig. 5.8B). However, ILF3-90 depletion showed a considerable increase in the viral yield while no effect was observed during CVB3 replicon replication. This may reflect the difference in the experimental systems used. In the replicon replication assay, cells are transfected with the RNA replicon, so many more RNA genomes are introduced into the cell compared to typical infection, making the replication less sensitive to the presence of antiviral factors directly binding viral RNA. However, in the titration assay, cells are infected with a low MOI, which much more closely reflects the natural infection in a host when few genomes start the replication process, and the cellular antiviral factors can effectively interfere with it

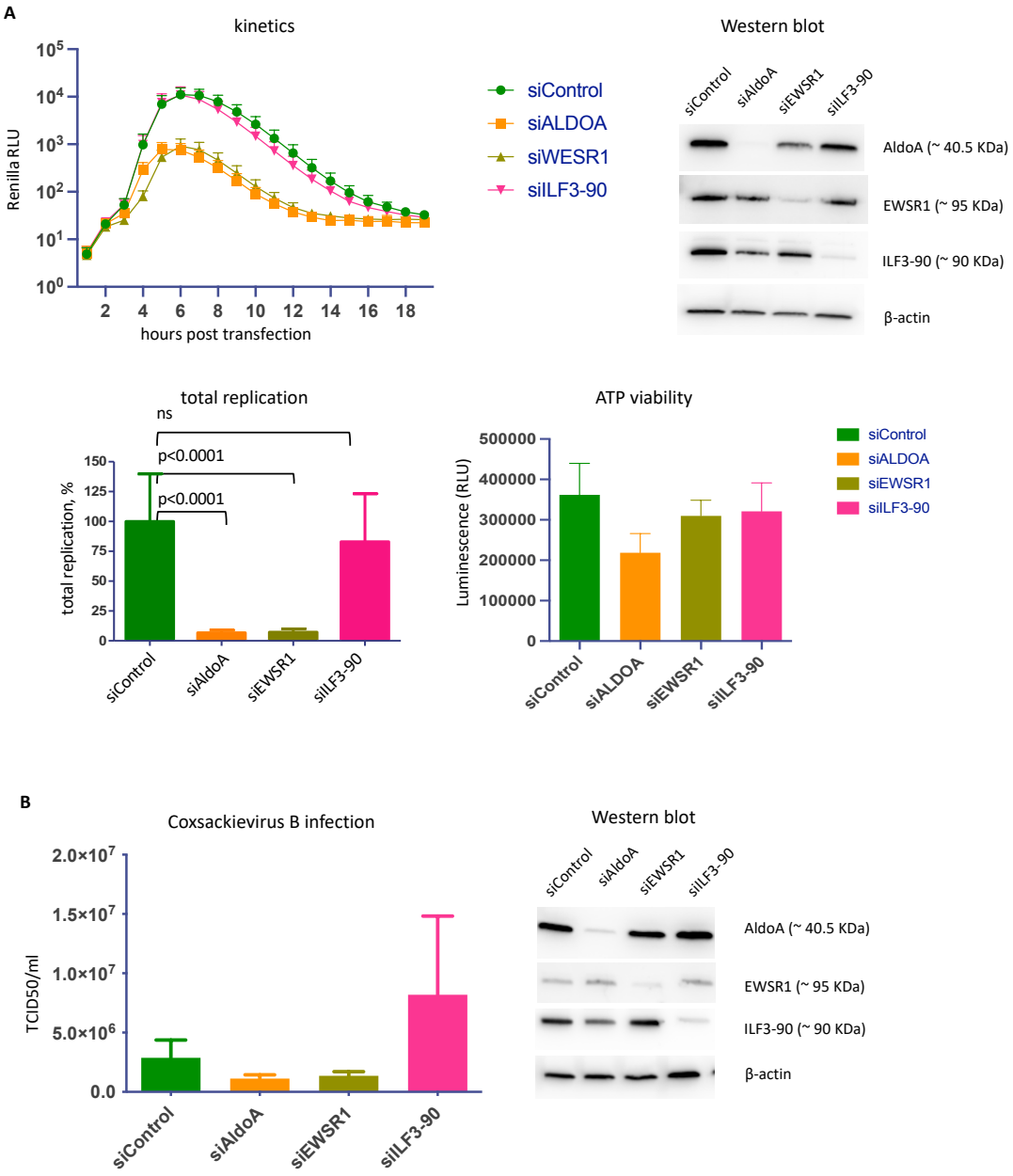

Figure 5.8 Distinct behavior of the selected proteins on the CVB3 RNA replication. (A) HeLa cells were transfected with siRNAs specific against AldoA, EWSR1 and ILF3-90, or non-targeting control siRNA, and CVB3 replicon replication assay was performed 72 h post siRNA transfection**.** The total replication was calculated as the area under the corresponding kinetics curves. No significant cell toxicity was observed after siRNA gene silencing for an individual protein of interest. The transfection efficiency for each protein knock down experiment was evaluated by western blot. **(B)** TCID50 assay was performed to measure viral yield after knocking down of an individual protein. The transfection efficiency for each protein knock down experiment was evaluated by western blot.

To further investigate if the depletion of these proteins affects the translation or replication of the viral RNA, a polio RNA replicon replication assay was performed in the absence or presence of 2 mM of Guanidine HCl (GuHCl), which is a potent inhibitor of viral replication. In the presence of the inhibitor, the signal reflects the translation of the original dose of the replicon RNA delivered into the cells by transfection at the first 2-3 h. While the viral replication (in the absence of GuHCl) was decreased in the AldoA-depleted cells compared with the control, the genome translation level (in the presence of GuHCl) was similar to the control (Fig. 5.9A). Similarly, ILF3-90 depletion did not affect the translation in the presence of the inhibitor (Fig. 5.9C). In contrast, EWSR1 depletion showed a negative effect on the translation step (Fig. 5.9B).

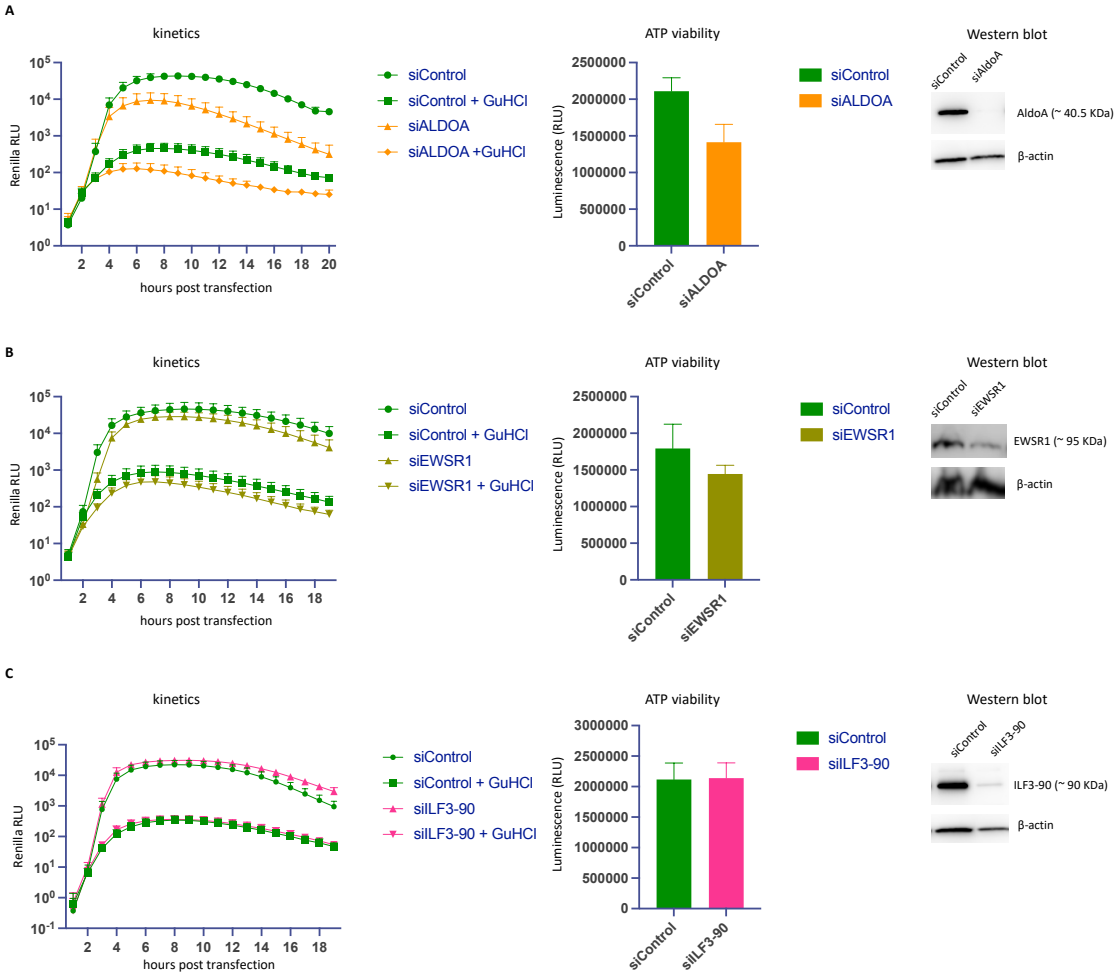

Figure 5.9 Evaluation of the selected proteins functions during in viral genome translation and replication. HeLa cells were transfected with siRNAs specific against AldoA **(A)**, EWSR1 **(B)** and ILF3-90 **(C)**, or non-targeting control siRNA, and polio replicon replication assay was performed 72 h post siRNA transfection in the absence or the presence of 2mM of guanidine-HCl (GuHCl). The signal in the GuHCl-containing probes reflects the translation of the input RNA. No significant cell toxicity was observed after siRNA gene silencing for an individual protein of interest. The transfection efficiency for each protein knock down experiment was evaluated by western blot.

5.2.3.4 Redistribution pattern of the selected proteins during poliovirus infection

We next evaluated the recruitment of the selected proteins to the replication organelles by microscopy. HeLa cells were infected with 50 PFU/cell poliovirus (or mock-infected), followed by staining with antibodies against the cellular proteins of interest and a viral protein (2B or 3B) as a marker of the replication sites. The localization of all selected proteins was significantly modified during poliovirus infection.

The redistribution pattern of EWSR1 resembled that of the stress granules (SGs) during enterovirus infection (Fig. 5.10A). The protein was exclusively detected in the nucleus in mock-infected cells. Although EWSR1 was mainly located in the nucleus at the early stage of infection (2 hpi), it appeared in multiple small granules throughout the cytoplasm in about 20% of the cells. At 4 hpi, weak nuclear localization of the EWSR1 signal was observed, and it was extensively redistributed into the cytoplasm or in the stress granules encircling the nucleus. Although the number of granules dropped compared with the previous time point, their size increased significantly, and almost all of the cells demonstrated a similar distribution pattern. By the end of the infectious cycle at 6 hpi, the number and size of the granules were remarkably reduced (Fig. 5.10A). At this point, no EWSR1 signal was detected in the nucleus, and about half of the cells lost the signal for EWSR1 granules in the cytoplasm. The cytoplasmic EWSR1 signal in infected cells outside of the punctae strongly colocalized with the structures positive for a viral antigen 3B (VPg). 3B signal may correspond to the RNA replication primer in a free form, or attached to the 5' of viral RNAs, but may also be detected as a part of intermediate polyprotein processing products ((Fig. 5.10B).

The cytoplasmic punctae pattern of EWSR1 was highly reminiscent of the development of stress granules upon poliovirus infection. To test that, we stained mock-infected and infected cells for EWSR1 and GTPase Activating Protein (SH3 Domain) Binding Protein 1 (G3BP1), a stress granule assembly factor known to be recruited to poliovirus-induced stress granules. Indeed, in infected cells, the cytoplasmic punctae of EWSR1 and GRBP1 signals colocalized perfectly confirming that these structures are stress granules (Fig. 5.10C). The detection of a stress granule protein upon proximity biotinylation by a GBF1-derived construct was somewhat unexpected since we are not aware of reports of GBF1 targeting to stress granules in infected or otherwise stressed cells. We analyzed the biotinylation pattern relative to the G3BP1 signal in APEX2-GARG-1060 cells. In infected cells we observed multiple bright biotinylation-positive punctae colocalizing with G3BP1-containing stress granules in the cytoplasm, explaining the stress granule protein labeling by APEX2-GARG-1060 construct (Fig. 5.10D). Whether endogenous GBF1 can be associated with stress granules upon infection, or this is a phenomenon specific to the artificial truncated GBF1 construct requires further investigation.

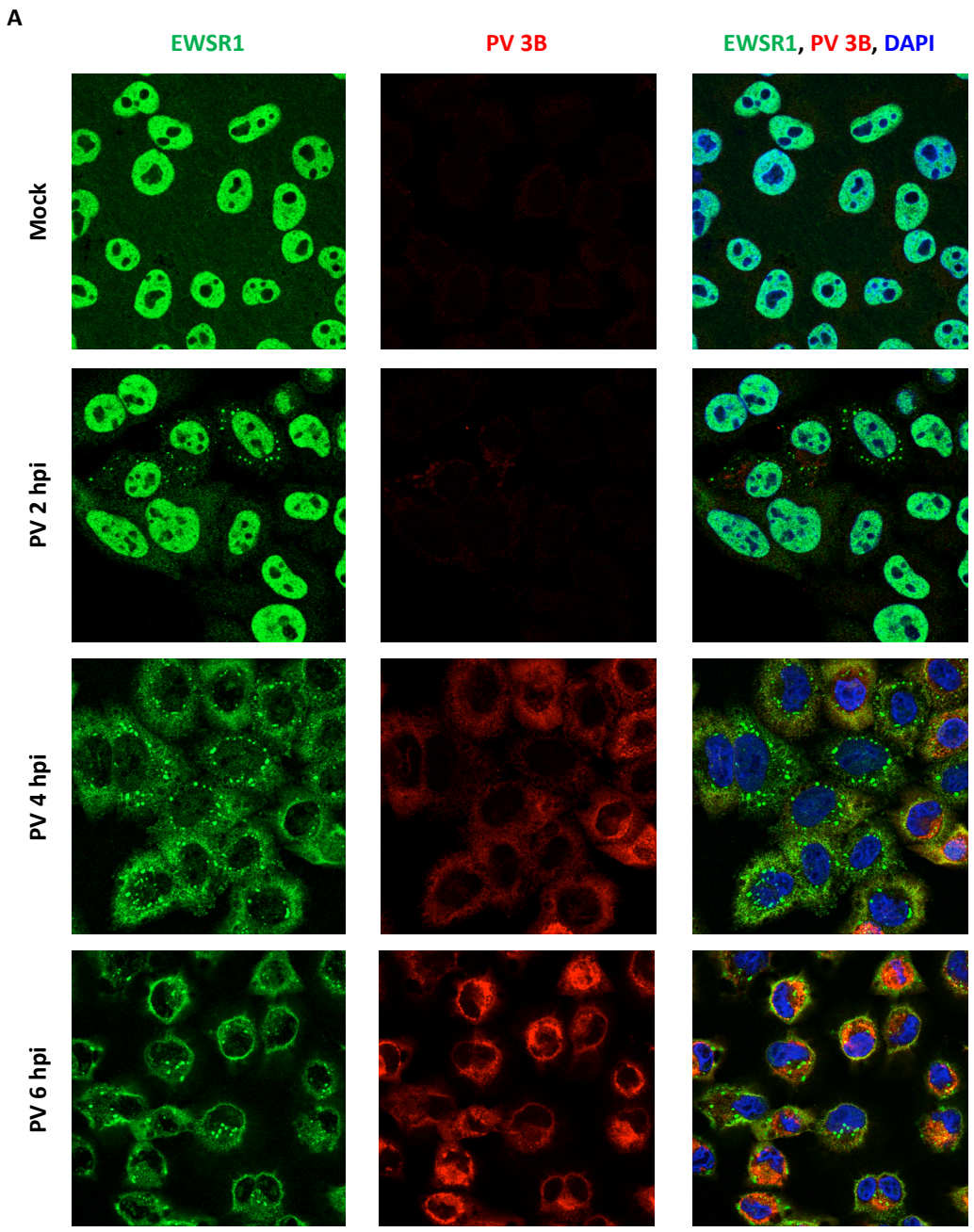
A
EWSR1
PV 3B
EWSR1, PV 3B, DAPI
Mock
PV 2 hpi
PV 4 hpi
PV 6 hpi

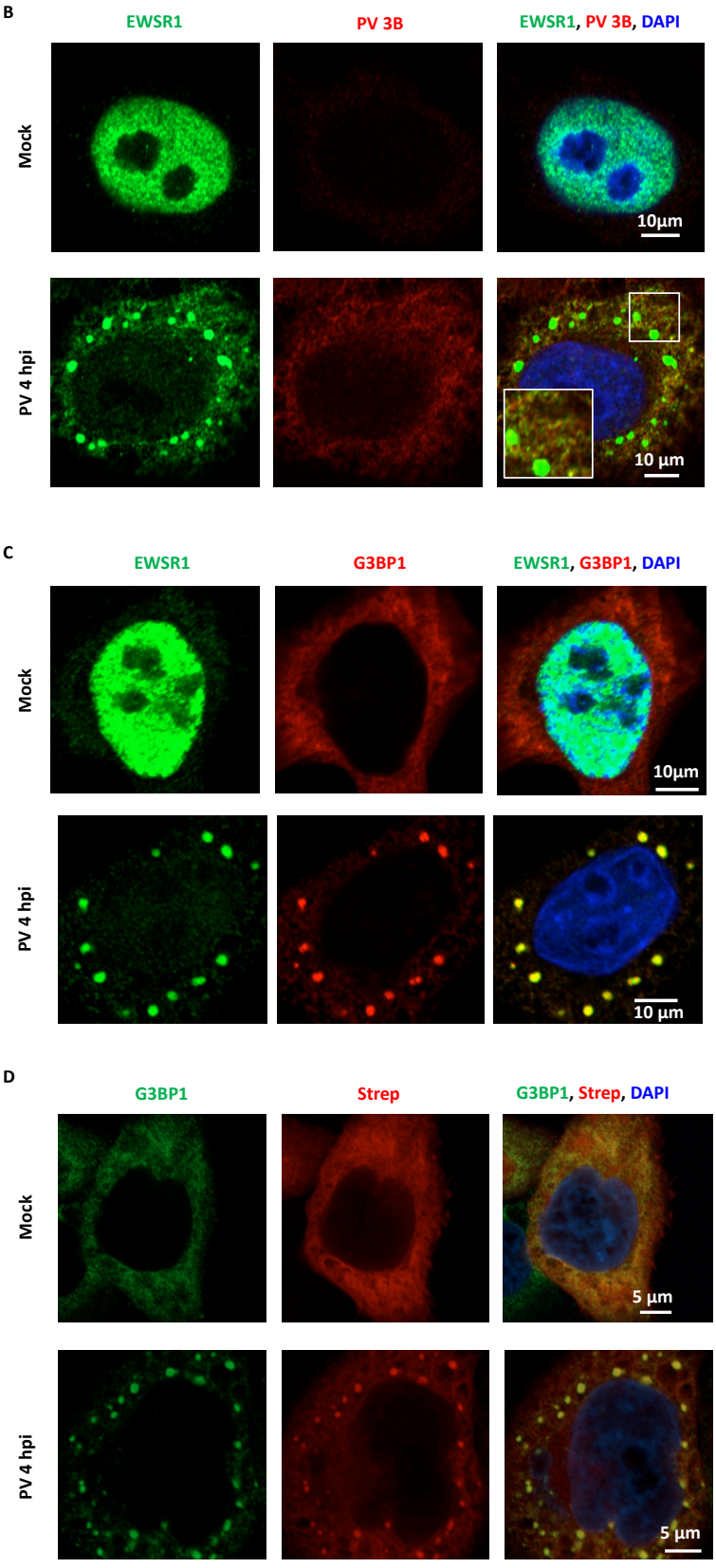
B
EWSR1
PV 3B
EWSR1, PV 3B, DAPI
Mock
10µm
PV 4 hpi
10 µm
C
EWSR1
G3BP1
EWSR1, G3BP1, DAPI
Mock
10µm
PV 4 hpi
10 µm
D
G3BP1
Strep
G3BP1, Strep, DAPI
Mock
5 µm
PV 4 hpi
5 µm

Figure 5.10 Dynamics of EWSR1 localization during different time course of poliovirus infection. (A) HeLa cells were mock or virus-infected with 50 PFU/ml of poliovirus for certain time points. Cells were then fixed and stained with antibodies recognizing EWSR1 (green) and the viral protein 3B (red). Nuclear DNA was stained by Hoechst 33342 (blue). **(B)** High magnification confocal images of HeLa cells infected (or mock-infected) and processed as in A at 4 hpi Note the association of cytoplasmic EWSR1 signal outside of stress granules with the 3B-positive structures. **(C)** Confocal images of HeLa cells infected (or mock-infected) as in A, fixed at 4 hpi and stained with the antibodies against EWSR1 (Green) and a stress granule component G3BP1 (red). **(D)** Confocal images of HeLa cells stably APEX2-GARG-1060 infected (or mock-infected) as in A, and processed at 4 hpi for biotinylation reaction and subsequent staining with antibodies against a stress granule component G3BP1 (green) and streptavidin Alexa conjugate (red). Nuclear DNA was stained by Hoechst 33342 (blue).

A unique distribution of ILF3-90 was observed in the polio-infected cells. HeLa cells were infected (or mock-infected) with 50 PFU/cell of poliovirus for 4 h, fixed and co-stained with antibodies against ILF3-90, and either 2B or dsRNA. In mock-infected cells, ILF3-90 was mainly in the nucleus. During virus infection, the protein translocated from the nucleus into the cytoplasm, where it encircled the viral replication organelles indicated by viral protein 2B (Fig. 5.11A). Such observation is consistent with our previous data showing an antiviral activity of the protein and indicates that it is inhibited from entry to the replication sites. Nevertheless, a slight colocalization of ILF3-90 and viral protein 2B in the ROs suggests that even though the virus attempts to limit the entry of factors with antiviral potentials into the replication sites, host cell immune responses countermeasure the infection by importing the antiviral factors into ROs. At the same time, ILF3-90 and dsRNA colocalized in multiple areas in the replication organelles, suggesting that the antiviral activity of ILF3-90 depends on its dsRNA-binding characteristics (Fig. 5.11B).

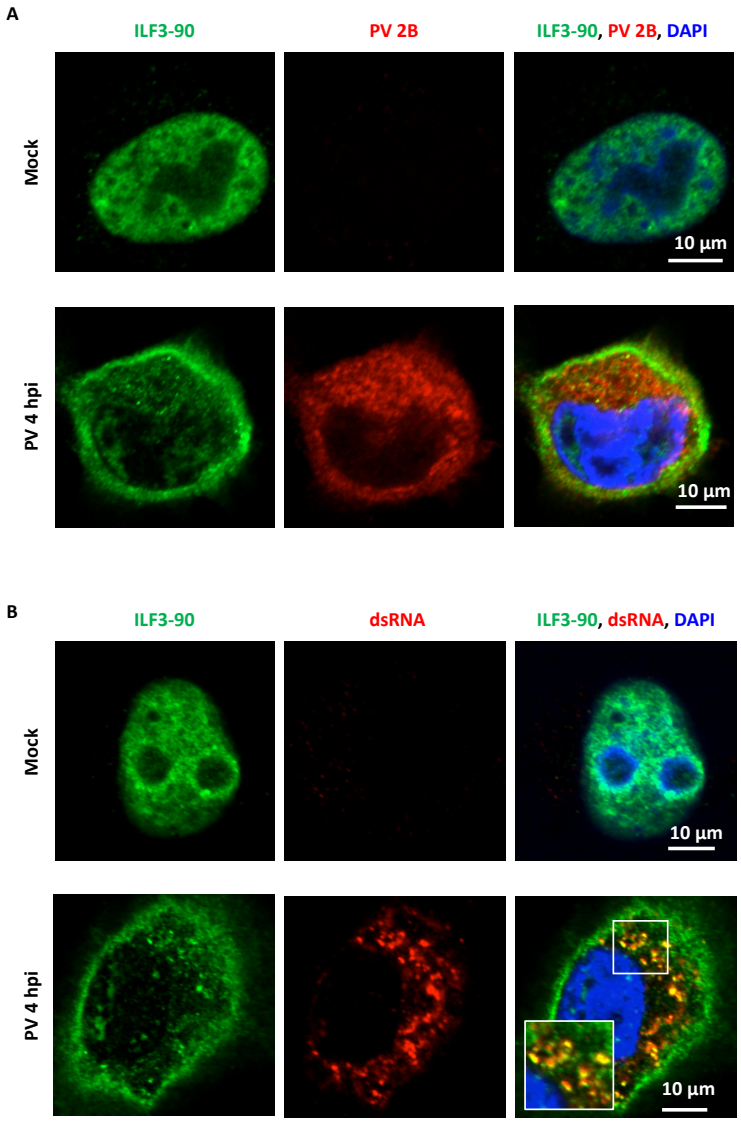

Figure 5.11 Redistribution pattern of ILF3-90 upon poliovirus infection. HeLa cells were mock or virus-infected with 50 PFU/ml of poliovirus for 4 h. Cells were then fixed and stained with antibodies recognizing ILF3-90 (green) and **(A)** the viral protein 2B or **(B)** an intermediate product of the viral RNA replication, dsRNA (red). Nuclear DNA was stained by Hoechst 33342 (blue).

AldoA was one of the several glycolytic enzymes biotinylated by APEX2-GBF1 in poliovirus-infected cells. HeLa cells were infected (or mock-infected) with 50 PFU/cell of poliovirus for 4 h, fixed and co-stained with antibodies against AldoA, and either 2B or dsRNA. In mock-infected cells, AldoA was distributed in the cytoplasm and the nucleus, while upon infection, more cytoplasmic localization of AlodA was detected in cells. We also observed multiple AldoA punctae inside the replication organelles; however, the signal for AldoA was separated from that of 2B or dsRNA (Fig. 12A and B).

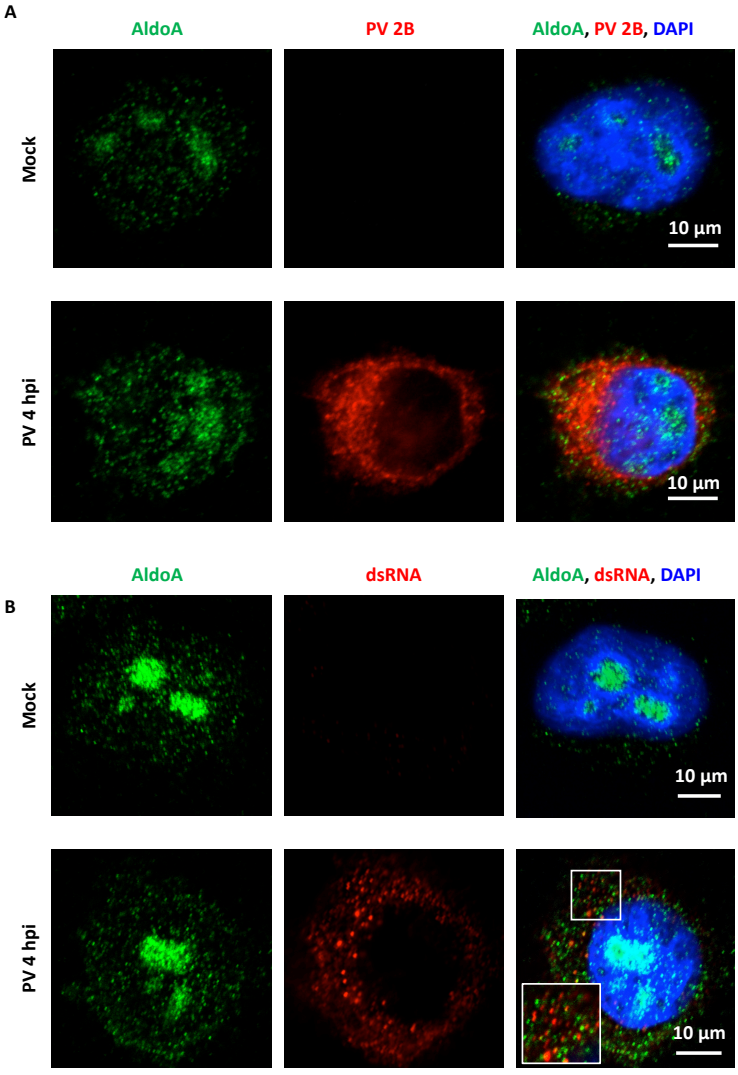

Figure 5.12 Redistribution pattern of AldoA upon poliovirus infection. HeLa cells were mock or virus-infected with 50 PFU/ml of poliovirus for 4 h. Cells were then fixed and stained with antibodies recognizing AldoA (green) and **(A)** the viral protein 2B or **(B)** an intermediate product of the viral RNA replication, dsRNA (red). Nuclear DNA was stained by Hoechst 33342 (blue).

5.3 Discussion

GBF1 is a cellular protein essential for enterovirus replication that interacts with the poliovirus protein 3A on the replication organelles. In this report, we implemented proximity biotinylation coupled with mass spectrometry to explore the protein composition in the vicinity of GBF1 in poliovirus-infected cells. A C-terminally truncated GBF1 mutant downstream of the HDS1 domain previously shown to be fully competent in polio replication was used to reduce the detection of proteins without critical roles in PV replication. We then replaced the Sec7d of GBF1 with the Sec7d of a BFA-insensitive Arf-GEF, ARNO, so that all the replication functions will be performed by this exogenously introduced BFA-resistant GBF1 in the presence of BFA in our experiments. The construct was finally N-terminally inserted into a FLAG-tagged APEX2 (APEX2-GARG-1060). We established a stable cell line expressing APEX2-GARG-1060 and showed that this construct could support poliovirus replication in the presence of BFA.

Fluorescence imaging showed a diffused cytoplasmic localization of APEX2-GARG-1060 in mock-infected cells, which is explained by the fact that the membrane-targeting determinants of GBF1 in the C-terminal domain were removed. At the same time, the biotinylated proteins were detected exclusively on the replication membranes, where they colocalized with the viral protein 3A. This indicates that APEX2-GARG-1060 was successfully recruited to the replication organelles and biotinylated the nearby proteins.

Accordingly, the biotinylated proteins isolated from infected cells were significantly higher than that of mock-infected cells. Also, more biotinylated proteins were observed as the infection progressed, with the highest at 6 hpi. These data indicate that we can efficiently characterize the biotin-labeled viral or cellular proteins nearby GBF1 in the mock and virus-infected cells.

Then, the biotin-labeled samples were evaluated for several cellular proteins previously shown to be involved in the functioning and/or development of the ROs of enteroviruses. PI4KIIIβ, OSBP, and ACBD3 were identified in western blot, indicating that these proteins are localized in the close vicinity of GBF1 on the replication membranes. At the same time, no signal was observed for other proteins tested, such as Arf GTPases, suggesting either they are not located nearby GBF1 or they were not properly exposed to the biotin-phenoxyl radicals in an electron-rich amino acid angel. Collectively, these data revealed that the proteome of the ROs nearby GBF1 is not enriched in all of the known cellular proteins functioning in virus replication, suggesting that the ROs are not biochemically homogeneous and likely have specialized domains.

Among the viral proteins identified in the biotinylated fraction, we detected an increased proportion of the incomplete products of the poliovirus polyprotein cleavage, including some of the fragments that could not be matched with the known intermediates of the polyprotein processing. This suggests that GBF1 on the replication membranes is localized close to the sites of active polyprotein processing. This would be consistent with the requirement of GBF1 activity for the functioning of the viral RNA replication complexes and the fact that viral replication complexes contain proteins that need to be assembled *in cis*, i.e., derived from the same polyprotein molecule (51, 168, 207, 209). On

the other hand, an artificial increase of the large polyprotein fragment signal due to a more efficient purification because of a higher proportion of biotinylated amino acids cannot be excluded. Interestingly, while the large precursors were easily detected in a western blot assay of purified biotinylated proteins, the mass-spectrometry analysis identified viral polypeptides overlapping the 3C-3D but not any other polyprotein cleavage sites, suggesting that most of the polyprotein processing events are very rapid.

The MS analysis of the biotin-labeled proteins identified in the polio-infected sample revealed that a major proportion of these proteins (85%) had not been previously studied in the context of enterovirus infection. Gene ontology analysis showed significant enrichment of RNA binding and mRNA metabolic processes, indicating that GBF1 is likely localized close to the RNA replication complexes. The predominant association of RNA-binding proteins can be explained by the fact that upon infection, enteroviruses protease $2A^{pro}$ specifically cleaves several nucleoporins, resulting in the inactivation of organized nucleocytoplasmic trafficking and leakage of the nuclear proteins into the cytoplasm where the virus can employ them for its benefits (18, 75, 165, 226).

The functional validation of several proteins with distinct cellular functions that were significantly enriched in the MS dataset from the infected cells was performed by an RNAi screen followed by either western blot detecting the level of viral protein 2C accumulation or polio replicon replication. AldoA was one of several glycolytic enzymes biotinylated by APEX2-GBF1 in poliovirus-infected cells, and its depletion significantly inhibited the viral replication. The infection-specific biotinylation of multiple glycolytic enzymes suggests an active supply of the replication organelles with the glycolysis pathway-derived metabolites. Recently, the recruitment of glycolytic enzymes to the

replication organelles of tombusviruses, a group of positive-strand plant viruses has been discovered, and it was shown that these enzymes are involved in generating a high local level of ATP required to support the viral replication (41, 134, 175). Interestingly, the siRNA knockdown of AldoA expression also resulted in a reduction of the cellular ATP level reflected in a lower signal of an ATP-based cell viability test. It is tempting to speculate that the local nucleotide synthesis sustained in part by the recruitment of the glycolytic enzymes generating the necessary substrates at the replication organelles is a conserved feature of the replication of positive-strand RNA viruses. The importance of *de novo* nucleotide synthesis on the replication organelles is highlighted by the previous observations that the partially purified membrane-associated picornavirus replication complexes more efficiently incorporate in the replicating RNA exogenously added nucleoside mono and diphosphates compared to nucleoside triphosphates (113). Staining data showed cytoplasmic and nuclear localization of AldoA in the mock-infected cells, while during poliovirus infection, most of the signal for the protein was detected in the cytoplasm. No colocalization of AldoA with viral protein 2B and dsRNA was observed.

The RNA metabolism proteins were highly enriched in the proteome recovered from the infected cells. Many of these proteins have RNA binding properties and normally have a predominantly nuclear localization where they participate in nuclear transcript processing. Among the RNA proteins, we focused on EWSR1 and ILF3, which showed the most robust and most consistent effects on viral replication in the preliminary screening. EWSR1 is an RNA and DNA binding multifunctional protein involved in different networks of regulation of gene expression (124). EWSR1 depletion significantly inhibited poliovirus genome translation and RNA replication. A similar inhibitory effect

was observed for CVB3 replication, suggesting a potential proviral activity of EWSR1 during enterovirus infection. The ILF3 gene is expressed as two major isoforms of 110 and 90 kDa, which both share the dsRNA binding domain and regulate multiple steps of RNA metabolism in the nucleus and the cytoplasm (37). Since the proteomics data did not distinguish the ILF3 isoforms, we separately targeted the expression of 110k and 90k proteins. Depletion of the 90 kDa isoform of ILF3 had a strong stimulatory effect on the replication of all enteroviruses tested.

The disruption of the nucleocytoplasmic barrier is caused by the cleavage of nucleoporins by enterovirus protease 2A, which also cleaves a translation initiation factor eIF4G. This would halt the mRNA export from the nucleus and cap-dependent translation of cellular mRNAs (18, 75, 165). In addition, the viral proteases 3C and 3CD cleave the core components of RNA polymerase II (116, 189). The rapid and profound inactivation of the cellular gene transcription and translation implies that the proteins present in the cell before infection must contain the full complement of factors required to support the viral replication. This also implies that the cells must dispose of some anti-viral measures ready to be deployed without significant input from the activation of new gene expression. The nuclear depot of RNA-binding proteins thus represents an important resource of both EWSR1 and ILF3-90 signals that were confined almost exclusively to the nuclei in non-infected cells and massively relocated to the cytoplasm upon infection.

Immunostaining data showed a resemblance in the redistribution pattern of EWSR1 into multiple dot-shaped organelles during the time course of infection to that of the enterovirus-induced stress granules, which was confirmed by observing a colocalization of EWSR1 and G3BP1, a marker for SGs. We showed a unique redistribution of ILF3-90

upon infection such that the ILF3-90 signal was mainly detected surrounding the replication organelles, indicated by viral protein 2B, with a slight colocalization with 2B on the replication membranes. This suggests that the antiviral proteins such as ILF3-90 are inhibited from entry to the replication sites although the host cell defense mechanisms find a way to internalize the antiviral factors to the replication membranes evidenced by identifying ILF3-90 nearby 3A-recruited GBF1 in our MS data.

Overall, our data demonstrated that the 3A-recruited GBF1 domain on the ROs is enriched in proteins with either proviral or antiviral activities, indicating that while the virus highjacks host proteins to support different steps of the life cycle, the host antiviral immune mechanisms are actively trying to interrupt the infection by recruiting antiviral factors to the viral replication sites.

Collectively, our work introduced a highly efficient system to investigate the proteome of the poliovirus ROs and revealed a unique protein composition of the GBF1-enriched environment in the replication sites.

Chapter 6: Conclusions and Future Works

In this work, we investigated the function of the GBF1-controlled network of host proteins during enterovirus infection.

Enterovirus genome replication occurs in remodeled membranous structures called the replication organelles, whose composition is important for the proper assembly and functioning of the viral replication complexes. GBF1 is an activator of small GTPases Arf, and its activity is important for the functioning of the cellular secretory pathway. During viral infection, GBF1 is recruited to the replication organelles through direct interaction with the viral protein 3A, and its Arf-GEF function is required to support virus replication. However, the mechanistic role of GBF1-activated Arf isoforms in supporting viral replication is much less understood.

This study revealed that all human Arf isoforms are redistributed to the enterovirus replication sites by the end of the infectious cycle. However, the kinetics of recruitment of distinct Arfs are different at the early-middle steps of infection, which implies the dynamic changes of the Arf-controlled biochemical environment of the replication organelles during the time course of infection. This may guide the transition of the infectious cycle from the early stage, when viral proteins and RNAs are accumulated, to the later phases associated with increasing virion assembly, maturation, and release. Besides, the simultaneous association of all Arf isoforms with the replication organelles likely creates a unique combination of Arf effectors that generate a biochemical environment never exists in organelles in non-infected cells.

Our work revealed novel data on the Arf6 recruitment to the enterovirus replication organelles. Arf6 is the most structurally divergent member of Arf GTPases, a BFA-

insensitive Arf-GEF ARNO normally activates it, and it is predominantly associated with the plasma membrane. However, Arf6 is also implicated in endocytic traffic, and the relocation of Arf6 to the replication membranes may be linked to the redirection of endocytic traffic required for the enrichment of the replication membranes in cholesterol from the plasma membrane depot (91). The possible involvement of Arf6 also implies that ARNO or other members of the cytohesin family of Arf-GEFs (203) may be other host factors essential for the development of infection.

We showed that in non-infected cells, Arfs undergo rapid cycling between membrane-associated GTP-bound and cytoplasmic GDP-bound forms. However, once recruited to the replication membranes, all Arfs except Arf3 became insensitive to the inhibition of Arf-GEF activity, indicating that they remain for a prolonged time in a GTP-bound form. This again underscores that the metabolism of Arf-associated reactions is very different between infected and non-infected cells.

The detailed analysis of the localization of viral antigens revealed that nonstructural protein 2B and the fully assembled virions show the strongest colocalization with Arf1-enriched membranes. However, the nonstructural proteins 2C and 3A with known membrane-targeting domains showed less colocalization with Arfs, especially at the early stages of infection. Only a minimal amount of the viral polymerase $3D^{Pol}$ was colocalizing with Arfs on replication membranes, with most of the protein found in the cytoplasm without apparent association with any membranous structures. Such extensive localization of the viral nonstructural proteins outside the replication organelles suggests that they have important replication-independent functions that remain virtually unexplored. Interestingly, while the signal for dsRNA was in close vicinity to that of Arf1, the two

signals were clearly separated. Collectively, our data indicate that the replication organelles are not homogenous membrane agglomerates but likely have compositionally and structurally distinct microdomains, most likely reflecting the different requirements during distinct stages of the viral life cycle.

To further elucidate the fine organization of the replication organelles, we will explore the localization of viral antigens and dsRNA relative to the Arf1-enriched domains using higher-resolution microscopy techniques.

The individual Arf siRNA depletion studies indicated the importance of Arf1 and, to a lesser extent, Arf6 on the GBF1-supported poliovirus replication. Together with the observations that Arf1 was the first Arf associated with the replication organelles at the beginning of infection, our data suggest that the GBF1-Arf1 axis is the most important contributor to the development and/or functioning of the replication organelles.

One plausible explanation for the importance of Arf1 and Arf6 during enterovirus replication is that Arf depletion prevents the recruitment of the effector proteins to the ROs. Thus, future experiments will focus on investigating the recruitment dynamics and importance of Arf1 and 6's effector proteins during enterovirus infection. To do so, we would first focus on Arf1 and 6's effectors identified in the PV replication sites in our proteomics data in this study, such as multifunctional protein ADE2, cytohesin-2, leucine-rich PPR motif-containing protein, and clathrin heavy chain-1. Of particular interest is cytohesin-2 since it is a GEF for Arf6, the second important Arf in polio replication. Then, we will inhibit the expression and/or activity of these proteins using siRNA or specific inhibitors where appropriate and perform a quantitative enterovirus replication assay (similar to the experiments for the functional validation in chapter 5).

In chapter 5, we explored the proteome composition of poliovirus replication organelles in the vicinity of the 3A-recruited GBF1 domains using an enzyme-based proximity assay followed by mass spectrometry. Detection of the biotin-labeled proteins exclusively on the replication membranes, colocalized with the viral protein 3A, in microscopy ascertained the efficiency of this assay to identify the proteins located nearby 3A-recruited GBF1 in the replication sites. This observation was confirmed by blotting, in which a higher level of biotinylated proteins was detected in the poliovirus-infected samples than in mock. Western blot analysis using antibodies against cellular proteins with known functions in the virus replication revealed that not all of them are located in the GBF1-contained regions of the replication organelles. We also showed that the viral proteins are not equally represented in the GBF1 environment. We found an accumulation of the viral precursor proteins nearby GBF1, suggesting that GBF1 surroundings may be associated with the viral polyprotein processing. Collectively, these data indicate that the GBF1-environment on the replication organelles features a unique combination of viral and cellular proteins, which may lead to functional differentiation of specific membranous domains within the ROs.

Gene ontology analysis of the proteomics data showed a strong enrichment of RNA-binding proteins nearby GBF1 on the replication organelles, which is consistence with the available data, although most of the RNA-binding proteins identified in this study were not previously reported in the context of enterovirus replication (133, 191). Functional analysis of the proteins identified in MS revealed that the GBF1-contained domains on the replication membranes are enriched in a combination of proteins with proviral or antiviral activities. This indicates that during infection, the virus highjacks

various host proteins to the replication sites to support the infectious cycle, and on the other hand, the host cell antiviral defense mechanisms countermeasure the infection by actively recruiting the proteins with antiviral functions to these sites.

Future experiments will provide more details on the mechanistic contributions of the proviral and antiviral proteins during viral infection.

Here, we selected a few highly abundant proteins for initial characterization; however, the abundance upon the proximity biotinylation-based detection reflects the combination of three variables, including the abundance of the protein in a cell, its retention close to the bait, and the exposure of the amino-acids that can accept the biotinphenoxyl radicals. This may skew the representation of the actual enrichment of proteins at the bait construct; thus, the less abundant proteins specifically detected at the replication organelles should also be investigated in the future.

In chapter 4, we showed the important contribution of the GBF1-Arf1 axis in the development/functioning of the ROs, and in chapter 5, we defined a unique combination of cellular and viral proteins nearby GBF1 on the replication membranes. Thus, we will aim to further explore the proteome nearby Arf1 to get a deeper insight into the proteins involved in this axis and in supporting viral replication. Besides, it would be interesting to identify the functions of the Arf-enriched and Arf-depleted micro-domain of the replication organelles.

Overall, our work elucidated important details of the dynamics of the GBF1-dependent activation of small Arf GTPases during enterovirus infection and documented the unique membrane environment of the replication organelles. Moreover, our data significantly increased the knowledge of the cellular proteins associated with the

enterovirus replication organelles and provided an important resource for the rational approach to developing antiviral strategies targeting conserved steps of enterovirus replication.

Bibliography

1. **Agol, V. I., G. A. Belov, K. Bienz, D. Egger, M. S. Kolesnikova, N. T. Raikhlin, L. I. Romanova, E. A. Smirnova, and E. A. Tolskaya.** 1998. Two types of death of poliovirus-infected cells: caspase involvement in the apoptosis but not cytopathic effect. Virology **252:**343-353.
2. **Agol, V. I., G. A. Belov, K. Bienz, D. Egger, M. S. Kolesnikova, L. I. Romanova, L. V. Sladkova, and E. A. Tolskaya.** 2000. Competing death programs in poliovirus-infected cells: commitment switch in the middle of the infectious cycle. J Virol **74:**5534-5541.
3. **Ahmed, N. S., L. M. Harrell, D. R. Wieland, M. A. Lay, V. F. Thompson, and J. C. Schwartz.** 2021. Fusion protein EWS-FLI1 is incorporated into a protein granule in cells. RNA (New York, N.Y.) **27:**920-932.
4. **Alexander, J. P., Jr., L. E. Chapman, M. A. Pallansch, W. T. Stephenson, T. J. Török, and L. J. Anderson.** 1993. Coxsackievirus B2 infection and aseptic meningitis: a focal outbreak among members of a high school football team. The Journal of infectious diseases **167:**1201-1205.
5. **Anbalagan, S., R. A. Hesse, and B. M. Hause.** 2014. First identification and characterization of porcine enterovirus G in the United States. PLoS One **9:**e97517-e97517.
6. **Andries, K., B. Dewindt, J. Snoeks, L. Wouters, H. Moereels, P. J. Lewi, and P. A. Janssen.** 1990. Two groups of rhinoviruses revealed by a panel of antiviral compounds present sequence divergence and differential pathogenicity. J Virol **64:**1117-1123.
7. **Arden, K. E., and I. M. Mackay.** 2009. Human rhinoviruses: coming in from the cold. Genome Medicine **1:**44.
8. **Ariav, Y., J. H. Ch'ng, H. R. Christofk, N. Ron-Harel, and A. Erez.** 2021. Targeting nucleotide metabolism as the nexus of viral infections, cancer, and the immune response. Sci Adv **7**.
9. **Arita, M., H. Kojima, T. Nagano, T. Okabe, T. Wakita, and H. Shimizu.** 2013. Oxysterol-binding protein family I is the target of minor enviroxime-like compounds. J Virol **87:**4252-4260.
10. **Arita, M., H. Kojima, T. Nagano, T. Okabe, T. Wakita, and H. Shimizu.** 2011. Phosphatidylinositol 4-kinase III beta is a target of enviroxime-like compounds for antipoliovirus activity. J Virol **85:**2364-2372.
11. **Baggen, J., H. J. Thibaut, J. Strating, and F. J. M. van Kuppeveld.** 2018. The life cycle of non-polio enteroviruses and how to target it. Nature reviews. Microbiology **16:**368-381.
12. **Basavappa, R., R. Syed, O. Flore, J. P. Icenogle, D. J. Filman, and J. M. Hogle.** 1994. Role and mechanism of the maturation cleavage of VP0 in poliovirus assembly: structure of the empty capsid assembly intermediate at 2.9 A resolution. Protein science : a publication of the Protein Society **3:**1651-1669.

13. **Belov, G. A.** 2016. Dynamic lipid landscape of picornavirus replication organelles. Current opinion in virology **19:**1-6.
14. **Belov, G. A.** 2014. Modulation of lipid synthesis and trafficking pathways by picornaviruses. Current opinion in virology **9:**19-23.
15. **Belov, G. A., N. Altan-Bonnet, G. Kovtunovych, C. L. Jackson, J. Lippincott-Schwartz, and E. Ehrenfeld.** 2007. Hijacking components of the cellular secretory pathway for replication of poliovirus RNA. J Virol **81:**558-567.
16. **Belov, G. A., Q. Feng, K. Nikovics, C. L. Jackson, and E. Ehrenfeld.** 2008. A critical role of a cellular membrane traffic protein in poliovirus RNA replication. PLoS pathogens **4:**e1000216.
17. **Belov, G. A., G. Kovtunovych, C. L. Jackson, and E. Ehrenfeld.** 2010. Poliovirus replication requires the N-terminus but not the catalytic Sec7 domain of ArfGEF GBF1. Cell Microbiol **12:**1463-1479.
18. **Belov, G. A., P. V. Lidsky, O. V. Mikitas, D. Egger, K. A. Lukyanov, K. Bienz, and V. I. Agol.** 2004. Bidirectional increase in permeability of nuclear envelope upon poliovirus infection and accompanying alterations of nuclear pores. J Virol **78:**10166-10177.
19. **Belov, G. A., V. Nair, B. T. Hansen, F. H. Hoyt, E. R. Fischer, and E. Ehrenfeld.** 2012. Complex dynamic development of poliovirus membranous replication complexes. J Virol **86:**302-312.
20. **Belov, G. A., L. I. Romanova, E. A. Tolskaya, M. S. Kolesnikova, Y. A. Lazebnik, and V. I. Agol.** 2003. The major apoptotic pathway activated and suppressed by poliovirus. J Virol **77:**45-56.
21. **Belov, G. A., and E. Sztul.** 2014. Rewiring of cellular membrane homeostasis by picornaviruses. J Virol **88:**9478-9489.
22. **Belov, G. A., and F. J. van Kuppeveld.** 2012. (+)RNA viruses rewire cellular pathways to build replication organelles. Current opinion in virology **2:**740-747.
23. **Belov, G. A., and F. J. M. van Kuppeveld.** 2019. Lipid Droplets Grease Enterovirus Replication. Cell host & microbe **26:**149-151.
24. **Benschop, K. S., H. G. van der Avoort, E. Duizer, and M. P. Koopmans.** 2015. Antivirals against enteroviruses: a critical review from a public-health perspective. Antiviral therapy **20:**121-130.
25. **Bergelson, J. M.** 2010. Receptors, p. 73-86, The Picornaviruses.
26. **Bergelson, J. M., M. P. Shepley, B. M. Chan, M. E. Hemler, and R. W. Finberg.** 1992. Identification of the integrin VLA-2 as a receptor for echovirus 1. Science (New York, N.Y.) **255:**1718-1720.
27. **Bersuker, K., C. W. H. Peterson, M. To, S. J. Sahl, V. Savikhin, E. A. Grossman, D. K. Nomura, and J. A. Olzmann.** 2018. A Proximity Labeling Strategy Provides Insights into the Composition and Dynamics of Lipid Droplet Proteomes. Developmental cell **44:**97-112 e117.
28. **Beske, O., M. Reichelt, M. P. Taylor, K. Kirkegaard, and R. Andino.** 2007. Poliovirus infection blocks ERGIC-to-Golgi trafficking and induces microtubule-dependent disruption of the Golgi complex. Journal of cell science **120:**3207-3218.

29. **Bhatt, J. M., W. Hancock, J. M. Meissner, A. Kaczmarczyk, E. Lee, E. Viktorova, S. Ramanadham, G. A. Belov, and E. Sztul.** 2019. Promiscuity of the catalytic Sec7 domain within the guanine nucleotide exchange factor GBF1 in ARF activation, Golgi homeostasis, and effector recruitment. Molecular biology of the cell **30:**1523-1535.
30. **Bhatt, J. M., E. G. Viktorova, T. Busby, P. Wyrozumska, L. E. Newman, H. Lin, E. Lee, J. Wright, G. A. Belov, R. A. Kahn, and E. Sztul.** 2016. Oligomerization of the Sec7 domain Arf guanine nucleotide exchange factor GBF1 is dispensable for Golgi localization and function but regulates degradation. American Journal of Physiology-Cell Physiology **310:**C456-C469.
31. **Blas-Machado, U., J. T. Saliki, M. J. Boileau, S. D. Goens, S. L. Caseltine, J. C. Duffy, and R. D. Welsh.** 2007. Fatal ulcerative and hemorrhagic typhlocolitis in a pregnant heifer associated with natural bovine enterovirus type-1 infection. Veterinary pathology **44:**110-115.
32. **Blyn, L. B., J. S. Towner, B. L. Semler, and E. Ehrenfeld.** 1997. Requirement of Poly(rC) binding protein 2 for translation of poliovirus RNA. Journal of Virology **71:**6243-6246.
33. **Cao, D., D. Haussecker, Y. Huang, and M. A. Kay.** 2009. Combined proteomic-RNAi screen for host factors involved in human hepatitis delta virus replication. RNA (New York, N.Y.) **15:**1971-1979.
34. **Casanova, J. E.** 2007. Regulation of Arf activation: the Sec7 family of guanine nucleotide exchange factors. Traffic (Copenhagen, Denmark) **8:**1476-1485.
35. **Casanova, V., F. H. Sousa, C. Stevens, and P. G. Barlow.** 2018. Antiviral therapeutic approaches for human rhinovirus infections. Future Virol **13:**505-518.
36. **Cassidy, H., R. Poelman, M. Knoester, C. C. Van Leer-Buter, and H. G. M. Niesters.** 2018. Enterovirus D68 - The New Polio? Front Microbiol **9:**2677-2677.
37. **Castella, S., R. Bernard, M. Corno, A. Fradin, and J. C. Larcher.** 2015. Ilf3 and NF90 functions in RNA biology. Wiley interdisciplinary reviews. RNA **6:**243-256.
38. **Chen, Z., K. Chumakov, E. Dragunsky, D. Kouiavskaia, M. Makiya, A. Neverov, G. Rezapkin, A. Sebrell, and R. Purcell.** 2011. Chimpanzee-human monoclonal antibodies for treatment of chronic poliovirus excretors and emergency postexposure prophylaxis. J Virol **85:**4354-4362.
39. **Cherry, J. D.** 2006. Chapter 24 - Enterovirus and Parechovirus Infections, p. 783-822. *In* J. S. Remington, J. O. Klein, C. B. Wilson, and C. J. Baker (ed.), Infectious Diseases of the Fetus and Newborn Infant (Sixth Edition). W.B. Saunders, Philadelphia.
40. **Chong, P., C. C. Liu, Y. H. Chow, A. H. Chou, and M. Klein.** 2015. Review of enterovirus 71 vaccines. Clinical infectious diseases : an official publication of the Infectious Diseases Society of America **60:**797-803.
41. **Chuang, C., K. R. Prasanth, and P. D. Nagy.** 2017. The Glycolytic Pyruvate Kinase Is Recruited Directly into the Viral Replicase Complex to Generate ATP for RNA Synthesis. Cell host & microbe **22:**639-652 e637.

42. **Cifuente, J. O., and G. Moratorio.** 2019. Evolutionary and Structural Overview of Human Picornavirus Capsid Antibody Evasion. Frontiers in Cellular and Infection Microbiology **9**.
43. **Clayton, E. L., S. Minogue, and M. G. Waugh.** 2013. Mammalian phosphatidylinositol 4-kinases as modulators of membrane trafficking and lipid signaling networks. Progress in lipid research **52:**294-304.
44. **Corona Velazquez, A., A. K. Corona, K. A. Klein, and W. T. Jackson.** 2018. Poliovirus induces autophagic signaling independent of the ULK1 complex. Autophagy **14:**1201-1213.
45. **de Breyne, S., J. M. Bonderoff, K. M. Chumakov, R. E. Lloyd, and C. U. Hellen.** 2008. Cleavage of eukaryotic initiation factor eIF5B by enterovirus 3C proteases. Virology **378:**118-122.
46. **De Coster, I., I. Leroux-Roels, A. S. Bandyopadhyay, C. Gast, K. Withanage, K. Steenackers, P. De Smedt, A. Aerssens, G. Leroux-Roels, M. S. Oberste, J. L. Konopka-Anstadt, W. C. Weldon, A. Fix, J. Konz, R. Wahid, J. Modlin, R. Clemens, S. A. Costa Clemens, N. S. Bachtiar, and P. Van Damme.** 2021. Safety and immunogenicity of two novel type 2 oral poliovirus vaccine candidates compared with a monovalent type 2 oral poliovirus vaccine in healthy adults: two clinical trials. The Lancet **397:**39-50.
47. **De Jesus, N. H.** 2007. Epidemics to eradication: the modern history of poliomyelitis. Virology Journal **4:**70.
48. **Delang, L., J. Paeshuyse, and J. Neyts.** 2012. The role of phosphatidylinositol 4-kinases and phosphatidylinositol 4-phosphate during viral replication. Biochemical pharmacology **84:**1400-1408.
49. **Delorme-Axford, E., S. Morosky, J. Bomberger, D. B. Stolz, W. T. Jackson, and C. B. Coyne.** 2014. BPIFB3 regulates autophagy and coxsackievirus B replication through a noncanonical pathway independent of the core initiation machinery. mBio **5:**e02147-e02147.
50. **Donaldson, J. G., and C. L. Jackson.** 2011. ARF family G proteins and their regulators: roles in membrane transport, development and disease. Nature reviews. Molecular cell biology **12:**362-375.
51. **Egger, D., N. Teterina, E. Ehrenfeld, and K. Bienz.** 2000. Formation of the Poliovirus Replication Complex Requires Coupled Viral Translation, Vesicle Production, and Viral RNA Synthesis. J Virol **74:**6570-6580.
52. **Ellie Ehrenfeld, E. D., Raymond P. Roos.** 2010. The Picornaviruses. American Society for Microbiology Press **Capter 1: Introduction to Picornavirus Biology:**3-32.
53. **Escribano-Romero, E., M. A. Jiménez-Clavero, and V. Ley.** 2000. Swine vesicular disease virus. Pathology of the disease and molecular characteristics of the virion. Animal health research reviews **1:**119-126.
54. **Fei, T., Y. Chen, T. Xiao, W. Li, L. Cato, P. Zhang, M. B. Cotter, M. Bowden, R. T. Lis, S. G. Zhao, Q. Wu, F. Y. Feng, M. Loda, H. H. He, X. S. Liu, and M. Brown.** 2017. Genome-wide CRISPR screen identifies HNRNPL as a prostate cancer dependency

regulating RNA splicing. Proceedings of the National Academy of Sciences of the United States of America **114:**E5207-E5215.

55. **Feng, Q., M. A. Langereis, and F. J. van Kuppeveld.** 2014. Induction and suppression of innate antiviral responses by picornaviruses. Cytokine & growth factor reviews **25:**577-585.
56. **Ferlin, J., R. Farhat, S. Belouzard, L. Cocquerel, A. Bertin, D. Hober, J. Dubuisson, and Y. Rouillé.** 2018. Investigation of the role of GBF1 in the replication of positive-sense single-stranded RNA viruses. The Journal of general virology **99:**1086-1096.
57. **Fernández de Castro, I., J. J. Fernández, D. Barajas, P. D. Nagy, and C. Risco.** 2017. Three-dimensional imaging of the intracellular assembly of a functional viral RNA replicase complex. Journal of cell science **130:**260-268.
58. **Fields B.N., K. D. M., Howley P.M., Griffin D.E. .** 2001. Fields Virology. 4th edition. Wolters Kluwer Health/Lippincott Williams & Wilkins, Philadelphia, PA, USA.
59. **Filippi, C. M., and M. G. von Herrath.** 2008. Viral trigger for type 1 diabetes: pros and cons. Diabetes **57:**2863-2871.
60. **Flather, D., J. H. C. Nguyen, B. L. Semler, and P. D. Gershon.** 2018. Exploitation of nuclear functions by human rhinovirus, a cytoplasmic RNA virus. Plos Pathogens **14**.
61. **Foeger, N., W. Glaser, and T. Skern.** 2002. Recognition of eukaryotic initiation factor 4G isoforms by picornaviral proteinases. The Journal of biological chemistry **277:**44300-44309.
62. **Fox, J. T., W. K. Shin, M. A. Caudill, and P. J. Stover.** 2009. A UV-responsive internal ribosome entry site enhances serine hydroxymethyltransferase 1 expression for DNA damage repair. The Journal of biological chemistry **284:**31097-31108.
63. **Gaaloul, I., S. Riabi, R. Harrath, T. Hunter, K. B. Hamda, A. B. Ghzala, S. Huber, and M. Aouni.** 2014. Coxsackievirus B detection in cases of myocarditis, myopericarditis, pericarditis and dilated cardiomyopathy in hospitalized patients. Molecular medicine reports **10:**2811-2818.
64. **Garg, R. R., and S. M. Karst.** 2016. Chapter 5.2 - Interactions Between Enteric Viruses and the Gut Microbiota, p. 535-544. *In* L. Svensson, U. Desselberger, H. B. Greenberg, and M. K. Estes (ed.), Viral Gastroenteritis. Academic Press, Boston.
65. **Gazina, E. V., J. M. Mackenzie, R. J. Gorrell, and D. A. Anderson.** 2002. Differential Requirements for COPI Coats in Formation of Replication Complexes among Three Genera of Picornaviridae. J Virol **76:**11113-11122.
66. **Gern, J. E., and W. W. Busse.** 1999. Association of rhinovirus infections with asthma. Clinical microbiology reviews **12:**9-18.
67. **Gingras, A. C., K. T. Abe, and B. Raught.** 2019. Getting to know the neighborhood: using proximity-dependent biotinylation to characterize protein complexes and map organelles. Current opinion in chemical biology **48:**44-54.
68. **Glenet, M., L. Heng, D. Callon, A. L. Lebreil, P. A. Gretteau, Y. Nguyen, F. Berri, and L. Andreoletti.** 2020. Structures and Functions of Viral 5' Non-Coding Genomic RNA Domain-I in Group-B Enterovirus Infections. Viruses **12**.

69. **Godi, A., A. Di Campli, A. Konstantakopoulos, G. Di Tullio, D. R. Alessi, G. S. Kular, T. Daniele, P. Marra, J. M. Lucocq, and M. A. De Matteis.** 2004. FAPPs control Golgi-to-cell-surface membrane traffic by binding to ARF and PtdIns(4)P. Nature cell biology **6:**393-404.
70. **Gomila, R. C., G. W. Martin, and L. Gehrke.** 2011. NF90 Binds the Dengue Virus RNA 3 ' Terminus and Is a Positive Regulator of Dengue Virus Replication. Plos One **6**.
71. **Gradi, A., Y. V. Svitkin, H. Imataka, and N. Sonenberg.** 1998. Proteolysis of human eukaryotic translation initiation factor eIF4GII, but not eIF4GI, coincides with the shutoff of host protein synthesis after poliovirus infection. Proceedings of the National Academy of Sciences of the United States of America **95:**11089-11094.
72. **Greninger, A. L., G. M. Knudsen, M. Betegon, A. L. Burlingame, and J. L. Derisi.** 2012. The 3A protein from multiple picornaviruses utilizes the golgi adaptor protein ACBD3 to recruit PI4KIIIβ. J Virol **86:**3605-3616.
73. **Gu, J., J. Wu, D. Fang, Y. Qiu, X. Zou, X. Jia, Y. Yin, L. Shen, and L. Mao.** 2020. Exosomes cloak the virion to transmit Enterovirus 71 non-lytically. Virulence **11:**32-38.
74. **Gür, S., M. Gürçay, and A. Seyrek.** 2019. A study regarding bovine enterovirus type 1 infection in domestic animals and humans: An evaluation from the zoonotic aspect. J Vet Med Sci **81:**1824-1828.
75. **Gustin, K. E., and P. Sarnow.** 2001. Effects of poliovirus infection on nucleo-cytoplasmic trafficking and nuclear pore complex composition. The EMBO journal **20:**240-249.
76. **Hahn, H., and A. C. Palmenberg.** 1995. Encephalomyocarditis viruses with short poly(C) tracts are more virulent than their mengovirus counterparts. J Virol **69:**2697-2699.
77. **Han, S., N. D. Udeshi, T. J. Deerinck, T. Svinkina, M. H. Ellisman, S. A. Carr, and A. Y. Ting.** 2017. Proximity Biotinylation as a Method for Mapping Proteins Associated with mtDNA in Living Cells. Cell chemical biology **24:**404-414.
78. **Heikkilä, O., P. Susi, G. Stanway, and T. Hyypiä.** 2009. Integrin alphaVbeta6 is a high-affinity receptor for coxsackievirus A9. The Journal of general virology **90:**197-204.
79. **Herold, J., and R. Andino.** 2001. Poliovirus RNA replication requires genome circularization through a protein-protein bridge. Mol Cell **7:**581-591.
80. **Hindiyeh, M., Q. H. Li, R. Basavappa, J. M. Hogle, and M. Chow.** 1999. Poliovirus mutants at histidine 195 of VP2 do not cleave VP0 into VP2 and VP4. J Virol **73:**9072-9079.
81. **Hixon, A. M., P. Clarke, and K. L. Tyler.** 2019. Contemporary Circulating Enterovirus D68 Strains Infect and Undergo Retrograde Axonal Transport in Spinal Motor Neurons Independent of Sialic Acid. J Virol **93**.
82. **Hogle, J. M.** 2002. Poliovirus cell entry: common structural themes in viral cell entry pathways. Annu Rev Microbiol **56:**677-702.

83. **Hornbeck, P. V., B. Zhang, B. Murray, J. M. Kornhauser, V. Latham, and E. Skrzypek.** 2015. PhosphoSitePlus, 2014: mutations, PTMs and recalibrations. Nucleic acids research **43:**D512-520.
84. **Hsu, N. Y., O. Ilnytska, G. Belov, M. Santiana, Y. H. Chen, P. M. Takvorian, C. Pau, H. van der Schaar, N. Kaushik-Basu, T. Balla, C. E. Cameron, E. Ehrenfeld, F. J. van Kuppeveld, and N. Altan-Bonnet.** 2010. Viral reorganization of the secretory pathway generates distinct organelles for RNA replication. Cell **141:**799-811.
85. **Hu, M. M., and H. B. Shu.** 2020. Innate Immune Response to Cytoplasmic DNA: Mechanisms and Diseases. Annual review of immunology **38:**79-98.
86. **Huang, H.-I., and S.-R. Shih.** 2015. Neurotropic Enterovirus Infections in the Central Nervous System. Viruses **7:**6051-6066.
87. **Hughes, L. E., and M. D. Ryan.** 2008. Enteroviruses of Animals, p. 123-129. *In* B. W. J. Mahy and M. H. V. Van Regenmortel (ed.), Encyclopedia of Virology (Third Edition). Academic Press, Oxford.
88. **Hung, V., S. S. Lam, N. D. Udeshi, T. Svinkina, G. Guzman, V. K. Mootha, S. A. Carr, and A. Y. Ting.** 2017. Proteomic mapping of cytosol-facing outer mitochondrial and ER membranes in living human cells by proximity biotinylation. eLife **6**.
89. **Hung, V., P. Zou, H.-W. Rhee, Namrata D. Udeshi, V. Cracan, T. Svinkina, Steven A. Carr, Vamsi K. Mootha, and Alice Y. Ting.** 2014. Proteomic Mapping of the Human Mitochondrial Intermembrane Space in Live Cells via Ratiometric APEX Tagging. Molecular cell **55:**332-341.
90. **Hwang, J., and P. J. Espenshade.** 2016. Proximity-dependent biotin labelling in yeast using the engineered ascorbate peroxidase APEX2. The Biochemical journal **473:**2463-2469.
91. **Ilnytska, O., M. Santiana, N. Y. Hsu, W. L. Du, Y. H. Chen, E. G. Viktorova, G. Belov, A. Brinker, J. Storch, C. Moore, J. L. Dixon, and N. Altan-Bonnet.** 2013. Enteroviruses harness the cellular endocytic machinery to remodel the host cell cholesterol landscape for effective viral replication. Cell host & microbe **14:**281-293.
92. **Isken, O., M. Baroth, C. W. Grassmann, S. Weinlich, D. H. Ostareck, A. Ostareck-Lederer, and S. E. Behrens.** 2007. Nuclear factors are involved in hepatitis C virus RNA replication. Rna **13:**1675-1692.
93. **Jackson, C. L.** 2014. Arf Proteins and Their Regulators: At the Interface Between Membrane Lipids and the Protein Trafficking Machinery, p. 151-180. *In* A. Wittinghofer (ed.), Ras Superfamily Small G Proteins: Biology and Mechanisms 2: Transport. Springer International Publishing, Cham.
94. **Jackson, C. L., and S. Bouvet.** 2014. Arfs at a glance. Journal of cell science **127:**4103-4109.
95. **Jacobs, S. E., D. M. Lamson, K. St George, and T. J. Walsh.** 2013. Human rhinoviruses. Clinical microbiology reviews **26:**135-162.
96. **Jacobson, S. J., D. A. Konings, and P. Sarnow.** 1993. Biochemical and genetic evidence for a pseudoknot structure at the 3' terminus of the poliovirus RNA genome and its role in viral RNA amplification. J Virol **67:**2961-2971.

97. **Ji, C., Y. Zhang, R. Sun, J. Ma, Z. Pan, and H. Yao.** 2021. Isolation and Identification of Type F Bovine Enterovirus from Clinical Cattle with Diarrhoea. Viruses **13:**2217.
98. **Jiao, X. Y., L. Guo, D. Y. Huang, X. L. Chang, and Q. C. Qiu.** 2014. Distribution of EV71 receptors SCARB2 and PSGL-1 in human tissues. Virus research **190:**40-52.
99. **Jin, L., J. Chun, C. Pan, G. N. Alesi, D. Li, K. R. Magliocca, Y. Kang, Z. G. Chen, D. M. Shin, F. R. Khuri, J. Fan, and S. Kang.** 2017. Phosphorylation-mediated activation of LDHA promotes cancer cell invasion and tumour metastasis. Oncogene **36:**3797-3806.
100. **Kaczmarek, B., J. M. Verbavatz, and C. L. Jackson.** 2017. GBF1 and Arf1 function in vesicular trafficking, lipid homoeostasis and organelle dynamics. Biol Cell **109:**391-399.
101. **Kafasla, P., H. Lin, S. Curry, and R. J. Jackson.** 2011. Activation of picornaviral IRESs by PTB shows differential dependence on each PTB RNA-binding domain. Rna **17:**1120-1131.
102. **Kafasla, P., N. Morgner, C. V. Robinson, and R. J. Jackson.** 2010. Polypyrimidine tract-binding protein stimulates the poliovirus IRES by modulating eIF4G binding. Embo J **29:**3710-3722.
103. **Käll, L., J. D. Storey, and W. S. Noble.** 2008. Non-parametric estimation of posterior error probabilities associated with peptides identified by tandem mass spectrometry. Bioinformatics **24:**i42-i48.
104. **Kärber., G.** Beitrag zur kollektiven Behandlung pharmakologischer Reihenversuche. Archiv f. experiment. Pathol. u. Pharmakol. **162:**480-483.
105. **Karnauchow, T. M., D. L. Tolson, B. A. Harrison, E. Altman, D. M. Lublin, and K. Dimock.** 1996. The HeLa cell receptor for enterovirus 70 is decay-accelerating factor (CD55). J Virol **70:**5143-5152.
106. **Kerekatte, V., B. D. Keiper, C. Badorff, A. Cai, K. U. Knowlton, and R. E. Rhoads.** 1999. Cleavage of Poly(A)-binding protein by coxsackievirus 2A protease in vitro and in vivo: another mechanism for host protein synthesis shutoff? J Virol **73:**709-717.
107. **Kim, D. I., K. C. Birendra, W. Zhu, K. Motamedchaboki, V. Doye, and K. J. Roux.** 2014. Probing nuclear pore complex architecture with proximity-dependent biotinylation. Proceedings of the National Academy of Sciences of the United States of America **111:**E2453-2461.
108. **Kim, D. I., and K. J. Roux.** 2016. Filling the Void: Proximity-Based Labeling of Proteins in Living Cells. Trends Cell Biol **26:**804-817.
109. **Knipe David M., H. P.** 2013. Fields Virology. Volume 1, chapter 3, Principles of Virus Structure; Lippincott Williams & Wilkins Press.
110. **Knoops, K., M. Kikkert, S. H. Worm, J. C. Zevenhoven-Dobbe, Y. van der Meer, A. J. Koster, A. M. Mommaas, and E. J. Snijder.** 2008. SARS-coronavirus replication is supported by a reticulovesicular network of modified endoplasmic reticulum. PLoS biology **6:**e226.
111. **Knowles, N. J.** 1988. The association of group III porcine enteroviruses with epithelial tissue. The Veterinary record **122:**441-442.

112. **Konopka-Anstadt, J. L., R. Campagnoli, A. Vincent, J. Shaw, L. Wei, N. T. Wynn, S. E. Smithee, E. Bujaki, M. Te Yeh, M. Laassri, T. Zagorodnyaya, A. J. Weiner, K. Chumakov, R. Andino, A. Macadam, O. Kew, and C. C. Burns.** 2020. Development of a new oral poliovirus vaccine for the eradication end game using codon deoptimization. npj Vaccines **5:**26.
113. **Koonin, E. V., and V. I. Agol.** 1984. Encephalomyocarditis virus replication complexes preferentially utilizing nucleoside diphosphates as substrates for viral RNA synthesis. Nucleotide kinases specifically associated with the complex channel RNA precursor. European journal of biochemistry **144:**249-254.
114. **Kopecka, H.** 1999. ECHOVIRUSES (PICORNAVIRIDAE), p. 411-417. *In* A. Granoff and R. G. Webster (ed.), Encyclopedia of Virology (Second Edition). Elsevier, Oxford.
115. **Kopek, B. G., G. Perkins, D. J. Miller, M. H. Ellisman, and P. Ahlquist.** 2007. Three-dimensional analysis of a viral RNA replication complex reveals a virus-induced mini-organelle. PLoS biology **5:**e220.
116. **Kundu, P., S. Raychaudhuri, W. Tsai, and A. Dasgupta.** 2005. Shutoff of RNA polymerase II transcription by poliovirus involves 3C protease-mediated cleavage of the TATA-binding protein at an alternative site: incomplete shutoff of transcription interferes with efficient viral replication. J Virol **79:**9702-9713.
117. **Lai, J. K., I. C. Sam, and Y. F. Chan.** 2016. The Autophagic Machinery in Enterovirus Infection. Viruses **8**.
118. **Lam, S. S., J. D. Martell, K. J. Kamer, T. J. Deerinck, M. H. Ellisman, V. K. Mootha, and A. Y. Ting.** 2015. Directed evolution of APEX2 for electron microscopy and proximity labeling. Nature Methods **12:**51-54.
119. **Langford, M. P., E. A. Anders, and M. A. Burch.** 2015. Acute hemorrhagic conjunctivitis: anti-coxsackievirus A24 variant secretory immunoglobulin A in acute and convalescent tear. Clin Ophthalmol **9:**1665-1673.
120. **Lanke, K. H., H. M. van der Schaar, G. A. Belov, Q. Feng, D. Duijsings, C. L. Jackson, E. Ehrenfeld, and F. J. van Kuppeveld.** 2009. GBF1, a guanine nucleotide exchange factor for Arf, is crucial for coxsackievirus B3 RNA replication. J Virol **83:**11940-11949.
121. **Laufman, O., J. Perrino, and R. Andino.** 2019. Viral Generated Inter-Organelle Contacts Redirect Lipid Flux for Genome Replication. Cell **178:**275-289 e216.
122. **Lawson, M. A., and B. L. Semler.** 1992. Alternate poliovirus nonstructural protein processing cascades generated by primary sites of 3C proteinase cleavage. Virology **191:**309-320.
123. **Lee, H. Y., C. J. Chen, Y. C. Huang, W. C. Li, C. H. Chiu, C. G. Huang, K. C. Tsao, C. T. Wu, and T. Y. Lin.** 2010. Clinical features of echovirus 6 and 9 infections in children. Journal of clinical virology : the official publication of the Pan American Society for Clinical Virology **49:**175-179.
124. **Lee, J., P. T. Nguyen, H. S. Shim, S. J. Hyeon, H. Im, M. H. Choi, S. Chung, N. W. Kowall, S. B. Lee, and H. Ryu.** 2019. EWSR1, a multifunctional protein, regulates cellular function and aging via genetic and epigenetic pathways. Biochimica et biophysica acta. Molecular basis of disease **1865:**1938-1945.

125. **Lee, S. Y., M. G. Kang, J. S. Park, G. Lee, A. Y. Ting, and H. W. Rhee.** 2016. APEX Fingerprinting Reveals the Subcellular Localization of Proteins of Interest. Cell reports **15:**1837-1847.
126. **Lenarcic, E. M., D. M. Landry, T. M. Greco, I. M. Cristea, and S. R. Thompson.** 2013. Thiouracil Cross-Linking Mass Spectrometry: a Cell-Based Method To Identify Host Factors Involved in Viral Amplification. Journal of Virology **87:**8697-8712.
127. **Lewis-Rogers, N., J. Seger, R. Adler Frederick, and S. Lyles Douglas.** Human Rhinovirus Diversity and Evolution: How Strange the Change from Major to Minor. J Virol **91:**e01659-01616.
128. **Li, L., J.-Y. Yin, F.-Z. He, M.-S. Huang, T. Zhu, Y.-F. Gao, Y.-X. Chen, D.-B. Zhou, X. Chen, L.-Q. Sun, W. Zhang, H.-H. Zhou, and Z.-Q. Liu.** 2017. Long noncoding RNA SFTA1P promoted apoptosis and increased cisplatin chemosensitivity via regulating the hnRNP-U-GADD45A axis in lung squamous cell carcinoma. Oncotarget **8:**97476-97489.
129. **Li, M.-L., S.-R. Shih, B. S. Tolbert, and G. Brewer.** 2021. Enterovirus A71 Vaccines. Vaccines (Basel) **9:**199.
130. **Li, X., C. X. Liu, W. Xue, Y. Zhang, S. Jiang, Q. F. Yin, J. Wei, R. W. Yao, L. Yang, and L. L. Chen.** 2017. Coordinated circRNA Biogenesis and Function with NF90/NF110 in Viral Infection. Mol Cell **67:**214-+.
131. **Li, X., M. Wang, A. Cheng, X. Wen, X. Ou, S. Mao, Q. Gao, D. Sun, R. Jia, Q. Yang, Y. Wu, D. Zhu, X. Zhao, S. Chen, M. Liu, S. Zhang, Y. Liu, Y. Yu, L. Zhang, B. Tian, L. Pan, and X. Chen.** 2020. Enterovirus Replication Organelles and Inhibitors of Their Formation. Front Microbiol **11:**1817-1817.
132. **Lim, H. X., and C. L. Poh.** 2019. Insights into innate and adaptive immune responses in vaccine development against EV-A71. Therapeutic advances in vaccines and immunotherapy **7:**2515135519888998.
133. **Lin, J. Y., T. C. Chen, K. F. Weng, S. C. Chang, L. L. Chen, and S. R. Shih.** 2009. Viral and host proteins involved in picornavirus life cycle. Journal of biomedical science **16:**103.
134. **Lin, W., Y. Liu, M. Molho, S. Zhang, L. Wang, L. Xie, and P. D. Nagy.** 2019. Co-opting the fermentation pathway for tombusvirus replication: Compartmentalization of cellular metabolic pathways for rapid ATP generation. PLoS pathogens **15:**e1008092.
135. **Liu, Y., M. G. Hill, T. Klose, Z. Chen, K. Watters, Y. A. Bochkov, W. Jiang, A. C. Palmenberg, and M. G. Rossmann.** 2016. Atomic structure of a rhinovirus C, a virus species linked to severe childhood asthma. Proceedings of the National Academy of Sciences **113:**8997-9002.
136. **Lu, Y., S. Song, and L. Zhang.** 2020. Emerging Role for Acyl-CoA Binding Domain Containing 3 at Membrane Contact Sites During Viral Infection. Front Microbiol **11:**608.
137. **Lyoo, H., H. M. van der Schaar, C. M. Dorobantu, H. H. Rabouw, J. Strating, and F. J. M. van Kuppeveld.** 2019. ACBD3 Is an Essential Pan-enterovirus Host Factor

That Mediates the Interaction between Viral 3A Protein and Cellular Protein PI4KB. mBio **10**.

138. **Martino, T. A., M. Petric, M. Brown, K. Aitken, C. J. Gauntt, C. D. Richardson, L. H. Chow, and P. P. Liu.** 1998. Cardiovirulent coxsackieviruses and the decay-accelerating factor (CD55) receptor. Virology **244:**302-314.
139. **Matsunaga, S., H. Takata, A. Morimoto, K. Hayashihara, T. Higashi, K. Akatsuchi, E. Mizusawa, M. Yamakawa, M. Ashida, T. M. Matsunaga, T. Azuma, S. Uchiyama, and K. Fukui.** 2012. RBMX: a regulator for maintenance and centromeric protection of sister chromatid cohesion. Cell reports **1:**299-308.
140. **McBride, A. E., A. Schlegel, and K. Kirkegaard.** 1996. Human protein Sam68 relocalization and interaction with poliovirus RNA polymerase in infected cells. P Natl Acad Sci USA **93:**2296-2301.
141. **McCleland, M. L., A. S. Adler, Y. Shang, T. Hunsaker, T. Truong, D. Peterson, E. Torres, L. Li, B. Haley, J. P. Stephan, M. Belvin, G. Hatzivassiliou, E. M. Blackwood, L. Corson, M. Evangelista, J. Zha, and R. Firestein.** 2012. An integrated genomic screen identifies LDHB as an essential gene for triple-negative breast cancer. Cancer research **72:**5812-5823.
142. **McKnight, K. L.** 2003. The human rhinovirus internal cis-acting replication element (cre) exhibits disparate properties among serotypes. Archives of virology **148:**2397-2418.
143. **Medicine, I. o.** 1996. Options for Poliomyelitis Vaccination in the United States: Workshop Summary. The National Academies Press, Washington, DC.
144. **Merrill, M. K., and M. Gromeier.** 2006. The double-stranded RNA binding protein 76 : NF45 heterodimer inhibits translation initiation at the rhinovirus type 2 internal ribosome entry site. Journal of Virology **80:**6936-6942.
145. **Mesmin, B., J. Bigay, J. Moser von Filseck, S. Lacas-Gervais, G. Drin, and B. Antonny.** 2013. A four-step cycle driven by PI(4)P hydrolysis directs sterol/PI(4)P exchange by the ER-Golgi tether OSBP. Cell **155:**830-843.
146. **Mesmin, B., J. Bigay, J. Polidori, D. Jamecna, S. Lacas-Gervais, and B. Antonny.** 2017. Sterol transfer, PI4P consumption, and control of membrane lipid order by endogenous OSBP. The EMBO journal **36:**3156-3174.
147. **Mi, H., D. Ebert, A. Muruganujan, C. Mills, L. P. Albou, T. Mushayamaha, and P. D. Thomas.** 2021. PANTHER version 16: a revised family classification, tree-based classification tool, enhancer regions and extensive API. Nucleic acids research **49:**D394-D403.
148. **Montagnac, G., J.-B. Sibarita, S. Loubéry, L. Daviet, M. Romao, G. Raposo, and P. Chavrier.** 2009. ARF6 Interacts with JIP4 to Control a Motor Switch Mechanism Regulating Endosome Traffic in Cytokinesis. Current Biology **19:**184-195.
149. **Mueller, S., E. Wimmer, and J. Cello.** 2005. Poliovirus and poliomyelitis: a tale of guts, brains, and an accidental event. Virus research **111:**175-193.
150. **Nakamura, N., T. Yamauchi, M. Hiramoto, M. Yuri, M. Naito, M. Takeuchi, K. Yamanaka, A. Kita, T. Nakahara, I. Kinoyama, A. Matsuhisa, N. Kaneko, H. Koutoku, M. Sasamata, H. Yokota, S. Kawabata, and K. Furuichi.** 2012. Interleukin

enhancer-binding factor 3/NF110 is a target of YM155, a suppressant of survivin. Mol Cell Proteomics **11:**M111.013243-M013111.013243.

151. **Nchoutmboube, J. A., E. G. Viktorova, A. J. Scott, L. A. Ford, Z. Pei, P. A. Watkins, R. K. Ernst, and G. A. Belov.** 2013. Increased long chain acyl-Coa synthetase activity and fatty acid import is linked to membrane synthesis for development of picornavirus replication organelles. PLoS pathogens **9:**e1003401.
152. **Nelsen-Salz, B., H. J. Eggers, and H. Zimmermann.** 1999. Integrin alpha(v)beta3 (vitronectin receptor) is a candidate receptor for the virulent echovirus 9 strain Barty. The Journal of general virology **80 (Pt 9):**2311-2313.
153. **Neufeld, K. L., O. C. Richards, and E. Ehrenfeld.** 1991. Purification, characterization, and comparison of poliovirus RNA polymerase from native and recombinant sources. Journal of Biological Chemistry **266:**24212-24219.
154. **Nikonov, O. S., E. S. Chernykh, M. B. Garber, and E. Y. Nikonova.** 2017. Enteroviruses: Classification, Diseases They Cause, and Approaches to Development of Antiviral Drugs. Biochemistry. Biokhimiia **82:**1615-1631.
155. **Nugent, C. I., K. L. Johnson, P. Sarnow, and K. Kirkegaard.** 1999. Functional coupling between replication and packaging of poliovirus replicon RNA. J Virol **73:**427-435.
156. **Oberste, M. S., K. Maher, D. R. Kilpatrick, and M. A. Pallansch.** 1999. Molecular evolution of the human enteroviruses: correlation of serotype with VP1 sequence and application to picornavirus classification. J Virol **73:**1941-1948.
157. **OHKA, S., C.-i. Nihei, M. Yamazaki, and A. Nomoto.** 2012. Poliovirus trafficking toward central nervous system via human poliovirus receptor-dependent and -independent pathway. Front Microbiol **3**.
158. **Oikarinen, M., S. Tauriainen, S. Oikarinen, T. Honkanen, P. Collin, I. Rantala, M. Mäki, K. Kaukinen, and H. Hyöty.** 2012. Type 1 diabetes is associated with enterovirus infection in gut mucosa. Diabetes **61:**687-691.
159. **Olkkonen, V. M.** 2015. OSBP-Related Protein Family in Lipid Transport Over Membrane Contact Sites. Lipid insights **8:**1-9.
160. **Olzmann, J. A., and P. Carvalho.** 2019. Dynamics and functions of lipid droplets. Nature Reviews Molecular Cell Biology **20:**137-155.
161. **Ooi, M. H., S. C. Wong, P. Lewthwaite, M. J. Cardosa, and T. Solomon.** 2010. Clinical features, diagnosis, and management of enterovirus 71. The Lancet. Neurology **9:**1097-1105.
162. **Oughtred, R., J. Rust, C. Chang, B. J. Breitkreutz, C. Stark, A. Willems, L. Boucher, G. Leung, N. Kolas, F. Zhang, S. Dolma, J. Coulombe-Huntington, A. Chatr-aryamontri, K. Dolinski, and M. Tyers.** 2021. The BioGRID database: A comprehensive biomedical resource of curated protein, genetic, and chemical interactions. Protein Sci **30:**187-200.
163. **Owino, C. O., and J. J. H. Chu.** 2019. Recent advances on the role of host factors during non-poliovirus enteroviral infections. Journal of biomedical science **26:**47.
164. **Owusu, I. A., O. Quaye, K. D. Passalacqua, and C. E. Wobus.** 2021. Egress of non-enveloped enteric RNA viruses. The Journal of general virology **102**.

165. **Park, N., T. Skern, and K. E. Gustin.** 2010. Specific cleavage of the nuclear pore complex protein Nup62 by a viral protease. The Journal of biological chemistry **285:**28796-28805.
166. **Parsley, T. B., J. S. Towner, L. B. Blyn, E. Ehrenfeld, and B. L. Semler.** 1997. Poly (rC) binding protein 2 forms a ternary complex with the 5'-terminal sequences of poliovirus RNA and the viral 3CD proteinase. Rna **3:**1124-1134.
167. **Pasamontes, L., D. Egger, and K. Bienz.** 1986. Production of monoclonal and monospecific antibodies against non-capsid proteins of poliovirus. The Journal of general virology **67 (Pt 11):**2415-2422.
168. **Pathak, H. B., H. S. Oh, I. G. Goodfellow, J. J. Arnold, and C. E. Cameron.** 2008. Picornavirus genome replication: roles of precursor proteins and rate-limiting steps in oriI-dependent VPg uridylylation. The Journal of biological chemistry **283:**30677-30688.
169. **Patino, C., A. L. Haenni, and S. Urcuqui-Inchima.** 2015. NF90 isoforms, a new family of cellular proteins involved in viral replication? Biochimie **108:**20-24.
170. **Paul, A. V., G. A. Belov, E. Ehrenfeld, and E. Wimmer.** 2009. Model of Picornavirus RNA Replication, p. 3-23. *In* K. D. Raney, M. Gotte, and C. E. Cameron (ed.), Viral Genome Replication. Springer US, Boston, MA.
171. **Pedley, A. M., and S. J. Benkovic.** 2017. A New View into the Regulation of Purine Metabolism: The Purinosome. Trends Biochem Sci **42:**141-154.
172. **Pestova, T. V., V. G. Kolupaeva, I. B. Lomakin, E. V. Pilipenko, I. N. Shatsky, V. I. Agol, and C. U. Hellen.** 2001. Molecular mechanisms of translation initiation in eukaryotes. Proceedings of the National Academy of Sciences of the United States of America **98:**7029-7036.
173. **Platt, L. R., C. F. Estívariz, and R. W. Sutter.** 2014. Vaccine-associated paralytic poliomyelitis: a review of the epidemiology and estimation of the global burden. The Journal of infectious diseases **210 Suppl 1:**S380-389.
174. **Pocognoni, C. A., E. G. Viktorova, J. Wright, J. M. Meissner, G. Sager, E. Lee, G. A. Belov, and E. Sztul.** 2018. Highly conserved motifs within the large Sec7 ARF guanine nucleotide exchange factor GBF1 target it to the Golgi and are critical for GBF1 activity. Am J Physiol Cell Physiol **314:**C675-C689.
175. **Prasanth, K. R., C. Chuang, and P. D. Nagy.** 2017. Co-opting ATP-generating glycolytic enzyme PGK1 phosphoglycerate kinase facilitates the assembly of viral replicase complexes. PLoS pathogens **13:**e1006689.
176. **Prevention, C. f. D. C. a.** 2020. Polio Disease and Poliovirus https://www.cdc.gov/cpr/polioviruscontainment/diseaseandvirus.htm.
177. **Putnak, J. R., and B. A. Phillips.** 1981. Picornaviral structure and assembly. Microbiol Rev **45:**287-315.
178. **Quiner, C. A., and W. T. Jackson.** 2010. Fragmentation of the Golgi apparatus provides replication membranes for human rhinovirus 1A. Virology **407:**185-195.

179. **Reichman, T. W., L. C. Muniz, and M. B. Mathews.** 2002. The RNA binding protein nuclear factor 90 functions as both a positive and negative regulator of gene expression in mammalian cells. Mol Cell Biol **22:**343-356.
180. **Richardson, S. J., and N. G. Morgan.** 2018. Enteroviral infections in the pathogenesis of type 1 diabetes: new insights for therapeutic intervention. Curr Opin Pharmacol **43:**11-19.
181. **Rivera, C. I., and R. E. Lloyd.** 2008. Modulation of enteroviral proteinase cleavage of poly(A)-binding protein (PABP) by conformation and PABP-associated factors. Virology **375:**59-72.
182. **Roberts, B. L., Z. C. Severance, R. C. Bensen, A. T. Le-McClain, C. A. Malinky, E. M. Mettenbrink, J. I. Nuñez, W. J. Reddig, E. L. Blewett, and A. W. G. Burgett.** 2019. Differing activities of oxysterol-binding protein (OSBP) targeting anti-viral compounds. Antiviral Res **170:**104548.
183. **Romero-Brey, I., A. Merz, A. Chiramel, J.-Y. Lee, P. Chlanda, U. Haselman, R. Santarella-Mellwig, A. Habermann, S. Hoppe, S. Kallis, P. Walther, C. Antony, J. Krijnse-Locker, and R. Bartenschlager.** 2012. Three-Dimensional Architecture and Biogenesis of Membrane Structures Associated with Hepatitis C Virus Replication. PLoS pathogens **8:**e1003056.
184. **Roulin, P. S., M. Lötzerich, F. Torta, L. B. Tanner, F. J. van Kuppeveld, M. R. Wenk, and U. F. Greber.** 2014. Rhinovirus uses a phosphatidylinositol 4-phosphate/cholesterol counter-current for the formation of replication compartments at the ER-Golgi interface. Cell host & microbe **16:**677-690.
185. **Roux, K. J., D. I. Kim, M. Raida, and B. Burke.** 2012. A promiscuous biotin ligase fusion protein identifies proximal and interacting proteins in mammalian cells. The Journal of cell biology **196:**801-810.
186. **Schwartz, M., J. Chen, M. Janda, M. Sullivan, J. den Boon, and P. Ahlquist.** 2002. A positive-strand RNA virus replication complex parallels form and function of retrovirus capsids. Molecular cell **9:**505-514.
187. **Seddon, J. H., and M. F. Duff.** 1971. Hand-foot-and-mouth disease: Coxsackie virus types A 5, A 10, and A 16 infections. The New Zealand medical journal **74:**368-373.
188. **Shafren, D. R., D. J. Dorahy, R. A. Ingham, G. F. Burns, and R. D. Barry.** 1997. Coxsackievirus A21 binds to decay-accelerating factor but requires intercellular adhesion molecule 1 for cell entry. J Virol **71:**4736-4743.
189. **Sharma, R., S. Raychaudhuri, and A. Dasgupta.** 2004. Nuclear entry of poliovirus protease-polymerase precursor 3CD: implications for host cell transcription shut-off. Virology **320:**195-205.
190. **Shemiakina, I. I., G. V. Ermakova, P. J. Cranfill, M. A. Baird, R. A. Evans, E. A. Souslova, D. B. Staroverov, A. Y. Gorokhovatsky, E. V. Putintseva, T. V. Gorodnicheva, T. V. Chepurnykh, L. Strukova, S. Lukyanov, A. G. Zaraisky, M. W. Davidson, D. M. Chudakov, and D. Shcherbo.** 2012. A monomeric red fluorescent protein with low cytotoxicity. Nature Communications **3:**1204.
191. **Shih, S. R., V. Stollar, and M. L. Li.** 2011. Host factors in enterovirus 71 replication. J Virol **85:**9658-9666.

192. **Simmonds, P., A. E. Gorbalenya, H. Harvala, T. Hovi, N. J. Knowles, A. M. Lindberg, M. S. Oberste, A. C. Palmenberg, G. Reuter, T. Skern, C. Tapparel, K. C. Wolthers, P. C. Y. Woo, and R. Zell.** 2020. Recommendations for the nomenclature of enteroviruses and rhinoviruses. Archives of virology **165:**793-797.
193. **Snijder, E. J., R. W. A. L. Limpens, A. H. de Wilde, A. W. M. de Jong, J. C. Zevenhoven-Dobbe, H. J. Maier, F. F. G. A. Faas, A. J. Koster, and M. Bárcena.** 2020. A unifying structural and functional model of the coronavirus replication organelle: Tracking down RNA synthesis. PLoS biology **18:**e3000715-e3000715.
194. **Sohda, M., Y. Misumi, A. Yamamoto, A. Yano, N. Nakamura, and Y. Ikehara.** 2001. Identification and characterization of a novel Golgi protein, GCP60, that interacts with the integral membrane protein giantin. The Journal of biological chemistry **276:**45298-45306.
195. **Sommergruber, W., H. Ahorn, H. Klump, J. Seipelt, A. Zoephel, F. Fessl, E. Krystek, D. Blaas, E. Kuechler, H. D. Liebig, and et al.** 1994. 2A proteinases of coxsackie- and rhinovirus cleave peptides derived from eIF-4 gamma via a common recognition motif. Virology **198:**741-745.
196. **Sonenberg, N., and A. G. Hinnebusch.** 2009. Regulation of translation initiation in eukaryotes: mechanisms and biological targets. Cell **136:**731-745.
197. **Spickler, C., J. Lippens, M.-K. Laberge, S. Desmeules, É. Bellavance, M. Garneau, T. Guo, O. Hucke, P. Leyssen, J. Neyts, F. H. Vaillancourt, A. Décor, J. O'Meara, M. Franti, and A. Gauthier.** 2013. Phosphatidylinositol 4-kinase III beta is essential for replication of human rhinovirus and its inhibition causes a lethal phenotype in vivo. Antimicrobial agents and chemotherapy **57:**3358-3368.
198. **Stagg, S. M., P. LaPointe, and W. E. Balch.** 2007. Structural design of cage and coat scaffolds that direct membrane traffic. Current opinion in structural biology **17:**221-228.
199. **Stark, C., B. J. Breitkreutz, T. Reguly, L. Boucher, A. Breitkreutz, and M. Tyers.** 2006. BioGRID: a general repository for interaction datasets. Nucleic Acids Res **34:**D535-D539.
200. **Steil, B. P., and D. J. Barton.** 2009. Cis-active RNA elements (CREs) and picornavirus RNA replication. Virus research **139:**240-252.
201. **Strating, J. R., L. van der Linden, L. Albulescu, J. Bigay, M. Arita, L. Delang, P. Leyssen, H. M. van der Schaar, K. H. Lanke, H. J. Thibaut, R. Ulferts, G. Drin, N. Schlinck, R. W. Wubbolts, N. Sever, S. A. Head, J. O. Liu, P. A. Beachy, M. A. De Matteis, M. D. Shair, V. M. Olkkonen, J. Neyts, and F. J. van Kuppeveld.** 2015. Itraconazole inhibits enterovirus replication by targeting the oxysterol-binding protein. Cell reports **10:**600-615.
202. **Sun, Z., and J. L. Brodsky.** 2019. Protein quality control in the secretory pathway. The Journal of cell biology **218:**3171-3187.
203. **Sztul, E., P. W. Chen, J. E. Casanova, J. Cherfils, J. B. Dacks, D. G. Lambright, F. S. Lee, P. A. Randazzo, L. C. Santy, A. Schürmann, I. Wilhelmi, M. E. Yohe, and R. A.**

Kahn. 2019. ARF GTPases and their GEFs and GAPs: concepts and challenges. Molecular biology of the cell **30:**1249-1271.

204. **Téoulé, F., C. Brisac, I. Pelletier, P.-O. Vidalain, S. Jégouic, C. Mirabelli, M. Bessaud, N. Combelas, A. Autret, F. Tangy, F. Delpeyroux, and B. Blondel.** 2013. The Golgi protein ACBD3, an interactor for poliovirus protein 3A, modulates poliovirus replication. J Virol **87:**11031-11046.
205. **Teterina, N. L., D. Egger, K. Bienz, D. M. Brown, B. L. Semler, and E. Ehrenfeld.** 2001. Requirements for assembly of poliovirus replication complexes and negative-strand RNA synthesis. J Virol **75:**3841-3850.
206. **Teterina, N. L., Y. Pinto, J. D. Weaver, K. S. Jensen, and E. Ehrenfeld.** 2011. Analysis of poliovirus protein 3A interactions with viral and cellular proteins in infected cells. J Virol **85:**4284-4296.
207. **Teterina, N. L., W. D. Zhou, M. W. Cho, and E. Ehrenfeld.** 1995. Inefficient complementation activity of poliovirus 2C and 3D proteins for rescue of lethal mutations. J Virol **69:**4245-4254.
208. **Thibaut, H. J., C. Lacroix, A. M. De Palma, D. Franco, M. Decramer, and J. Neyts.** 2016. Toward antiviral therapy/prophylaxis for rhinovirus-induced exacerbations of chronic obstructive pulmonary disease: challenges, opportunities, and strategies. Reviews in medical virology **26:**21-33.
209. **Towner, J. S., M. M. Mazanet, and B. L. Semler.** 1998. Rescue of defective poliovirus RNA replication by 3AB-containing precursor polyproteins. J Virol **72:**7191-7200.
210. **Toyoda, H., D. Franco, K. Fujita, A. V. Paul, and E. Wimmer.** 2007. Replication of poliovirus requires binding of the poly(rC) binding protein to the cloverleaf as well as to the adjacent C-rich spacer sequence between the cloverleaf and the internal ribosomal entry site. Journal of Virology **81:**10017-10028.
211. **Trinkle-Mulcahy, L.** 2019. Recent advances in proximity-based labeling methods for interactome mapping. F1000Research **8**.
212. **Tuthill, T. J., E. Groppelli, J. M. Hogle, and D. J. Rowlands.** 2010. Picornaviruses. Curr Top Microbiol Immunol **343:**43-89.
213. **Ulferts, R., S. M. de Boer, L. van der Linden, L. Bauer, H. R. Lyoo, M. J. Maté, J. Lichière, B. Canard, D. Lelieveld, W. Omta, D. Egan, B. Coutard, and F. J. van Kuppeveld.** 2016. Screening of a Library of FDA-Approved Drugs Identifies Several Enterovirus Replication Inhibitors That Target Viral Protein 2C. Antimicrobial agents and chemotherapy **60:**2627-2638.
214. **van der Schaar, H. M., P. Leyssen, H. J. Thibaut, A. de Palma, L. van der Linden, K. H. Lanke, C. Lacroix, E. Verbeken, K. Conrath, A. M. Macleod, D. R. Mitchell, N. J. Palmer, H. van de Poël, M. Andrews, J. Neyts, and F. J. van Kuppeveld.** 2013. A novel, broad-spectrum inhibitor of enterovirus replication that targets host cell factor phosphatidylinositol 4-kinase IIIβ. Antimicrobial agents and chemotherapy **57:**4971-4981.
215. **Van Dyke, T. A., and J. B. Flanegan.** 1980. Identification of poliovirus polypeptide P63 as a soluble RNA-dependent RNA polymerase. J Virol **35:**732-740.

216. **Viktorova, E. G., S. Gabaglio, J. M. Meissner, E. Lee, S. Moghimi, E. Sztul, and G. A. Belov.** 2019. A Redundant Mechanism of Recruitment Underlies the Remarkable Plasticity of the Requirement of Poliovirus Replication for the Cellular ArfGEF GBF1. Journal of Virology **93**.
217. **Viktorova, E. G., S. Gabaglio, J. M. Meissner, E. Lee, S. Moghimi, E. Sztul, G. A. Belov, and S. López.** 2019. A Redundant Mechanism of Recruitment Underlies the Remarkable Plasticity of the Requirement of Poliovirus Replication for the Cellular ArfGEF GBF1. J Virol **93:**e00856-00819.
218. **Viktorova, E. G., S. Khattar, S. Samal, and G. A. Belov.** 2018. Poliovirus Replicon RNA Generation, Transfection, Packaging, and Quantitation of Replication. Current protocols in microbiology **48:**15H 14 11-15H 14 15.
219. **Viktorova, E. G., J. A. Nchoutmboube, L. A. Ford-Siltz, E. Iverson, and G. A. Belov.** 2018. Phospholipid synthesis fueled by lipid droplets drives the structural development of poliovirus replication organelles. PLoS pathogens **14:**e1007280-e1007280.
220. **Virgen-Slane, R., J. M. Rozovics, K. D. Fitzgerald, T. Ngo, W. Chou, G. J. van der Heden van Noort, D. V. Filippov, P. D. Gershon, and B. L. Semler.** 2012. An RNA virus hijacks an incognito function of a DNA repair enzyme. Proceedings of the National Academy of Sciences of the United States of America **109:**14634-14639.
221. **Volpicelli-Daley, L. A., Y. Li, C. J. Zhang, and R. A. Kahn.** 2005. Isoform-selective effects of the depletion of ADP-ribosylation factors 1-5 on membrane traffic. Molecular biology of the cell **16:**4495-4508.
222. **Walker, P. J., S. G. Siddell, E. J. Lefkowitz, A. R. Mushegian, E. M. Adriaenssens, P. Alfenas-Zerbini, A. J. Davison, D. M. Dempsey, B. E. Dutilh, M. L. García, B. Harrach, R. L. Harrison, R. C. Hendrickson, S. Junglen, N. J. Knowles, M. Krupovic, J. H. Kuhn, A. J. Lambert, M. Łobocka, M. L. Nibert, H. M. Oksanen, R. J. Orton, D. L. Robertson, L. Rubino, S. Sabanadzovic, P. Simmonds, D. B. Smith, N. Suzuki, K. Van Dooerslaer, A. M. Vandamme, A. Varsani, and F. M. Zerbini.** 2021. Changes to virus taxonomy and to the International Code of Virus Classification and Nomenclature ratified by the International Committee on Taxonomy of Viruses (2021). Archives of virology **166:**2633-2648.
223. **Wang, J., J. Du, and Q. Jin.** 2014. Class I ADP-ribosylation factors are involved in enterovirus 71 replication. PLoS One **9:**e99768-e99768.
224. **Wang, Y. J., W. S. Wang, L. Xu, X. Y. Zhou, E. Shokrollahi, K. Felczak, L. J. W. van der Laan, K. W. Pankiewicz, D. Sprengers, N. J. H. Raat, H. J. Metselaar, M. P. Peppelenbosch, and Q. W. Pan.** 2016. Cross Talk between Nucleotide Synthesis Pathways with Cellular Immunity in Constraining Hepatitis E Virus Replication. Antimicrob Agents Ch **60:**2834-2848.
225. **Watson, S. F., N. Bellora, and S. Macias.** 2020. ILF3 contributes to the establishment of the antiviral type I interferon program. Nucleic Acids Res **48:**116-129.

226. **Watters, K., B. Inankur, J. C. Gardiner, J. Warrick, N. M. Sherer, J. Yin, and A. C. Palmenberg.** 2017. Differential Disruption of Nucleocytoplasmic Trafficking Pathways by Rhinovirus 2A Proteases. J Virol **91**.
227. **Welsch, S., S. Miller, I. Romero-Brey, A. Merz, C. K. Bleck, P. Walther, S. D. Fuller, C. Antony, J. Krijnse-Locker, and R. Bartenschlager.** 2009. Composition and three-dimensional architecture of the dengue virus replication and assembly sites. Cell host & microbe **5:**365-375.
228. **Wessels, E., D. Duijsings, K. H. Lanke, W. J. Melchers, C. L. Jackson, and F. J. van Kuppeveld.** 2007. Molecular determinants of the interaction between coxsackievirus protein 3A and guanine nucleotide exchange factor GBF1. J Virol **81:**5238-5245.
229. **Wessels, E., D. Duijsings, K. H. Lanke, S. H. van Dooren, C. L. Jackson, W. J. Melchers, and F. J. van Kuppeveld.** 2006. Effects of picornavirus 3A Proteins on Protein Transport and GBF1-dependent COP-I recruitment. J Virol **80:**11852-11860.
230. **Wessels, E., D. Duijsings, T. K. Niu, S. Neumann, V. M. Oorschot, F. de Lange, K. H. Lanke, J. Klumperman, A. Henke, C. L. Jackson, W. J. Melchers, and F. J. van Kuppeveld.** 2006. A viral protein that blocks Arf1-mediated COP-I assembly by inhibiting the guanine nucleotide exchange factor GBF1. Developmental cell **11:**191-201.
231. **Wright, J., R. A. Kahn, and E. Sztul.** 2014. Regulating the large Sec7 ARF guanine nucleotide exchange factors: the when, where and how of activation. Cellular and molecular life sciences : CMLS **71:**3419-3438.
232. **Xiang, W., A. Cuconati, D. Hope, K. Kirkegaard, and E. Wimmer.** 1998. Complete protein linkage map of poliovirus P3 proteins: interaction of polymerase 3Dpol with VPg and with genetic variants of 3AB. J Virol **72:**6732-6741.
233. **Yang, S., Y. Wang, Q. Shen, W. Zhang, and X. Hua.** 2013. Prevalence of porcine enterovirus 9 in pigs in middle and eastern China. Virol J **10:**99.
234. **Yogo, Y., and E. Wimmer.** 1972. Polyadenylic acid at the 3'-terminus of poliovirus RNA. Proceedings of the National Academy of Sciences of the United States of America **69:**1877-1882.
235. **Youn, J. Y., W. H. Dunham, S. J. Hong, J. D. R. Knight, M. Bashkurov, G. I. Chen, H. Bagci, B. Rathod, G. MacLeod, S. W. M. Eng, S. Angers, Q. Morris, M. Fabian, J. F. Côté, and A. C. Gingras.** 2018. High-Density Proximity Mapping Reveals the Subcellular Organization of mRNA-Associated Granules and Bodies. Molecular cell **69:**517-532 e511.
236. **Ypma-Wong, M. F., P. G. Dewalt, V. H. Johnson, J. G. Lamb, and B. L. Semler.** 1988. Protein 3CD is the major poliovirus proteinase responsible for cleavage of the P1 capsid precursor. Virology **166:**265-270.
237. **Zell, R., A. Krumbholz, M. Dauber, E. Hoey, and P. Wutzler.** 2006. Molecular-based reclassification of the bovine enteroviruses. The Journal of general virology **87:**375-385.

238. **Zevakov, V. F., S. Semak, V. I. Titarenko, N. V. Andreĭchenko, and O. V. Gedzul.** 1987. [Role of poliomyelitis viruses in the etiology of serous meningitis in Odessa 1979-1983]. Voprosy virusologii **32:**459-464.
239. **Zhai, X., S. Wu, L. Lin, T. Wang, X. Zhong, Y. Chen, W. Xu, L. Tong, Y. Wang, W. Zhao, and Z. Zhong.** 2018. Stress Granule Formation is One of the Early Antiviral Mechanisms for Host Cells Against Coxsackievirus B Infection. Virol Sin **33:**314-322.
240. **Zhang, C. S., S. A. Hawley, Y. Zong, M. Li, Z. Wang, A. Gray, T. Ma, J. Cui, J. W. Feng, M. Zhu, Y. Q. Wu, T. Y. Li, Z. Ye, S. Y. Lin, H. Yin, H. L. Piao, D. G. Hardie, and S. C. Lin.** 2017. Fructose-1,6-bisphosphate and aldolase mediate glucose sensing by AMPK. Nature **548:**112-116.
241. **Zhang, J., Z. Zhang, V. Chukkapalli, J. A. Nchoutmboube, J. Li, G. Randall, G. A. Belov, and X. Wang.** 2016. Positive-strand RNA viruses stimulate host phosphatidylcholine synthesis at viral replication sites. Proceedings of the National Academy of Sciences of the United States of America **113:**E1064-1073.
242. **Zhang, Z., G. He, N. A. Filipowicz, G. Randall, G. A. Belov, B. G. Kopek, and X. Wang.** 2019. Host Lipids in Positive-Strand RNA Virus Genome Replication. Front Microbiol **10:**286.
243. **Zhu, L., Z. Xing, X. Gai, S. Li, Z. San, and X. Wang.** 2014. Identification of a novel enterovirus E isolates HY12 from cattle with severe respiratory and enteric diseases. PLoS One **9:**e97730-e97730.